Any Way the Wind Blows

Dynamics of Greenhouse Gas Exchange in Northeastern Siberian Tundra

Frans-Jan Parmentier

Cover photo: midnight sky at the Kytalyk resource reserve, August 2008, Northeastern Siberia.

Any Way the Wind Blows
Dynamics of Greenhouse Gas Exchange in Northeastern Siberian Tundra
(PhD Thesis, VU University Amsterdam)
In dutch: Waarheen de Wind Waait
Dynamiek van Broeikasgasuitwisseling in Noordoost-Siberische Toendra
(Academisch Proefschrift, Vrije Universiteit Amsterdam)

This research was funded by the Darwin Center for Biogeosciences (142.16.1041) and the Dutch Russian research cooperation programme of NWO, entitled "Long term observation of soil carbon and methane fluxes in Siberian tundra" (047.017.037)

ISBN 978-90-5335-404-9
NUR 935
Printed by Ridderprint BV, Ridderkerk

Subject headings:
Methane / Carbon Dioxide / Tundra / Peatland / Eddy Covariance / Flux Chamber Measurements / Carbon / Permafrost

VRIJE UNIVERSITEIT

Any Way the Wind Blows

Dynamics of Greenhouse Gas Exchange in Northeastern Siberian Tundra

ACADEMISCH PROEFSCHRIFT

ter verkrijging van de graad Doctor aan
de Vrije Universiteit Amsterdam,
op gezag van de rector magnificus
prof.dr. L.M. Bouter,
in het openbaar te verdedigen
ten overstaan van de promotiecommissie
van de faculteit der Aard- en Levenswetenschappen
op maandag 30 mei 2011 om 15.45 uur
in de aula van de universiteit,
De Boelelaan 1105

door

Franciscus Jan Willem Parmentier

geboren te Bonn-Duisdorf, Duitsland

promotor: prof.dr. A.J. Dolman
copromotor: dr. J. van Huissteden

ΦAKKO & CAKKO


ALS ONDERZOEKER NAAR SIBERIË GE-STUURD WORDEN-
... HET HEEFT IETS STALINISTISCH!
Rom 24/01/07
Jean-Marc V tol

reading committee: prof.dr. R. Aerts
prof.dr. W. Bleuten
dr. T. Friborg
dr. D.M.D. Hendriks
dr. R.A.M. de Jeu
dr. E.M. Veenendaal

Contents

Acknowledgements

At the start of the summer of 2006, when I was in the midst of writing my Masters thesis, Han invited me 'to chat about Russia'. A signed contract and a few months later, I started the research that is presented before you in this book. At that time, I had no idea of the scale of the task that lay ahead of me. Today, more than four years later, I have learned so much and I've been so lucky to have great experiences in distant places such as Siberia and Alaska. In those places, but also back home, there are many people who I want to thank for helping me get so far.

At the VU I want to thank my professor, Han Dolman, for making it possible for me to do research in such a beautiful, remote place and his guidance into making this thesis come together. Ko van Huissteden, for a tremendous work, trying to circumvent all the bureaucratic pitfalls that are inherent to research in Russia. Because of your tenaciousness, we were able to get the results we wanted in the end. Michiel, for teaching me everything about eddy covariance and for showing me the way on the tundra. Rob, Hans, Niek and the others from the workshop for not just making great fieldwork equipment but also for thinking practically about what was needed in the field. Ron from the electronics department, for his expertise and his help in setting up the fieldwork in 2008, despite the logistical problems. And a big thanks go out to my colleagues, for all the great lunches and thursday afternoon drinks: Margriet, Lieselotte, Dimmie, Brett, Uros, Josepha, Paolo and many others.

I want to thank my parents of course, who supported me throughout the long years that I worked to obtain my Masters degree, which led me to this research, and who always made it possible for me to pursue those things that I wanted to do the most. Janna, for being around in the first couple of years. My sisters Alice and Annemarie. And Dennis, for going along all the way to the tundra in the spring of 2009 (next time, we'll bring a real snowboard, not a plank!). And of course Carline, with whom I ventured through the last critical months of continuous writing.

There are also many people in Russia that I want to thank for the help they have shown with every visit. From the IBPC: Sergey, for the much appreciated (and needed) assistance in the field, without which it would never have been possible to perform all the required measurements. Sasha and Roman, for the humor they brought into the field. Trofim, for overseeing our cooperation. And many thanks to Dima, Ayal, Stas and Vasha also. In Chokurdakh: Tanja for the logistical support, making sure we were able to travel to the site. Sergey Ilitsj, for being there at the crucial moments and for the wonderful meals from his wife when we came back from the field. And of course thanks go out to the rangers Valera, Jegor, Kostja and many others who drove the snowmobiles in winter or the speedboats in summer. Also, a big thanks to Lena who cooked for us in the first summer and Alya who has been such a good and friendly cook ever since.

And many thanks go out to the people who accompanied me on the tundra: Daan, for all the summers we spent in endless clouds of mosquitos and sharing the experience. Maarten, Frida and Ruben for the fun we had out there. And there are so many more that I met. In Alaska, I want to thank Katey for letting me stay in Fairbanks and learn so much. Laura, for taking me out into the field and having me along on the beautiful trip up to Toolik Lake.

I'd like to thank the reading committee, Thomas Friborg, Rien Aerts, Wladimir Bleuten, Elmar van Veenendaal, Dimmie Hendriks and Richard de Jeu for critically evaluating this thesis and for their wise remarks. And last, but not least, I want to thank the Darwin Center for Biogeosciences for funding this research and NWO for providing additional funds that made our life in Siberia so much easier.

Chapter 1

Introduction

1.1 Background

Since the start of the industrial revolution, the atmospheric concentration of carbon dioxide, CO_2, has risen from around 260-280 ppm (parts per million) to about 389 ppm at the current day (*Indermuhle et al.*, 1999; *Conway et al.*, 2010). In the same time span, the second most important greenhouse gas, methane or CH_4, has more than doubled from a concentration of 730 ppb (parts per billion) to about 1800 ppb (*Blunier et al.*, 1995; *Dlugokencky et al.*, 2009). Caused by human activities such as fossil fuel burning, the clearing of forests, agriculture and animal husbandry, this increase in greenhouse gases has led to a rise in the average global surface air temperature of about 0.7 degrees (*Hegerl et al.*, 2007; *Smith et al.*, 2008).
While this increase in temperature seems small, there are large regional differences and one of the regions where global warming is felt more strongly in particular, is the Arctic. Arctic temperatures are rising much faster than in the rest of the world and this is expected to have, or already has had, large effects on i.e. the extent of sea ice, the onset of snowmelt, vegetation growth and the melting of permafrost. In turn, these changes have an influence on the natural exchange of greenhouse gases with the atmosphere, directly or indirectly. To better understand the influence of these external forcing factors to these ecosystems, we need to understand the underlying processes better.
This thesis therefore discusses the natural exchange of CO_2 and methane with the atmosphere, with a special emphasis on the Arctic. Research has been performed at a study site in Northeastern Siberia and additionally a part of the research has been performed at a peatland in the Netherlands. To obtain an integrated view of the area, the studied topics vary spatially and temporally: from very localized processes at the plot level, to measurements integrated over hundreds of meters and from processes occurring in minutes to inter-annual variations in fluxes. Together, these studies paint a larger picture of the greenhouse gas exchange of these ecosystems. Ultimately, this will lead to a better understanding of the response of these ecosystems to future climate change.

1.2 Objectives

The main objective of this thesis was to determine the size and variability of the fluxes of CO_2 and CH_4 from tundra in Northeastern Siberia, and their sensitivity to climate change and the

spatial variability within landscapes with a complementary set of approaches. Before focusing on the Arctic however, as a first objective, it was determined whether respiration and evaporation of a peatland in the Netherlands were sensitive to changes in water level. Although that site has a very different climate to the tundra, many of the studied processes hold true for both areas since certain aspects of the soil and vegetation are comparable. For example, both areas have a wet soil with a high organic content and vegetation is dominated by grasses, sedges and shrubs in tundra as in the studied peatland. Relationships found in the peatland are therefore likely to be helpful in explaining processes in the tundra as well.
The remaining objectives focused on processes that were studied solely at the research site in Northeastern Siberia: the second objective was to study the influence that methanotrophic bacteria, living in a cooperation with *Sphagnum*, have on the spatial variation of methane emissions from tundra. Following this detailed study, our third objective was to determine the integrated methane emission of tundra with eddy covariance and to clarify its temporal and spatial dynamics with the use of a non-linear model. Finally, the inter-annual variation and stability of photosynthesis, ecosystem respiration and the net exchange of CO_2 of tundra along growing season length and summer temperatures was studied.

1.3 Approach and outline of this thesis

Before these challenges are approached, this thesis is put in a larger perspective in the second chapter, which provides a general background. Herein, the tundra ecosystem, permafrost, ecological changes under climate change, the carbon cycle and measurement techniques such as the chamber flux method and the eddy covariance technique are discussed.
In chapter 3, to assess the influence of water table changes on evaporation and respiration in a peatland, eddy covariance measurements were combined with water table measurements, soil analysis and a process model to ascertain whether evaporation and respiration in a peatland showed any variation with water table depth when water availability remains high.
Subsequently, this thesis focuses on greenhouse gas emissions from tundra. In chapter 4, the influence of endophytic methanotrophic bacteria on net methane emissions was studied by careful measurement of methane fluxes from inundated vegetation types with and without *Sphagnum* but with similar soil temperatures and active layer depth. Samples from submerged *Sphagnum* vegetation were analyzed for methanotrophic activity and to identify the key underlying processes, fluxes of both vegetation types were modeled with a well-established process model.
In chapter 5, to investigate the temporal and area integrated dynamics of tundra methane fluxes, eddy covariance measurements were compared with parameters such as atmospheric stability, water level and temperature while keeping in mind the spatial heterogeneity of tundra. These relationships were used in a non-linear model that was tuned separately for three different source areas that showed significantly different fluxes and independently compared with flux chamber measurements performed in the vicinity of the eddy covariance tower.
Finally, in chapter 6, to investigate the inter-annual variation of CO_2 fluxes, eddy covariance measurements of the net ecosystem exchange of 8 consecutive growing seasons was split up into its components, photosynthesis and ecosystem respiration. These fluxes were compared to growing season length and summer temperatures to investigate whether a longer growing season would not only lead to more photosynthesis but also to a higher net uptake of carbon.

References

Blunier, T., J. Chappellaz, J. Schwander, B. Stauffer, and D. Raynaud, Variations in atmospheric methane concentration during the Holocene epoch, *Nature*, *374*(6517), 46--49, 1995.

Conway, T. J., P. M. Lang, and K. A. Masarie, Atmospheric Carbon Dioxide Dry Air Mole Fractions from the NOAA ESRL Carbon Cycle Cooperative Global Air Sampling Network, 1968-2009, *Version: 2010-09-08, Path: ftp://ftp.cmdl.noaa.gov/ccg/co2/flask/month/*, 2010.

Dlugokencky, E. J., et al., Observational constraints on recent increases in the atmospheric CH_4 burden, *Geophysical Research Letters*, *36*, L18,803, 2009.

Hegerl, G. C., F. W. Zwiers, P. Braconnot, N. P. Gillett, Y. Luo, J. A. Marengo Orsini, N. Nicholls, J. E. Penner, and P. A. Stott, Understanding and Attributing Climate Change, *Climate Change 2007: The Physical Science Basis. Contribution of Working Group I to the Fourth Assessment Report of the Intergovernmental Panel on Climate Change [Solomon, S., D. Qin, M. Manning, Z. Chen, M. Marquis, K.B. Averyt, M. Tignor and H.L. Miller*, 2007.

Indermuhle, A., et al., Holocene carbon-cycle dynamics based on CO_2 trapped in ice at Taylor Dome, Antarctica, *Nature*, *398*(6723), 121--126, 1999.

Smith, T. M., R. W. Reynolds, T. C. Peterson, and J. Lawrimore, Improvements to NOAA's historical merged land-ocean surface temperature analysis (1880-2006), *Journal Of Climate*, *21*(10), 2283--2296, 2008.

Chapter 2

The Tundra Ecosystem, Climate and Greenhouse Gas Exchange

2.1 Introduction

In the past century, global temperatures have risen about 0.7 degrees on average, which is commonly attributed to the increase of greenhouse gases in the atmosphere (*Hegerl et al.*, 2007; *Smith et al.*, 2008). Because this is an average temperature increase, it obscures the fact that large differences occur in between regions. For example, certain parts of the Arctic have shown exceptionally high temperature increases of 0.2 to 0.4 °C per decade and this trend is expected to continue (*Zwiers*, 2002; *Chapin III et al.*, 2005; *Serreze and Francis*, 2006). To understand how these temperature changes affect the Arctic as a carbon sink, it is critical to understand the functioning of greenhouse gas exchange in arctic ecosystems. In this chapter, the tundra ecosystem, geomorphology and climate is described, followed by an explanation on the specifics of the exchange of CO_2 and methane in tundra. The chapter concludes with an elaboration on the methods that are typically used to quantify greenhouse gas exchange in the Arctic.

2.2 Vegetation, geomorphology and climate sensitivity

2.2.1 The tundra ecosystem

The tundra climate, according to the Köppen-Geiger classification, falls within the polar climate group under designation ET, which is defined as the area where the temperature of the hottest month is above freezing but below 10 °C on average (*Peel et al.*, 2007). Excluding alpine tundra, this climate region occurs mostly in the most Northern parts of the American and Eurasian continents. Precipitation is quite low in these areas with a typical yearly precipitation of 150 to 250 mm on average, of which most usually falls as rain in summertime and as snow in the rest of the year. Although this amount of precipitation is rather low, total evaporation is also low and thus soils remain wet. Due to the short summers, combined with the low temperatures, tree growth is hindered and therefore most tundra is characterized by low growing vegetation such as shrubs, sedges, grasses, mosses and lichens.
The study area of this research has a highly heterogenous vegetation, which is mostly due to

Figure 2.1: Occurrence of permafrost in the Northern hemisphere. Areas of continuous permafrost are indicated with dark purple. Areas with discontinuous, sporadic and isolated permafrost have been indicated with ever lighter shades of purple. Original image by Philippe Rekacewicz and the International Permafrost Asssociation.

differences in water level. In dry areas, vegetation consists of *Betula nana* and *Salix pulchra* dwarf shrubs or hummocks of the sedge *Eriophorum vaginatum* with *Salix pulchra* in between. In these areas a moss and lichen ground cover is common. In the transition zone from a dry to a wet area, mosses and lichens are replaced by *Sphagnum spp.* and shrub cover is largely reduced. In these parts, *Potentilla palustris* occurs and sedge cover increases to 50% with species such as *Eriophorum angustifolium* and *Carex aquatilis*. These sedges dominate the wet, flooded parts of terrain depressions and polygon centers where *Sphagnum* is absent and sedge cover is around 80 to 100%.

2.2.2 Permafrost and geomorphology

Due to the cold temperatures, most tundra ecosystems are underlain by permafrost. Permafrost is defined as a soil which is below or at the freezing point of water for at least two consecutive years. While permafrost can extend up to several hundreds of meters into the earth, normally the top layer of the soil thaws in summer and this part of the soil, where most soil microbial processes occur, is called the active layer. This active layer can extend up to 2 meters in the taiga, while in tundra ecosystems active layer depths of 30 to 50 cm are more

typical.
The continuous thawing and freezing of the top layer of the soil leads to geomorphological features in the landscape, such as ice wedges, thermokarst lakes and palsas, that are typical for areas with an arctic climate. Ice wedges are created due to thermal contraction cracks in the ground which fill up with water during the summer season. When the water in these cracks freezes, the ice expands and this widens the crack. In following winters, thermal contraction cracks occur in the same places and the process is repeated, thus creating ever expanding ice wedges which also raise the top soil in the process, creating ridges. In arctic regions ice wedges usually join together forming ice wedge polygons in the landscape.
When ice wedges are exposed and melt completely, ponds are created in the surface. The relatively warm water in these ponds leads to a deeper active layer beneath the ponds and if these are deep enough, they do not completely freeze during winter. In the following summer they expand again and the successful succession of this process eventually leads to thermokarst lakes, a common feature of the arctic landscape. The anaerobic conditions at the bottom of thermokarst lakes are perfectly suited for methane production and it has been shown that these lakes are a significant global source of methane (*Walter et al.*, 2006).
A third common feature of the Arctic are palsas, which are small mounds in the landscape. These higher areas are created by frost heaving. This process occurs in areas where water saturated soil freezes, forming an ice lens in the soil. These ice lenses are able to grow larger and larger, provided there is enough water in the surrounding area which they can accumulate. Eventually these ice lenses lift the soil surface, creating frost heaves. These higher areas are more exposed to the winter cold due to a thinner snow cover. This promotes the growth of the ice lens even more, ultimately creating palsas.
While many more periglacial features can be identified, such as pingos and frost boils, the features described above are the most relevant in this thesis. The micro-topographical features created by ice wedges and palsas lead to changes in water availability and thus vegetation. These features therefore govern the spatial variability in greenhouse gas exchange of tundra. Furthermore, ponds and thermokarst lakes are significant emitters of methane, the second most important greenhouse gas.

2.2.3 Sensitivity to climate change

Since global warming occurs two to three times faster in the Arctic compared to the rest of the world, changes to climate change are expected earlier. The currently observed changes are occurring at a rate that has not been witnessed since the end of the last ice age and large effects are observed throughout the Arctic. Sea ice is breaking up earlier and refreezing later, while seasonal minimal extent of sea ice has declined by 45.000 km^2 per year (*Parkinson and Cavalieri*, 2008), furthermore the extent of snow cover has been reduced in the northern hemisphere (*Serreze et al.*, 2000) and these changes are expected to continue.
These changes in temperature and snow cover have a direct effect on the vegetation. Plants flower earlier in the year with earlier snowmelt and changes by as much as 20 days have been reported (*Høye et al.*, 2007). Studies from satellite data have confirmed that the growing season is lengthening across the Arctic and plant growth has increased over the 1980's and 1990's (*Myneni et al.*, 1997; *Stow et al.*, 2004). It has been suggested that this is due to an expansion of shrubs and recently it has been found that this might actually reduce summer permafrost thaw in tundra (*Blok et al.*, 2010). Furthermore, a longer growing season with higher plant activity might lead to more carbon uptake (*Churkina et al.*, 2005).

However, besides these positive effects, higher temperatures also lead to more soil respiration, reducing net carbon uptake (*Euskirchen et al.*, 2006) and seasonal effects might be highly important into explaining differences in the net uptake of carbon (*Randerson et al.*, 1999; *Piao et al.*, 2008). These changes in the net carbon exchange in tundra are important since arctic soils hold large deposits of carbon. Estimates of carbon stores in permafrost regions are currently as high as 1672 Pg or half the amount of carbon stored in soils worldwide (*Tarnocai et al.*, 2009). Recently, it has been shown that carbon released from deeper layers in the soil are also quite sensitive to higher temperatures, increasing the likeliness that respiration can compensate for the higher uptake of carbon due to a longer growing season (*Schuur et al.*, 2008; *Dorrepaal et al.*, 2009). Thus, higher arctic temperatures might lead to less uptake of carbon, which would lead to a higher buildup of CO_2 in the atmosphere and even higher temperatures.

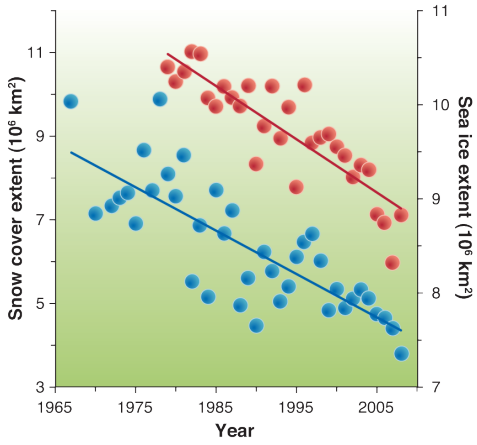

Figure 2.2: Reductions in terrestrial snow cover (blue) and sea ice (red) extent during June to August for the past since the 1960's and 1970's. Original image by Eric Post.

Furthermore, the aforementioned changes in snowmelt and sea ice extent do not only affect arctic flora but can also have large effects on arctic fauna. For example, it has been reported that the migration of caribou to their summer ranges starts due to a change in day length while the flowering of plants is linked to temperature. If the cues to these two processes start to differ in time, these animals can miss the peak of resource availability, which has consequences for successful reproduction (*Post and Forchhammer*, 2008). Furthermore, the reduction in sea ice also puts many marine animals such as seals and polar bears under increasing pressure (*Laidre et al.*, 2008), although recently it has been suggested that greenhouse gas mitigation might be able to help reverse this trend (*Amstrup et al.*, 2010).

2.3 Greenhouse gas exchange in tundra

2.3.1 Photosynthesis and respiration

While human activities release large amounts of CO_2 into the atmosphere, plants take up carbon through photosynthesis. In this process, plants combine water and CO_2 together with sunlight to create sugars, releasing oxygen in the process. The general equation of oxygenic photosynthesis is shown in Equation 2.1

$$2nCO_2 + 2nH_2O + \text{sunlight} \rightarrow 2(CH_2O)_n + 2nO_2 \tag{2.1}$$

The sugars created in this process can be used to create plant tissue or the energy stored within can be used by the plant when and where this energy is needed. This last process is done

through cellular respiration and is described in Equation 2.2.

$$C_6H_{12}O_6 + 6O_2 \rightarrow 6CO_2 + 6H_2O \tag{2.2}$$

This process not only releases energy for use by the plant, it also returns CO_2 to the atmosphere. The net carbon uptake of a plant therefore depends on both photosynthesis and plant respiration. Photosynthesis is commonly referred to as gross primary production, GPP, while the difference between GPP and plant respiration is referred to as net primary production, NPP.

Although plants accumulate carbon in their tissue throughout their lifetime, this organic matter is transferred to the soil once plants die or shed leaves. This plant matter is then respired back to the atmosphere by decomposers in the litter layer and the soil, such as bacteria. When considering whole ecosystems it is often difficult to accurately distinguish between this type of respiration and plant respiration. Therefore, usually only the sum of both types of respiration, known as ecosystem respiration, R_{eco}, is discussed. The difference between GPP and R_{eco} is commonly known as net ecosystem exchange, NEE. If GPP is larger than ecosystem respiration, NEE is negative and the ecosystem is taking up carbon from the atmosphere.

Soil temperature and water level are critical in creating the conditions for a net uptake of carbon. Low soil temperatures limit the ability of bacteria to respire carbon and beneath the water table, no oxygen is available for respiration. Areas where large amount of carbon have been stored in the soil are therefore characterized by low temperatures and wet conditions, such as in tundra and peatlands. Due to permafrost melt, these carbon stocks can become more readily available for respiration and in theory these carbon deposits can be respired back into the atmosphere.

2.3.2 Methane

While ecosystems such as tundra and peatlands are usually carbon sinks that have removed large amounts of CO_2 from the atmosphere, the greenhouse gas function of these ecosystems is possibly quite different. Below the water table, where respiration is limited due to the lack of oxygen, organic matter is decomposed by microorganisms known as methanogens, releasing methane in the process. Although this process can follow several pathways, the most commonly known involve CO_2 and hydrogen or acetic acid and are described in Equation 2.3 and Equation 2.4:

$$CO_2 + 4H_2 \rightarrow CH_4 + 2H_2O \tag{2.3}$$

$$CH_3COOH \rightarrow CH_4 + CO_2 \tag{2.4}$$

The methane formed through this methanogenesis has a global warming potential which is 25 times stronger than CO_2 on a per weight basis. Therefore, if enough methane is being emitted, ecosystems such as tundra can be a sink for carbon but at the same time also a source of greenhouse gases in terms of global warming potential. It is therefore critical to understand the processes that determine the emission of methane.

Since methane production only occurs in the anaerobic part of the soil, changes in the water table can have a large effect on emissions, as shown in Figure 2.3. If the top part of the soil is aerobic due to a low water table, methanotrophic bacteria in this part of the soil use oxygen

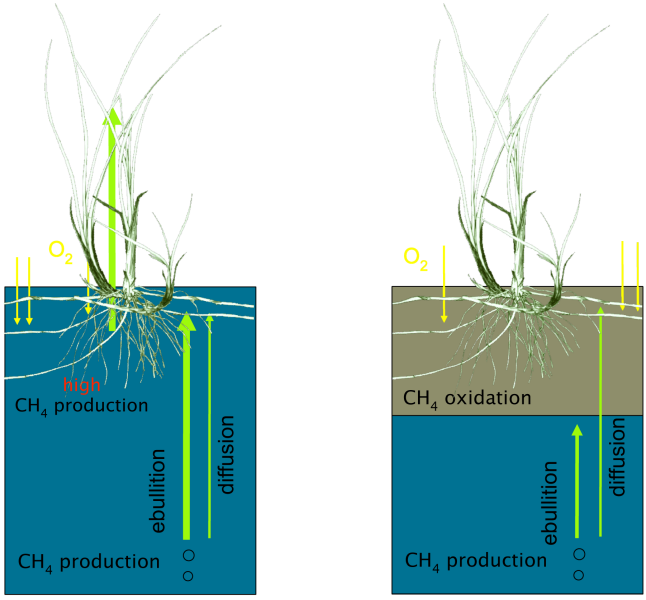

Figure 2.3: Methane pathways in the soil. If water table is high, as on the left, methane (indicated with green arrows) can be transported to the atmosphere directly. If water table is low, as on the right, emissions are limited due to oxidation in the aerobic part of the soil but plants can provide a bypass through this part of the soil. Original image by Ko van Huissteden.

to convert methane into CO_2. Therefore, methane that is produced in deeper soil layers will not reach the atmosphere if the water table is too low.

However, this aerobic part of the soil can be bypassed in certain cases where vascular plants root deep enough to reach the anaerobic part of the soil. Through the aerenchyma of plants, methane can be transported upwards without being oxidized. Therefore, methane emissions are often highest in areas with a large amount of vascular plants (*Joabsson et al.*, 1999; *Greenup et al.*, 2000; *Christensen et al.*, 2003; *Ström et al.*, 2005), although it has been shown that the aerenchyma of plants also provide a pathway for oxygen into the soil, increasing oxidation of methane (*Popp et al.*, 2000; *Whalen*, 2005). Additionally, vascular plants influence the production of methane by providing fresh substrate to the methanogens, which is easier to convert to methane than old and more recalcitrant organic matter (*Ström et al.*, 2005). Since these plants influence methane emissions and because vegetation composition is also related to water availability, vegetation composition can be used as an indicator of the spatial variation of methane emissions (*van Huissteden et al.*, 2005).

Apart from these relationships with vegetation, methane emissions are also increased by higher soil temperatures. In tundra, higher soil temperatures lead to a deeper active layer and this provides a larger reservoir in the soil for methane production to occur. However, higher temperatures also increase evaporation and a deeper active layer possibly increases drainage, which would both influence the water table in the soil. Localized conditions therefore strongly determine the size of methane fluxes and methane emissions are very heterogeneous spatially.

2.4 Measurement techniques

In the past, many different methods have been used to measure fluxes of CO_2 and methane, such as chamber flux measurements, mass balance techniques, eddy covariance, relaxed eddy accumulation and flux gradient methods (*Denmead*, 2008). It is beyond this thesis to discuss all these techniques separately and therefore we limit ourselves to the methods used most in this study, namely the flux chamber method and the eddy covariance technique.

2.4.1 Flux chambers

A widely used method to perform measurements of trace gas fluxes, soil respiration and methane emissions in particular, is the flux chamber technique (*Moore and Roulet*, 1991). This method has the advantage that it's portable and applicable to small areas (< 1 m^2), which makes it ideal to study small scale differences in fluxes. The general application is to place a closed chamber on top of a collar that is placed firmly into the top soil, to avoid leakage to the sides. Subsequently, the concentration increase of the gas of interest within the chamber is measured at regular intervals. By extrapolating the linear relationship between time and concentration, the flux of the gas can be calculated from the volume of the chamber and its base footprint.
The first closed chamber flux measurements were performed as early as the 1960's and 1970's. These early studies used either KOH to absorb CO_2 or they took air samples of the trace gas for analysis in a laboratory afterwards (*Witkamp*, 1966; *Schulze*, 1967; *Kanemasu et al.*, 1974; *Crill et al.*, 1988). Because this practice significantly limited temporal resolution, it was improved upon by performing continuous measurements with an infrared gas analyzer (IRGA) (*Edwards and Sollins*, 1973). This made continuous measurements possible but portability was reduced since a large trailer was needed for the IRGA equipment. After the miniaturization of this technique, chamber flux measurements provided both a high temporal resolution as well as portability (*Vourlitis et al.*, 1993; *Silvola et al.*, 1996).
The flux chamber technique can therefore provide a detailed view on the emission of methane and its spatial variability. If relevant environmental parameters are measured together with the flux measurement, the processes that drive these fluxes can be recognized readily (*van Huissteden et al.*, 2005). However, flux chamber measurements also have many downsides. First of all, measurements are very labor intensive because every plot has to be visited separately. Furthermore, fluxes can be disturbed during the measurement due to, among others, leakage, ebullition (natural or caused by disturbance from the person performing the measurement), heating of the chamber and non-linear concentration increases. Most of these problems can be solved by applying automatic chambers. However, irregular events such as ebullition will still be captured poorly while atmospheric effects such as turbulence are excluded with the closed flux chamber technique. Furthermore, the method is only applicable to low standing vegetation such as grasses and sedges, since chamber sizes are required to be relatively small.

2.4.2 Eddy covariance

Theory

Most of the disadvantages mentioned above do not apply to the eddy covariance technique. This technique can measure trace gas fluxes over an integrated area and continuously. The

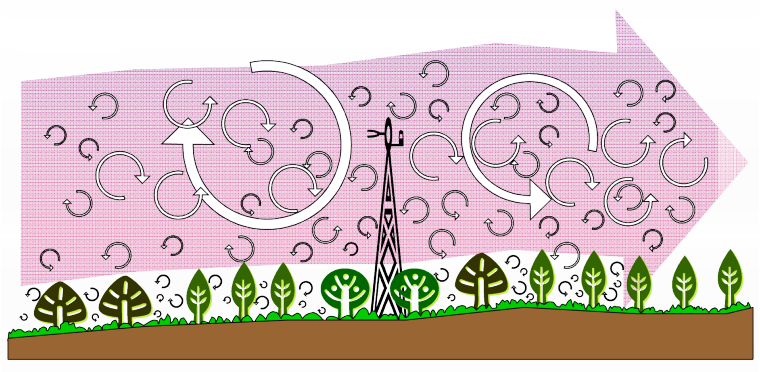

Figure 2.4: On this picture, the air flow is represented by the large pink arrow that passes through the tower and consists of different size of eddies. Conceptually, this is the framework for atmospheric eddy transport. Original image created by George Burba.

method combines measurements of wind speed and concentrations of the trace gas to approximate the average flux through statistical methods. Measurements are performed in open air and therefore atmospheric effects are incorporated. Also, measurements can be performed over larger vegetation such as forests.
Figure 2.4 shows the concept of atmospheric eddy transport. The large pink arrow represents the general airflow while within this airflow many different deviations from the average occur, caused by turbulent eddies. These eddies each have a certain concentration of trace gas and a speed associated and if these concentrations and vertical movements are measured in time, one can determine the flux. For example, if a moving parcel of air has a concentration of s1 and a speed of w1 in an upward direction, while a following parcel of air has a concentration of s2 and w2 in a downward direction, the average will determine how many molecules have traveled up or down and provides us with the flux. In eddy covariance these small eddies are measured as deviations from the average airflow and together with the simultaneously measured deviations of the concentration of the studied gas from the average, the flux can be calculated according to Equation 2.5.

$$F_s = \overline{w's'} = \frac{1}{t_2 - t_1} \int_{t_1}^{t_2} w'(t)s'(t)dt \tag{2.5}$$

Here F_s is the atmospheric flux of the studied gas (i.e. CO_2, CH_4 or H_2O), w' the deviation of the vertical wind speed from the mean, s' the deviation of the concentration of the studied gas from the mean and t_1 and t_2 the start and end of the studied time period.

Equipment

Since the measured eddies vary at a high frequency, the equipment to measure these fluctuations should measure at a high frequency too. Commonly, equipment measures wind speed and gas concentrations at a minimal frequency of 10 Hz and measurements need to be precise, highly accurate and stable over time. These requirements and data storage issues prevented a general application of eddy covariance before the 1980's (*Lloyd et al.*, 1984; *Businger*, 1986;

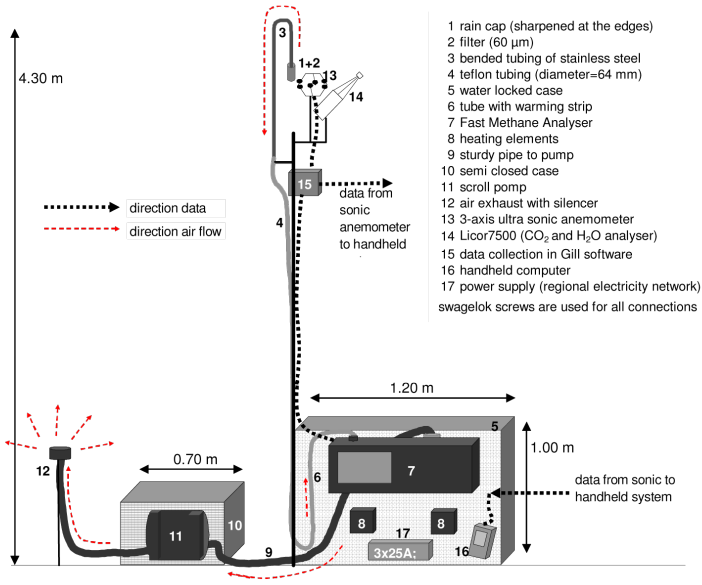

Figure 2.5: Diagram of an eddy covariance tower with a closed path setup for methane measurements and an open path setup for CO_2 and H_2O fluxes. Original image created by Dimmie Hendriks.

Verma et al., 1986; *McMillen*, 1988; *Valentini et al.*, 1991), although the theory was developed as early as the 1950's (*Swinbank*, 1951).

While these early studies used varying techniques, most eddy covariance studies on fluxes of CO_2 or water vapor use a sonic anemometer combined with an infrared gas analyzer (IRGA). A sonic anemometer measures wind speed by measuring the speed of sound between pairs of transducers. Since the speed of sound is also dependent on temperature, it can be derived from these measurements as well. A typical sonic anemometer in eddy covariance studies uses three pairs of transducers which are positioned in such a way that they provide a three dimensional measurement of wind speed and direction.

The IRGA's and other gas analyzers that are used in eddy covariance studies can be divided into two categories: closed and open-path. A closed path setup is often used if the analyzer is too large to place near the sonic anemometer. Instead, an inlet of a tube is situated near the sonic anemometer and from here a gas sample is drawn through this tube towards the gas analyzer. However, the air flow through the tube must be fast enough to replace the air in the measurement cell at the required frequency. Therefore, closed path setups often use a large pump and this increases power requirements.

In an open path setup, the analyzer is much smaller and measurements of gas concentrations are performed in open air. This eliminates the need for a pump and measurements require much less power. However, measurements are more easily disturbed by fog, raindrops on the instrument or radiant heat from the device itself (*Burba et al.*, 2008). This means that additional correction factors are needed and more data has to be filtered out with these types of setups. Even so, the introduction of open-path CO_2/H_2O analyzers such as the Licor-7500 (Licor, Lincoln, NE, USA) greatly simplified eddy covariance setups and made it possible to apply the technique in remote areas with limited power supply.

Since, many studies on CO_2 fluxes have used this equipment over a wide range of terrain but before recently, eddy covariance measurements of CH_4 still had to rely on close-path setups. These setups normally made use of a fast response tunable diode laser spectrometer (TDL) which was shown to give good results (*Verma et al.*, 1992; *Zahniser et al.*, 1995). However, this system had the large drawback that it needed to be cooled, with either liquid nitrogen or a cryogenic system, and that they required regular calibration with a standard gas. These requirements made the system of limited use in remote areas where either liquid nitrogen, calibration gases or the required power are logistically difficult. Recently, an off-axis integrated cavity output spectroscopy method was introduced that does not require cooling or regular calibration (*Hendriks et al.*, 2008). While this method still requires a large pump to obtain the required air flow for high frequency measurements, it is much more applicable in remote areas, provided a stable power supply is present.

Networks and Standardization

Many of the early studies were performed in short campaigns at varying locations with varying techniques. However, this approach makes it difficult to integrate observations to a regional scale or parameterization of models. Therefore, several regional networks (i.e. Euroflux/CarboEurope, Ameriflux and Asiaflux) have been established in the second half of the 1990's to standardize methods, initiate long-term observations and exchange data. Since 1998, these regional networks function under the umbrella organization 'Fluxnet' and currently over 500 long-term tower sites are associated. Through this network large steps towards standardization have been taken. For example, (*Aubinet et al.*, 2000) established the Euroflux methodology that standardized flux calculations of CO_2, H_2O and energy. Also, standard methods for gapfilling and error estimates have been established (*Papale et al.*, 2006). However, these methods mostly focused on CO_2 fluxes and standardization in eddy covariance measurements of methane and post-processing of data is still less defined.

References

Amstrup, S. C., E. T. DeWeaver, D. C. Douglas, B. G. Marcot, G. M. Durner, C. M. Bitz, and D. A. Bailey, Greenhouse gas mitigation can reduce sea-ice loss and increase polar bear persistence, *Nature*, *468*(7326), 955--U351, 2010.

Aubinet, M., et al., Estimates of the annual net carbon and water exchange of forests: The EUROFLUX methodology, *Advances In Ecological Research, Vol 30*, *30*, 113--175, 2000.

Blok, D., M. P. D. Heijmans, G. Schaepman-Strub, A. V. Kononov, T. C. Maximov, and F. Berendse, Shrub expansion may reduce summer permafrost thaw in Siberian tundra, *Global Change Biology*, *16*(4), 1296--1305, 2010.

Burba, G. G., D. K. McDermitt, A. Grelle, D. J. Anderson, and L. Xu, Addressing the influence of instrument surface heat exchange on the measurements of CO_2 flux from open-path gas analyzers, *Global Change Biology*, *14*(8), 1854--1876, 2008.

Businger, J. A., Evaluation of the accuracy with which dry deposition can be measured with current micrometeorological techniques, *Journal Of Climate And Applied Meteorology*, *25*(8), 1100--1124, 1986.

Chapin III, F. S., et al., Role of land-surface changes in Arctic summer warming, *Science*, *310*(5748), 657--660, 2005.

Christensen, T. R., N. S. Panikov, M. Mastepanov, A. Joabsson, A. Stewart, M. Oquist, M. Sommerkorn, S. Reynaud, and B. Svensson, Biotic controls on CO_2 and CH_4 exchange in wetlands - a closed environment study, *Biogeochemistry*, *64*(3), 337--354, 2003.

Churkina, G., D. Schimel, B. H. Braswell, and X. M. Xiao, Spatial analysis of growing season length control over net ecosystem exchange, *Global Change Biology*, *11*(10), 1777--1787, 2005.

Crill, P. M., K. B. Bartlett, R. C. Harriss, E. Gorham, E. S. Verry, D. I. Sebacher, L. Madzar, and W. Sanner, Methane flux from Minnesota peatlands, *Global Biogeochemical Cycles*, *2*(4), 371--384, 1988.

Denmead, O. T., Approaches to measuring fluxes of methane and nitrous oxide between landscapes and the atmosphere, *Plant And Soil*, *309*(1-2), 5--24, 2008.

Dorrepaal, E., S. Toet, R. S. P. van Logtestijn, E. Swart, M. J. van de Weg, T. V. Callaghan, and R. Aerts, Carbon respiration from subsurface peat accelerated by climate warming in the subarctic, *Nature*, *460*(7255), 616--U79, 2009.

Edwards, N. T., and P. Sollins, Continuous measurement of carbon-dioxide evolution from partitioned forest floor components, *Ecology*, *54*(2), 406--412, 1973.

Euskirchen, E. S., et al., Importance of recent shifts in soil thermal dynamics on growing season length, productivity, and carbon sequestration in terrestrial high-latitude ecosystems, *Global Change Biology*, *12*(4), 731--750, 2006.

Greenup, A. L., M. A. Bradford, N. P. McNamara, P. Ineson, and J. A. Lee, The role of Eriophorum vaginatum in CH_4 flux from an ombrotrophic peatland, *Plant And Soil*, *227*(1-2), 265--272, 2000.

Hegerl, G. C., F. W. Zwiers, P. Braconnot, N. P. Gillett, Y. Luo, J. A. Marengo Orsini, N. Nicholls, J. E. Penner, and P. A. Stott, Understanding and Attributing Climate Change, *Climate Change 2007: The Physical Science Basis. Contribution of Working Group I to the Fourth Assessment Report of the Intergovernmental Panel on Climate Change [Solomon, S., D. Qin, M. Manning, Z. Chen, M. Marquis, K.B. Averyt, M. Tignor and H.L. Miller*, 2007.

Hendriks, D. M. D., A. J. Dolman, M. K. van der Molen, and J. van Huissteden, A compact and stable eddy covariance set-up for methane measurements using off-axis integrated cavity output spectroscopy, *Atmospheric Chemistry And Physics*, *8*(2), 431--443, 2008.

Høye, T. T., E. Post, H. Meltofte, N. M. Schmidt, and M. C. Forchhammer, Rapid advancement of spring in the High Arctic, *Current Biology*, *17*(12), R449--R451, 2007.

Joabsson, A., T. R. Christensen, and B. Wallen, Vascular plant controls on methane emissions from northern peatforming wetlands, *Trends In Ecology & Evolution*, *14*(10), 385--388, 1999.

Kanemasu, E. T., W. L. Powers, and J. W. Sij, Field Chamber Measurements of CO_2 Flux From Soil Surface, *Soil Science*, *118*, 233--237, 1974.

Laidre, K. L., I. Stirling, L. F. Lowry, O. Wiig, M. P. Heide-Jorgensen, and S. H. Ferguson, Quantifying the sensitivity of arctic marine mammals to climate-induced habitat change, *Ecological Applications*, *18*(2), S97--S125, 2008.

Lloyd, C. R., W. J. Shuttleworth, J. H. C. Gash, and M. Turner, A microprocessor system for eddy-correlation, *Agricultural and Forest Meteorology*, *33*(1), 67--80, 1984.

McMillen, R. T., An eddy-correlation technique with extended applicability to non-simple terrain, *Boundary-Layer Meteorology*, *43*(3), 231--245, 1988.

Moore, T. R., and N. T. Roulet, A comparison of dynamic and static chambers for methane emission measurements from sub-arctic fens, *Atmosphere-Ocean*, *29*(1), 102--109, 1991.

Myneni, R. B., C. D. Keeling, C. J. Tucker, G. Asrar, and R. R. Nemani, Increased plant growth in the northern high latitudes from 1981 to 1991, *Nature*, *386*(6626), 698--702, 1997.

Papale, D., et al., Towards a standardized processing of Net Ecosystem Exchange measured with eddy covariance technique: algorithms and uncertainty estimation, *Biogeosciences*, *3*(4), 571--583, 2006.

Parkinson, C. L., and D. J. Cavalieri, Arctic sea ice variability and trends, 1979-2006, *Journal Of Geophysical Research-Oceans*, *113*(C7), C07,003, 2008.

Peel, M. C., B. L. Finlayson, and T. A. McMahon, Updated world map of the Köppen-Geiger climate classification, *Hydrology And Earth System Sciences*, *11*(5), 1633--1644, 2007.

Piao, S., et al., Net carbon dioxide losses of northern ecosystems in response to autumn warming, *Nature*, *451*(7174), 49--U3, 2008.

Popp, T. J., J. P. Chanton, G. J. Whiting, and N. Grant, Evaluation of methane oxidation in the rhizosphere of a Carex dominated fen in north central Alberta, Canada, *Biogeochemistry*, *51*(3), 259--281, 2000.

Post, E., and M. C. Forchhammer, Climate change reduces reproductive success of an Arctic herbivore through trophic mismatch, *Philosophical Transactions Of The Royal Society B-Biological Sciences*, *363*(1501), 2369--2375, 2008.

Randerson, J. T., C. B. Field, I. Y. Fung, and P. P. Tans, Increases in early season ecosystem uptake explain recent changes in the seasonal cycle of atmospheric CO_2 at high northern latitudes, *Geophysical Research Letters*, *26*(17), 2765--2768, 1999.

Schulze, E.-D., Soil respiration of tropical vegetation types, *Ecology*, *48*(4), 652--&, 1967.

Schuur, E. A. G., et al., Vulnerability of permafrost carbon to climate change: Implications for the global carbon cycle, *Bioscience*, *58*(8), 701--714, 2008.

Serreze, M. C., and J. A. Francis, The arctic amplification debate, *Climatic Change*, *76*(3-4), 241--264, 2006.

Serreze, M. C., et al., Observational evidence of recent change in the northern high-latitude environment, *Climatic Change*, *46*(1-2), 159--207, 2000.

Silvola, J., J. Alm, U. Ahlholm, H. Nykänen, and P. J. Martikainen, CO_2 fluxes from peat in boreal mires under varying temperature and moisture conditions, *Journal of Ecology*, *84*(2), 219--228, 1996.

Smith, T. M., R. W. Reynolds, T. C. Peterson, and J. Lawrimore, Improvements to NOAA's historical merged land-ocean surface temperature analysis (1880-2006), *Journal Of Climate*, *21*(10), 2283--2296, 2008.

Stow, D. A., et al., Remote sensing of vegetation and land-cover change in Arctic Tundra Ecosystems, *Remote Sensing of Environment*, *89*(3), 281--308, 2004.

Ström, L., M. Mastepanov, and T. R. Christensen, Species-specific effects of vascular plants on carbon turnover and methane emissions from wetlands, *Biogeochemistry*, *75*(1), 65--82, 2005.

Swinbank, W. C., The measurement of vertical transfer of heat and water vapor by eddies in the lower atmosphere, *Journal Of Meteorology*, *8*(3), 135--145, 1951.

Tarnocai, C., J. G. Canadell, E. A. G. Schuur, P. Kuhry, G. Mazhitova, and S. A. Zimov, Soil organic carbon pools in the northern circumpolar permafrost region, *Global Biogeochemical Cycles*, *23*, GB2023, 2009.

Valentini, R., G. E. S. Mugnozza, P. Deangelis, and R. Bimbi, An experimental test of the eddy correlation technique over a Mediterranean macchia canopy, *Plant, Cell and Environment*, *14*(9), 987--994, 1991.

van Huissteden, J., T. C. Maximov, and A. J. Dolman, High methane flux from an arctic floodplain (Indigirka lowlands, eastern Siberia), *Journal of Geophysical Research-Biogeosciences*, *110*(G2), G02,002, 2005.

Verma, S. B., D. D. Baldocchi, D. E. Anderson, D. R. Matt, and R. J. Clement, Eddy fluxes of CO_2, water vapor, and sensible heat over a deciduous forest, *Boundary-Layer Meteorology*, *36*(1-2), 71--91, 1986.

Verma, S. B., F. G. Ullman, D. Billesbach, R. J. Clement, J. Kim, and E. S. Verry, Eddy-correlation measurements of methane flux in a northern peatland ecosystem, *Boundary-Layer Meteorology*, *58*(3), 289--304, 1992.

Vourlitis, G. L., W. C. Oechel, S. J. Hastings, and M. A. Jenkins, A system for measuring in situ CO_2 and CH_4 flux in unmanaged ecosystems - an arctic example, *Functional Ecology*, *7*(3), 369--379, 1993.

Walter, K. M., S. A. Zimov, J. P. Chanton, D. Verbyla, and F. S. Chapin III, Methane bubbling from Siberian thaw lakes as a positive feedback to climate warming, *Nature*, *443*(7107), 71--75, 2006.

Whalen, S. C., Biogeochemistry of methane exchange between natural wetlands and the atmosphere, *Environmental Engineering Science*, *22*(1), 73--94, 2005.

Witkamp, M., Rates of carbon dioxide evolution from forest floor, *Ecology*, *47*(3), 492--&, 1966.

Zahniser, M. S., D. D. Nelson, J. B. McManus, and P. L. Kebabian, Measurement of trace gas fluxes using tunable diode-laser spectroscopy, *Philosophical Transactions of The Royal Society Of London Series A*, *351*(1696), 371--381, 1995.

Zwiers, F. W., Climate change - The 20-year forecast, *Nature*, *416*(6882), 690--691, 2002.

Chapter 3

CO_2 fluxes and evaporation on a peatland in the Netherlands appear not affected by water table fluctuations[1]

Abstract
The effect of shallow water table fluctuations on the evaporation and CO_2 fluxes in a peatland is investigated. The fluxes of evaporation and net ecosystem exchange of carbon were measured from mid-spring to end of summer in 2005 and 2006 and simulated independently with process models. The observed and modelled data were then compared along a gradient of water levels. Any variation along the gradient would imply an influence of the water table on the flux. It became evident that changes in the water table had no effect on the evaporation and CO_2 fluxes of the peatland. A probable cause could be the high water content of the soil, even for the low water tables, and the stable thermal conductivity of the soil. This study has implications for current land use management, which is aimed at reducing CO_2-emissions. Regulations are currently concerned with water table while this study shows that soil water content should be focused on as well.

3.1 Introduction

Peatlands cover around 3.5 x 10^6 km^2 globally and store around 455 Pg of carbon (*Gorham*, 1991) or one-third of the total carbon stored in soils. Changes in fluxes from this pool are therefore an important factor in the global carbon cycle. Accumulation of carbon takes place as plants sequester carbon from the atmosphere through photosynthesis and dead organic matter is transferred to the peat. Release of carbon occurs when the dead organic matter is metabolized by bacteria into CO_2 in the unsaturated zone. Together with the CO_2 release

[1]The content of this chapter has been published as Parmentier et al., CO_2 fluxes and evaporation on a peatland in the Netherlands appear not affected by water table fluctuations, Agricultural and Forest Meteorology (2009) vol. 149 (6-7) pp. 1201-1208

by plants, also called dark respiration, this comprises the ecosystem respiration. In peatlands respiration is mostly lower than photosynthesis and thus a net accumulation of carbon occurs. Below the water table bacteria are unable to metabolize the organic matter into CO_2 because of the lack of oxygen. Under these anaerobic conditions, the removal of carbon occurs by methanogenic bacteria that process substrate into CH_4. When this gas travels up through the unsaturated zone, methanotrophic bacteria oxidize part or all of the CH_4, converting it to CO_2. The balance between ecosystem respiration, photosynthesis and net methane emissions thus determines whether a peatland is a sink or a source for greenhouse gases.
Taking this into account, it is intuitive that carbon fluxes of peatlands should be controlled by water table. A low water table will increase respiration and reduce methane emissions while a high water table will reduce respiration but increase methane emissions (*Bubier*, 1995; *Christensen et al.*, 1995). And although this effect has been reproduced for methane emissions (*Moore and Roulet*, 1993; *Updegraff et al.*, 2001; *van Huissteden et al.*, 2005), past research has lead to conflicting results on the effect of the water table on ecosystem respiration (*Lloyd*, 2006).
For example (*Silvola et al.*, 1996) investigated the influence of water table on CO_2 fluxes and found a clear relation. A lowering of the water table with just 1 cm led to an increase of 7.1 mg CO_2 m^{-2} h^{-1} and a linear relation for the first 30-40 cm of drawdown was shown. (*Oechel et al.*, 1998) also found water table to have a large influence on the carbon fluxes of a peatland. In a laboratory study a lowering of the water table by just 10 cm changed the soils from a small sink into a large source in just 80 days. Although these and other studies acknowledge the influence of temperature on ecosystem respiration, they generally agree that water table is more important. However, other research has suggested that respiration depends more on temperature than water table. (*Lafleur et al.*, 2005) found that in their research site ecosystem respiration was very strongly correlated to changes in temperature and not to water table. This is similar to (*Updegraff et al.*, 2001) who found that respiration was only correlated to temperature and not to other measured variables. This debate has major implications on water management of peatlands, since current policy is aimed at raising the water table with the intention of increasing carbon storage and decreasing greenhouse gas emissions. If respiration is mainly controlled by temperature, a higher water table will probably have little effect on ecosystem respiration but a large effect on CH_4 emissions. In that case a higher water table would only increase greenhouse gas emissions.
In this research we aim to address this problem by quantifying the effect of groundwater fluctuations on CO_2 fluxes. Extra emphasis will be laid on the variation of soil water content and thermal properties of the soil to analyse these results. To further support the analysis, the effect of water table on evaporation is also studied. For the CO_2 fluxes this is important since high water suction in the root zone of the soil causes stomata to close and this reduces the exchange of water and CO_2 to the atmosphere. If photosynthesis is limited by water, evaporation should also diminish with low water tables.

3.2 Site description and instrumentation

The research site (52°14'25"N, 5°04'17"E) is located in the south of the Horstermeer polder, a former wetland area of about 800 ha in size that was drained in 1882. The polder is located in the centre of the Netherlands in a region that was historically used for peat excavation and is now a mosaic of lakes, land reclamations and wetlands. The local hydrology of the area is dominated by the river Vecht, to the west, and by seepage emanating from higher lain lakes,

bordering the area north and south. Average annual precipitation is 797 mm and the average temperature is 9.8 °C.
The site is located in the southern part of the polder where the water level has been raised for nature conservation purposes. Ground level is at 2.2 m below sea level and spatially the area can be split up in 10% ditches, 20% land that is saturated annually (alongside the ditches) and 70% relatively dry land with a fluctuating water table that is about 15 cm below the surface on average. Management consists only of a fixed overflow to allow water to leave the area and which prevents the site from flooding. Water enters the area only through seepage and precipitation and during drought the water table is not additionally managed. No cattle grazing or harvesting takes place, the only removal of vegetation consists of sporadic grazing by roe deer. Vegetation consists of different types of grasses (dominant species *Holcus lanatus*, *Phalaris arundinacea*, *Glyceria fluitans*), horsetail (*Equisetum palustre, fluviatile*) reeds (*Phragmites australis*, *Typha latifolia*) and high forbs (*Urtica diocia*, *Cirsium arvense, palustre*). Vegetation, litter and bare soil cover around 80, 15 and 5% of the total area, respectively. For a more elaborate description of the site we refer to (*Hendriks et al.*, 2007).

3.2.1 Hydrology and soil

Groundwater fluctuations were recorded with a pressure transducer installed in an access tube at 1 m depth in the clayey peat layer in the dry part of the site. The water levels were measured within a 60-minute time interval. In 24-hour periods, variations in water level were relatively small (within the order of 3 cm) and therefore averaged daily values were used in this study. Furthermore, the studied period was constrained to the dates shown in figure 3.1, when variations in fluxes and water level were largest but changes in leaf area index were relatively small. In addition 15 soil samples with a standard volume (100 cm^3) were taken at the root zone depth ($\sim$15 cm) and analysed in a laboratory. The samples were acclimatised at various levels of soil water suction. At each pF value the samples were weighed and a pF curve was derived for the root zone depth with a pF range of 0-2. At the same time the thermal conductivity, λ, of the samples were measured with the use of a needle probe similar to the design of (*Bristow et al.*, 2001). Changes in the thermal properties of the soil have significant impact on the energy-balance and can therefore clarify our observations. At the end of the experiment organic and mineral fractions of the samples were determined with a FlashEA 1112 C/N analyser (Thermo Fisher Scientific, Waltham, MA, USA).
The relation between soil moisture and water table fluctuations was analysed with historical water table and tensiometer (Eijkelkamp, T4, NL) data of 2002 and 2003 (see Figure 3.2). The tensiometer used to measure soil water suction was installed at the root zone depth and measured the soil suction within a 10-minute interval. This tensiometer data were used to convert water table to soil moisture values with the derived pF curve.

3.2.2 Eddy covariance

Eddy covariance measurements of CO_2 concentration, water vapour, wind speed and air temperature were performed with a Licor 7500 open path infrared gas analyser (IRGA, LI-COR, Lincoln, NE, USA) and a Windmaster Pro 3 axis Ultrasonic Anemometer (GILL Instruments Limited, Hampshire, UK). IRGA and anemometer are installed at 4.3 m above the surface. The EUROFLUX method (*Aubinet et al.*, 2000) was applied to the eddy correlation data to calculate the fluxes of momentum, sensible and latent heat and CO_2. The method of (*Nakai et al.*, 2006) was used to apply the angle of attack dependent calibration (*Gash and Dolman*,

2003; *van der Molen et al.*, 2004).
On a separate tower, incoming and reflected shortwave radiation (Kipp & Zonen, Delft, the Netherlands) and up and downward long wave radiation (Eppley Pyrgeometers, Eppley laboratory Inc., Model Precision Infrared Radiometers (PIR)) were measured. As backup of these radiation-balance measurements the net radiation was measured (Campbell Scientific, Q7). All radiometers are installed at a height of 2.5 m (except incoming long wave radiation at 1.6 m height). For a more detailed description of the equipment used at the research site, we refer again to (*Hendriks et al.*, 2007).

3.3 Methods

3.3.1 Modelling of evaporation

For a well-watered grassland, it has been shown that evaporation, LE, is only limited by radiation and vapour pressure deficit (*Priestley and Taylor*, 1972).

$$\mathrm{LE} = \alpha \frac{s}{s+\gamma} + (R_n - G) \tag{3.1}$$

Here α is the Priestley-Taylor parameter, s the slope of the saturation water vapour-temperature curve at air temperature, γ the psychometric constant, R_n the net radiation and G the soil heat flux. Since this equation only uses net radiation and air temperature, it is independent of the water table (soil heat flux is negligible on a daily scale). In this equation the Priestley-Taylor parameter usually has a value of 1.26 for a well-watered reference grass. To calculate the actual heat fluxes for our situation, the value for α was determined by optimizing the model.
The observed and modelled evaporation are then subtracted from each other and this residual is plotted as a function of the water table (DWT). If it can be shown that the observed flux is reasonably modelled without using DWT as a parameter and that the residual of modelled vs. observed fluxes is invariant with water level, we conclude that it has little or no influence on the measured fluxes.

3.3.2 Modelling of ecosystem respiration, R_{eco}

During the night photosynthesis is zero and all measured CO_2 fluxes should then be due solely to ecosystem respiration. However, when the atmosphere is stable, CO_2 fluxes may be stored below the measurement height. To avoid this problem only fluxes for nights with enough turbulence, defined by a $u^* > 0.2$ m s^{-1}, were used, which is a comfortable limit for this site (*Hendriks et al.*, 2007). This estimate of ecosystem respiration was then plotted against the soil temperature to derive a Q_{10}, according to the equation listed below:

$$R_{eco} = R_{ref} \cdot Q_{10}^{(T_{soil}/10)} \tag{3.2}$$

Here R_{eco} is the ecosystem respiration, R_{ref} the reference respiration at T = 10 °C, and T_{soil} the soil temperature integrated over the top 3 cm. This relation was then used with soil temperature data to extrapolate the respiration to the entire day. Again, model results were compared with observed data and the residuals were plotted as a function of DWT to test the

dependence of R_{eco} to water levels. If respiration is invariant from DWT no variation over the water table gradient is expected.

3.3.3 Modelling of gross primary production, GPP

We used the photosynthesis module of the vegetation model ORCHIDEE (*Krinner et al.*, 2005; *Morales et al.*, 2005), to simulate GPP one-dimensionally as a function of radiation, surface temperature, air humidity, air pressure, precipitation, CO_2 concentration and surface conductance. Precipitation was only used for determining the amount of water left on leaves after rain to determine surface conductance. No soil water dynamics were simulated and water table was not used as a variable in this model. Since the eddy covariance method only measures NEE, GPP is obtained with the use of equation 3.3:

$$\text{GPP} = \text{NEE} - R_{eco} \tag{3.3}$$

Here R_{eco} is obtained from equation 3.2. Again, like for LE and R_{eco}, the residual of observed minus modelled will be plotted against DWT. If GPP is invariant with water table, we should see no variation for the residual with DWT.

3.4 Results

3.4.1 Hydrology and soil

During the period of record, water table varied between the surface level and -51 cm in the field. The water level experiences six cycles between these two extremes (figure 3.1) and shows a high dependence on precipitation. Dry periods occur mostly in spring and summer, periods when incoming radiation is highest.
Figure 3.2 shows the relation between soil water suction and water level from the historical tensiometer data and also gives the results of the laboratory analysis of 15 soil samples that have been taken from the root zone.
From figure 3.2 we see that the observed water tables of 0 and -51 cm can be extrapolated to pF values at the root zone between 0 and 1.8. For these values of soil water suction, the volumetric water content varies from 89% to 72%. Volumetric fractions of the organic and mineral components were determined to be 3.2% ($\pm$ 1.6) and 7.7% ($\pm$ 5.2). From this figure we also see that the variation of soil thermal conductivity, λ, with observed soil water content is negligible. A one-way analysis of variance (ANOVA) indeed shows that all measurements with a V_w lower than 89% can be described by the same mean value (1.12 $\pm$ 0.15) and that only the measurement at full saturation (1.01 $\pm$ 0.08, V_w=89%) differs significantly from the other measurements. However, this difference is still relatively small.

3.4.2 Evaporation

In the left panel of figure 3.3, the performance of the evaporation model is shown. In the graph the correlation coefficient and significance are given and a 1:1 line is plotted to show model performance both numerically and visually. On the right panel the residual is shown, by subtracting modelled from observed fluxes, and these are plotted vs. water level. The value of the Priestley-Taylor parameter, α, was determined to be 0.75. Compared to the standard

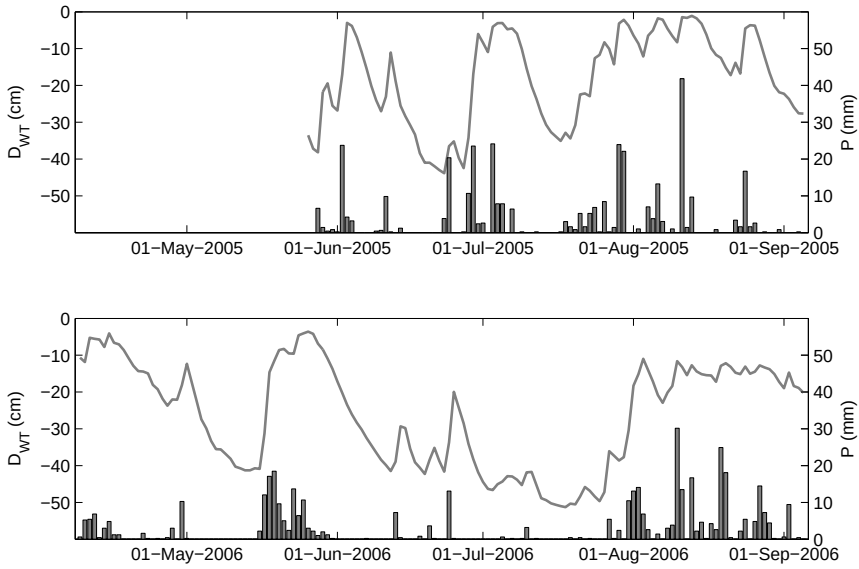

Figure 3.1: Water table and precipitation for the observed period in 2005 and 2006.

value of 1.26 this is rather low and an explanation may lie in the fact that soil heat flux was measured with a certain type of heat flux plate, which has been known to underestimate fluxes (*Sauer et al.*, 2003). Since the Priestley-Taylor parameter was determined by optimizing the model, an underestimation of G would lower our value of α. On the other hand, similar low values for α have been reported before (*Kellner*, 2001; *Petrone et al.*, 2007).
From this figure we see that the model for evaporation, LE, performs well and that the residual of observed and modelled values showed no significant correlation with water level.

3.4.3 CO_2 fluxes

In figure 3.4, the models for ecosystem respiration, R_{eco}, and gross primary production, GPP, are given in the same way as for evaporation. On the left model performance is given, again with the correlation coefficient and a 1:1 line while on the right side the remaining variance is plotted as a function of water level.
Both models for R_{eco} and GPP show good model performance. When the residual is plotted against water level we see no significant variation. Correlation coefficients are near zero and significance is low.

3.5 Discussion

The models of evaporation and CO_2 fluxes all performed well for this site. For evaporation the graph of the residual vs. water table showed that any variation left in the signal was uncorrelated with DWT and thus evaporation is independent from the water table. An explanation

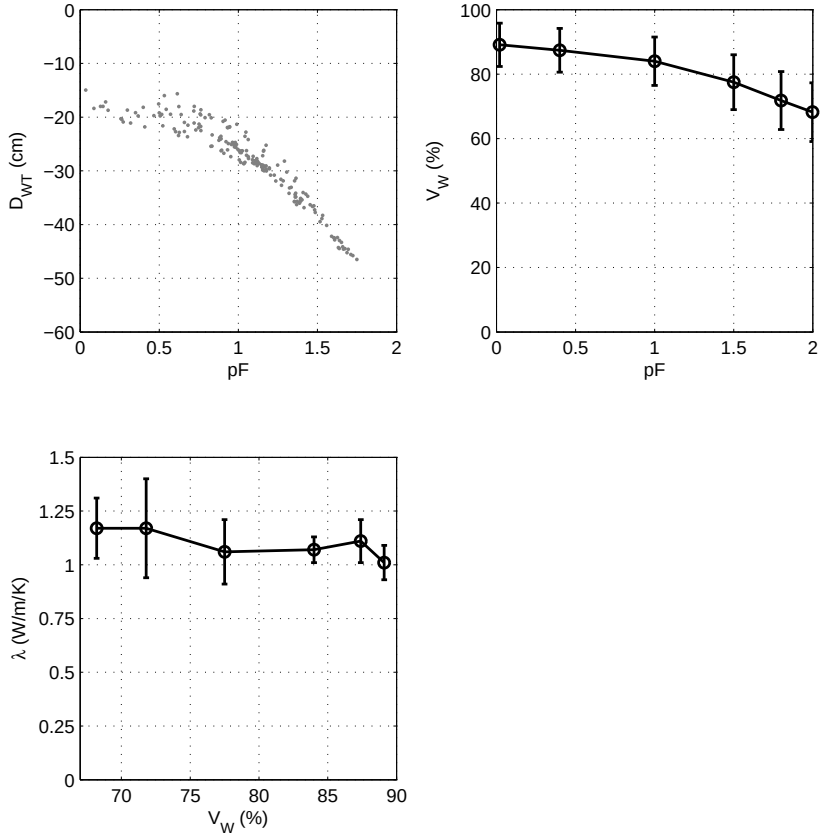

Figure 3.2: (a) Daily values of pF at the root zone depth vs. the water table, measured from July 2002 to July 2003. (b) V_w of the 15 soil samples from the root zone with applied soil water suction in pF. (c) Measured values for thermal conductivity (λ) of the soil against volumetric water content, V_w.

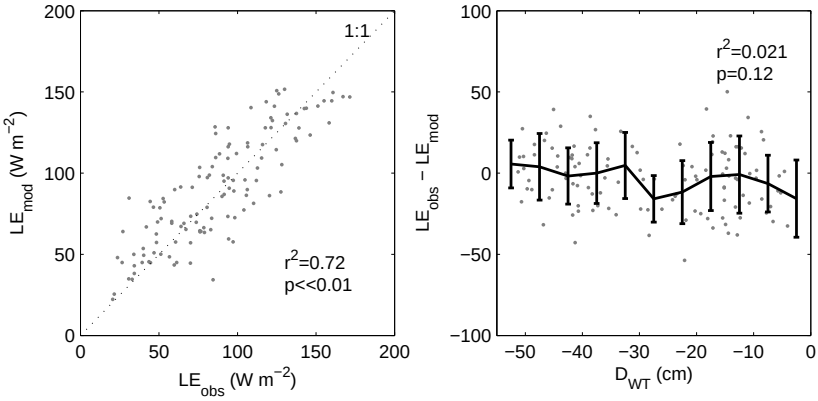

Figure 3.3: Model results for evaporation. The left panel shows model performance by giving the r^2 value with significance and a 1:1 plot. On the right the residual of observed vs. modelled evaporation are plotted against water table with r^2 values and significance. A binned average is added for clarity.

for this result comes from the soil analysis and the knowledge that vegetation cover is very high for this site, thus dominating LE. Figure 3.2 shows that even for low water levels, the volumetric water content of the soil at the root zone remains high. V_w lowers from 89% to 72% in the observed extremes for this study. When converting these values to soil water suction, we see that the highest observed pF was 1.8. For these pressures, soil water is still readily available to plants and not a limiting factor on transpiration (*Kramer*, 1983). Furthermore, the lack of variation of LE with DWT is independently confirmed by our analysis of the thermal conductivity of the soil. It has been shown that λ did not change along the observed gradient of soil water content. This means that the amount of energy that can be transferred to the soil and be made available for evaporation was also not affected by changes in the water table (*Milly*, 1984). Together with the high water content of the soil this explains why LE did not change with water table changes.

It was further shown that R_{eco} and GPP did not vary with DWT. As explained earlier from the results of the soil analysis, water availability and thermal properties of the soil did not change enough to limit GPP, which was therefore constricted by other factors such as radiation and air temperature. The findings for R_{eco} are consistent with prior research that also found temperature to be more important than water table (*Lafleur et al.*, 2005; *Updegraff et al.*, 2001).

However, there are also many studies that have found contrary results (*Lloyd*, 2006; *Tenhunen et al.*, 1995). An explanation could be that R_{eco} is mostly studied in relation to the water table while the majority of the studies lack to report the associated soil water content. The studies that do report soil water content showed that R_{eco} does vary along a soil moisture content gradient (*Flanagan and Johnson*, 2005; *Lafleur et al.*, 2005). Furthermore, (*Jacobs et al.*, 2007), who compared peatlands in the Netherlands, found a temperature relation for all sites but large differences in base respiration between sites. This difference and the remaining scatter in the Q_{10} fit was suggested to be due to soil moisture differences. It is therefore still likely that a lowering of the water table will have an effect on ecosystem respiration if this lowering is persistent and thus results in a lowering of the soil moisture content. In the current research, variations in water table are relatively large but variations in soil water content are relatively

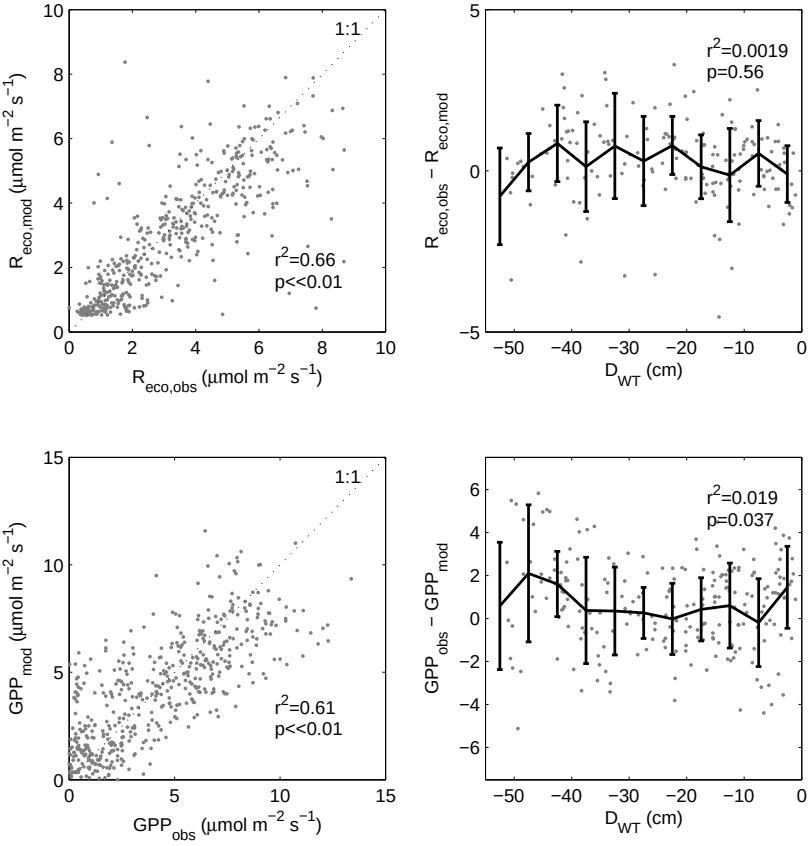

Figure 3.4: Model results for the CO_2 fluxes. The left panels show model performance by giving the r^2 value with significance and a 1:1 plot. On the right the residual of observed vs. modelled flux are plotted against water table with r^2 values and significance. A binned average is added for clarity.

small. The low dependency on water table could thus be explained by the small variation in soil water content.
As a final check on these results we assessed the contribution of a possible hysteresis effect of a lowering vs. a rising water table. The residual of modelled minus observed fluxes were plotted against the change in water level by calculating the slope of the graph in figure 3.1. These results gave no distinct relationship (r^2 of about 0.05 or smaller) and therefore hysteresis effects are not likely to have influenced these results.

3.6 Conclusion

In this study, evaporation and CO_2 fluxes of a peatland could be well modelled without water table as a parameter. Earlier studies have shown that CO_2 fluxes may vary with water table (*Oechel et al.*, 1998; *Silvola et al.*, 1996; *Tenhunen et al.*, 1995) while other studies have found contrary results (*Lafleur et al.*, 2005; *Updegraff et al.*, 2001). We address this inconsistency by showing that the water table can lower significantly with little change in soil water content and that soil water suction in the root zone does not become critical for plants. Evaporation therefore did not diminish and photosynthesis and ecosystem respiration were not affected by water table. This observation was further supported by showing that thermal conductivity of the soil did not change with a lowering of the water table, restricting the influence of the water table on heat fluxes.
This study does not refute the fact that changes have been observed for CO_2 fluxes with different water tables by other researchers. However, it is possible that the conflicting conclusions on the controlling factors of respiration are caused by different changes in soil moisture content and soil water suction with the same water table drawdown due to different hydraulic conductivity of the soils at the studied sites. In soil types with high water retention, like our site, changes in soil water content will be relatively small and slow compared to the changes in the water table. Due to the enduring wet soil conditions, changes in respiration will therefore be more controlled by temperature than by water table. On the other hand, in soil types with low water retention capacity, changes in soil water level have a direct effect on soil water content. Ecosystem respiration will therefore show more variation with changing water levels in those types of systems. Unfortunately many studies on the relation between water and carbon fluxes only consider water table and give little or no information about soil water content or soil water suction (*Funk et al.*, 1994; *Moore and Dalva*, 1993; *Updegraff et al.*, 2001; *Laine et al.*, 2007). We therefore suggest that soil moisture content and water suction changes should be included in further studies on the interaction between water and the energy- or carbon-balance to better compare between different sites.
This finding might also have implications on land use management that is focused on reducing CO_2-emissions by raising the water table. Although this is a practical parameter to control from a policy point of view, it is arguably not the single best parameter to determine a reduction in greenhouse gas emissions due to the heterogeneity in hydrology between sites. If ecosystem respiration is controlled more by soil moisture content than by water level, a rise in water level will only reduce respiration in those sites where a significant increase from lower to higher soil moisture content is to be expected. If the relative change in soil moisture content is small, no large effect on ecosystem respiration is likely.
At the same time CH_4-emissions will surely be increased with a high water table (*Moore and Roulet*, 1993; *Hendriks et al.*, 2007). Since CH_4 is 23 times stronger as a greenhouse gas (*Forster et al.*, 2007) this means that the raising of the water table with the intent of reducing

greenhouse gas emissions could be less straightforward than was previously assumed. In theory it is conceivable that this will even lead to an increase in net greenhouse gas emissions and a rise in water table should therefore be considered wisely. On the other hand, a low water table combined with low soil moisture content will certainly, as shown by previous research, turn peatlands into a source of carbon. Therefore, when altering the hydrology of a peatland with the intent of reducing greenhouse gas emissions, soil moisture content can be a valuable additional tool to find the optimal balance between CO_2 uptake and CH_4-emissions.

References

Aubinet, M., et al., Estimates of the annual net carbon and water exchange of forests: The EUROFLUX methodology, *Advances In Ecological Research, Vol 30*, *30*, 113--175, 2000.

Bristow, K. L., G. J. Kluitenberg, C. J. Goding, and T. S. Fitzgerald, A small multi-needle probe for measuring soil thermal properties, water content and electrical conductivity, *Computers and Electronics in Agriculture*, *31*(3), 265--280, 2001.

Bubier, J. L., The relationship of vegetation to methane emission and hydrochemical gradients in northern peatlands, *Journal of Ecology*, *83*(3), 403--420, 1995.

Christensen, T. R., S. Jonasson, T. V. Callaghan, and M. Havstrom, Spatial variation in high-latitude methane flux along a transect across siberian and european tundra environments, *Journal Of Geophysical Research-Atmospheres*, *100*(D10), 21,035--21,045, 1995.

Flanagan, L. B., and B. G. Johnson, Interacting effects of temperature, soil moisture and plant biomass production on ecosystem respiration in a northern temperate grassland, *Agricultural and Forest Meteorology*, *130*(3-4), 237--253, 2005.

Forster, P., et al., Changes in Atmospheric Constituents and in Radiative Forcing, *Climate Change 2007: The Physical Science Basis. Contribution of Working Group I to the 4th Assessment Report of the Intergovernmental Panel on Climate Change [Solomon, S., D. Qin, M. Manning, Z. Chen, M. Marquis, K.B. Averyt, M.Tignor and H.L. Miller (ed*, 2007.

Funk, D. W., E. R. Pullman, K. M. Peterson, P. M. Crill, and W. D. Billings, Influence of water table on carbon dioxide, carbon monoxide and methane fluxes from taiga bog microcosms, *Global Biogeochemical Cycles*, *8*(3), 271--278, 1994.

Gash, J. H. C., and A. J. Dolman, Sonic anemometer (co)sine response and flux measurement I. The potential for (co)sine error to affect sonic anemometer-based flux measurements, *Agricultural and Forest Meteorology*, *119*(3-4), 195--207, 2003.

Gorham, E., Northern peatlands - role in the carbon-cycle and probable responses to climatic warming, *Ecological Applications*, *1*(2), 182--195, 1991.

Hendriks, D. M. D., J. van Huissteden, A. J. Dolman, and M. K. van der Molen, The full greenhouse gas balance of an abandoned peat meadow, *Biogeosciences*, *4*(3), 411--424, 2007.

Jacobs, C. M. J., et al., Variability of annual CO_2 exchange from Dutch grasslands, *Biogeosciences*, *4*(5), 803--816, 2007.

Kellner, E., Surface energy fluxes and control of evapotranspiration from a Swedish Sphagnum mire, *Agricultural and Forest Meteorology*, *110*(2), 101--123, 2001.

Kramer, P. J., Water Relations of Plants - Chapter 4: Soil and Water, *Water Relations of Plants*, 1983.

Krinner, G., N. Viovy, N. de Noblet-Ducoudré, J. Ogée, J. Polcher, P. Friedlingstein, P. Ciais, S. Sitch, and I. C. Prentice, A dynamic global vegetation model for studies of the coupled atmosphere-biosphere system, *Global Biogeochemical Cycles*, *19*(1), GB1015, 2005.

Lafleur, P. M., T. R. Moore, N. T. Roulet, and S. Frolking, Ecosystem respiration in a cool temperate bog depends on peat temperature but not water table, *Ecosystems*, *8*(6), 619--629, 2005.

Laine, A., K. A. Byrne, G. Kiely, and E.-S. Tuittila, Patterns in vegetation and CO_2 dynamics along a water level gradient in a lowland blanket bog, *Ecosystems*, *10*(6), 890--905, 2007.

Lloyd, C. R., Annual carbon balance of a managed wetland meadow in the Somerset Levels, UK, *Agricultural and Forest Meteorology*, *138*(1-4), 168--179, 2006.

Milly, P. C. D., A Simulation Analysis of Thermal Effects on Evaporation From Soil, *Water Resources Research*, *20*(8), 1087--1098, 1984.

Moore, T. R., and M. Dalva, The influence of temperature and water-table position on carbon-dioxide and methane emissions from laboratory columns of peatland soils, *Journal of Soil Science*, *44*(4), 651--664, 1993.

Moore, T. R., and N. T. Roulet, Methane flux: Water table relations in northern wetlands, *Geophysical Research Letters*, *20*(7), 587--590, 1993.

Morales, P., et al., Comparing and evaluating process-based ecosystem model predictions of carbon and water fluxes in major European forest biomes, *Global Change Biology*, *11*(12), 2211--2233, 2005.

Nakai, T., M. K. van der Molen, J. H. C. Gash, and Y. Kodama, Correction of sonic anemometer angle of attack errors, *Agricultural and Forest Meteorology*, *136*(1-2), 19--30, 2006.

Oechel, W. C., G. L. Vourlitis, S. J. Hastings, R. P. Ault, and P. Bryant, The effects of water table manipulation and elevated temperature on the net CO_2 flux of wet sedge tundra ecosystems, *Global Change Biology*, *4*(1), 77--90, 1998.

Petrone, R. M., U. Silins, and K. J. Devito, Dynamics of evapotranspiration from a riparian pond complex in the Western Boreal Forest, Alberta, Canada, *Hydrological Processes*, *21*(11), 1391--1401, 2007.

Priestley, C. H. B., and R. T. Taylor, On the assessment of surface heat-flux and evaporation using large-scale parameters, *Monthly Weather Review*, *100*(2), 81--&, 1972.

Sauer, T. J., D. W. Meek, T. E. Ochsner, A. R. Harris, and R. Horton, Errors in Heat Flux Measurement by Flux Plates of Contrasting Design and Thermal Conductivity, *Vadose Zone Journal*, *2*(4), 580--588, 2003.

Silvola, J., J. Alm, U. Ahlholm, H. Nykänen, and P. J. Martikainen, CO_2 fluxes from peat in boreal mires under varying temperature and moisture conditions, *Journal of Ecology*, *84*(2), 219--228, 1996.

Tenhunen, J. D., C. T. Gillespie, S. F. Oberbauer, A. Sala, and S. Whalen, Climate effects on the carbon balance of tussock tundra in the Philip-Smith-Mountains, Alaska, *Flora*, *190*(3), 273--283, 1995.

Updegraff, K., S. D. Bridgham, J. Pastor, P. Weishampel, and C. Harth, Response of CO_2 and CH_4 emissions from peatlands to warming and water table manipulation, *Ecological Applications*, *11*(2), 311--326, 2001.

van der Molen, M. K., J. H. C. Gash, and J. A. Elbers, Sonic anemometer (co)sine response and flux measurement - II. The effect of introducing an angle of attack dependent calibration, *Agricultural and Forest Meteorology*, *122*(1-2), 95--109, 2004.

van Huissteden, J., T. C. Maximov, and A. J. Dolman, High methane flux from an arctic floodplain (Indigirka lowlands, eastern Siberia), *Journal of Geophysical Research-Biogeosciences*, *110*(G2), G02,002, 2005.

Chapter 4

The role of endophytic methane oxidizing bacteria in submerged *Sphagnum* in determining methane emissions of Northeastern Siberian tundra[1]

Abstract
The role of the microbial processes governing methane emissions from tundra ecosystem is receiving increasing attention. Recently, cooperation between methanotrophic bacteria and submerged *Sphagnum* was shown to reduce methane emissions but also to supply CO_2 for photosynthesis for the plant. Although this process was shown to be important in the laboratory, the differences that exist in methane emissions from inundated vegetation types with or without *Sphagnum* in the field have not been linked to these bacteria before.
In this study, chamber flux measurements, an incubation study and flux modeling were used to investigate the drivers and controls on the relative difference in methane emissions between a submerged *Sphagnum*/sedge vegetation and an inundated sedge vegetation without *Sphagnum*. It was found that methane emissions in the *Sphagnum* dominated vegetation type were 50% lower than in the vegetation type without *Sphagnum*. A model sensitivity analysis showed that these differences could not sufficiently be explained by differences in methane production and plant transport.
The model, combined with an incubation study, indicated that methane oxidation by endophytic bacteria, living in cooperation with submerged *Sphagnum*, plays a significant role in methane cycling at this site. This result is important for spatial upscaling spatially as oxidation by these bacteria plays a large role in 15% of the net methane emissions at this tundra site. Our findings support the notion that methane oxidizing bacteria are an important factor in understanding the processes behind methane emissions in tundra.

[1]The content of this chapter has been submitted as "The role of endophytic methane oxidizing bacteria in submerged *Sphagnum* in determining methane emissions of Northeastern Siberian tundra" to Biogeosciences

4.1 Introduction

Improved understanding of the controls and drivers of tundra methane emissions is important in the study of the global carbon cycle. While the cold tundra climate and the wet character of its soils have both led to a large buildup of carbon (*Post et al.*, 1982; *Tarnocai et al.*, 2009), these same wet soils are also a source of methane (*Corradi et al.*, 2005; *van der Molen et al.*, 2007; *Wille et al.*, 2008), the second most important greenhouse gas (*Frolking et al.*, 2006). It has been hypothesized that these emissions might increase under a warmer climate (*Zhuang et al.*, 2004; *McGuire et al.*, 2009), and therefore an improved understanding of the biogeochemical functioning of tundra is needed to better appreciate its response to these changes.
Methane is formed by archaea below the water table, in the anoxic part of the soil as the final step in the series of processes that degrade organic matter (*Whalen*, 2005). The methane produced is then either emitted to the atmosphere or oxidized to CO_2 above the water table in the aerated part of the soil by other microorganisms. The balance of production and oxidation therefore determines the amount of methane emitted by the ecosystem. For example, if the aerated part of the soil is deep enough, and the oxidation zone large, most or all of the methane can be consumed (*Whalen and Reeburgh*, 1990). On the other hand, methane emissions are at their highest when the water table is situated close to or at the surface.
In tundra, these wet areas tend to be dominated by sedges such as *Eriophorum* spp., *Carex* spp. and mosses such as *Sphagnum* spp. The vascular plants in this vegetation type further facilitate a release of methane through their aerenchyma that provide a direct pathway to the atmosphere, bypassing oxic zones in the soil where methane would normally be oxidized (*Joabsson and Christensen*, 2001; *Greenup et al.*, 2000; *Christensen et al.*, 2003; *Ström et al.*, 2005). However, this plant structure also increases the transfer of oxygen into the soil, which can lead to significant oxidation of methane at the rhizosphere (*Popp et al.*, 2000; *Whalen*, 2005). However, there have also been studies that show that little or no oxidation can occur in the sedges *Eriophorum angustifolium* and *Eriophorum vaginatum* (*Frenzel and Rudolph*, 1998). Furthermore, vegetation also influences the quality of substrate that is available for carbohydrate oxidation. Methane production is higher in the presence of more labile carbon than with dominantly stable organic matter and it has been shown that sedges such as *Eriophorum* spp. provide fresh substrate through their roots, which is then converted into methane (*Ström et al.*, 2005).
In contrast to the higher fluxes in the presence of vascular plants, it has been shown that methane emissions are lower in areas that have a *Sphagnum* cover (*Hines et al.*, 2008). This has mostly been contributed to the low coverage of vascular plants in these areas, limiting plant transport of methane from the anoxic zone to the atmosphere. It has also been found that oxidation of methane is particularly high in *Sphagnum* (*Vecherskaya et al.*, 1993; *Sundh et al.*, 1995).
Recently it has been shown that oxidation in *Sphagnum* can also occur below the water table by a cooperation between methanotrophic bacteria and *Sphagnum* (*Raghoebarsing et al.*, 2005). In this cooperation, the plant provides oxygen which allows the bacteria to oxidize methane into CO_2, which is then returned to the plant to be used for photosynthesis. Furthermore, it has been shown that methane derived carbon in *Sphagnum* can be as high as up to 35% (*Kip et al.*, 2010) and this system could thus explain the high carbon burial found in *Sphagnum* peatlands. These methanotrophic endophytes are very common around the world (*Kip et al.*, 2010), with varying rates of oxidation. However, there are very few studies that relate field observations of methane emissions from submerged *Sphagnum* to this specific

type of bacteria since most studies on the spatial variations of methane fluxes focus on water level, NPP, vascular plant cover or oxidation in the aerated part of *Sphagnum* (*Fechner and Hemond*, 1992; *Bubier*, 1995; *Frenzel and Rudolph*, 1998; *Greenup et al.*, 2000; *Joabsson and Christensen*, 2001; *Christensen et al.*, 2003; *Kutzbach et al.*, 2004; *Basiliko et al.*, 2004; *Ström et al.*, 2005; *Minkkinen and Laine*, 2006; *Hines et al.*, 2008), while oxidation in inundated areas with *Sphagnum* vegetation is much less studied (*Kip et al.*, 2010; *Larmola et al.*, 2010). Field studies in the Siberian Arctic are virtually not known due to logistical constraints. In this paper, we compare two inundated vegetation types in Northeastern Siberian tundra and show that methane emissions are significantly lower in a submerged *Sphagnum*/sedge vegetation type, in comparison to sedge vegetation with no *Sphagnum* presence, and ascertain that oxidation in submerged *Sphagnum* likely attributes to this difference.

4.2 Materials and Methods

4.2.1 Study site

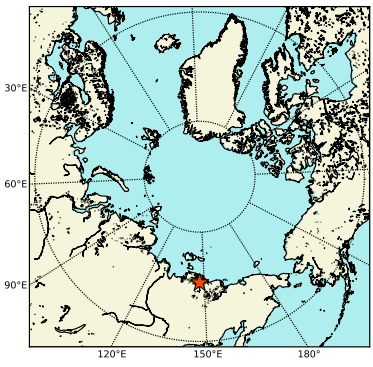

Figure 4.1: Location of the research site within Northeastern Siberia

The study site is located in the nature reserve 'Kytalyk' in Northeastern Siberia (70°49'44.9" N, 147°29'39.4" E), about 30 km NW from the town of Chokurdakh in the Sakha Republic (Yakutia), Russian Federation (as shown in Figure 4.1). While this location is extremely remote, only reachable by air during most of the year and few carbon cycling studies have been performed previously in the region, this makes it an ideal and unique area for studying pristine and undisturbed tundra. The research area itself is situated in a former thermokarst lake that drained in the past when it was intersected to the south by the Berelekekh (Yelon) river, a tributary to the Indigirka river. The floodplain along the river and the former lakebed have different vegetation, soil and hydrology. Measurements in this research focus on the tundra terrace, in the former lakebed.

The climate is cold and continental with an average annual temperature of -10.5°C and extremes as low as -25 to -45°C in winter and 5 to 25°C in summer. Snowmelt usually occurs at the start of June and while most snow is gone in mid June, bud break does not occur before the end of June or early July, together with the first warm days of the year. Since half way through September temperatures start to drop below zero again, the growing season is limited to the months of July and August. Summer temperatures are highly variable due to the large contrast between winds from the North and South. Northern winds blow cold air from the East Siberian sea (approx. 100 km away) while Southern winds bring hot summer air from the Siberian interior. This dependency on wind direction also means that the daily air temperature can drop by as much as 20°C in just two days if the wind direction changes from South to North. Since methane emissions are sensitive to temperature change, this also

Table 4.1: Description of the studied vegetation classes

Code	Site class	Soil	Water table	Vegetation	Vascular plant cover
TW1	depression, diffuse drainage	organic on mineral	0-15 cm	*Eriophorum angustifolium*, *Carex aquatilis*	40% to 90%
TW4	low polygon centre, other depressions	organic	0-10 cm	*Sphagnum*, *Eriophorum angustifolium*, *Carex aquatilis*, *Comarum palustre*	20% to 30%

has an obvious effect on emissions on the short-term.
Annual precipitation is about 200 to 250 mm with approximately half of it falling as rain during the growing season. The other half falls in the rest of the year, mostly as snow. Although this amount of precipitation is similar to the yearly total in semi-arid areas, total evaporation is much lower and thus the soil remains very wet and plenty of water is available for plant growth.
The vegetation is classified as graminoid tundra (tussock-sedge, dwarf shrub, moss tundra, cf. circumpolar arctic vegetation map (*Walker et al.*, 2005)). The spatial heterogeneity of the vegetation is related to the presence of ice-wedge polygon micro-topography leading to differences in soil water saturation. The higher and drier parts are dominated by either *Betula nana* and *Salix pulchra* dwarf shrubs with mosses or *Eriophorum vaginatum* hummocks interspersed with *Salix pulchra* dwarf shrubs and mosses. Towards the center of a polygon soil conditions get wetter; *Betula nana* is no longer present and *Salix pulchra* cover gets more sparse while *Sphagnum* spp. cover increases and *Carex aquatilis* and *Eriophorum angustifolium* appear. Dominant *Sphagnum* species include *S. balticum*, *S. compactum*, *S. subsecundum* and *S. squarrosum*. The center, lowest part of polygons are usually inundated and vegetation is dominated by *Carex aquatilis* and *Eriophorum angustifolium* while *Sphagnum* spp. cover is largely reduced or absent. Similar vegetation exists at the edges of ponds that are created by melting ice wedges, although transitions can be more abrupt. A more elaborate site description and comparison with other sites has previously been given by *van Huissteden et al.* (2005) and *van der Molen et al.* (2007).

4.2.2 Methane flux measurements

To find areas that were suitable for comparison, the vegetation at each measurement location was classified according to vegetation, geomorphology and water availability as described by *van Huissteden et al.* (2005). This classification identifies 12 different classes. Of these 12, the vegetation types TW1 and TW4, as described in Table 4.1, were used to compare between plots with and without *Sphagnum*. These vegetation types are responsible for almost all methane emissions of the tundra terrace and both are usually inundated, which means there is no aerated part of the soil or *Sphagnum* layer. TW1 is a vegetation type dominated by *Eriophorum angustifolium* and *Carex aquatilis* (typical cover of 40 to 95%), where *Sphagnum* is mostly absent. TW4 is a vegetation type that is dominated by *Sphagnum* (cover of 50 to 100%) but a substantial amount of vascular plants such as *Carex aquatilis*, *Eriophorum angustifolium* and *Comarum palustre* remain (typical cover of 20 to 30%). This difference in vascular plant cover is possibly due to competition between *Sphagnum* and vascular plants, resulting in a lower cover of the latter (*Heijmans et al.*, 2002).
The other ten classes were not considered here since they either referred to dry vegetation types with a water table below the surface or to areas with *Sphagnum* where the water table

was below the top of the *Sphagnum*. Furthermore, the study of *van Huissteden et al.* (2005) also reported high methane emissions from the floodplain along the river but in this area no *Sphagnum* is present and since hydrology, soil and vegetation are completely different from the tundra terrace, these vegetation types were not included in the comparison.
Measurements were performed on 5 plots of the TW1 vegetation type and 4 plots of the TW4 vegetation type, for which the spatial variation of vegetation within each class was taken into account visually. The plots were located in close vicinity to each other, often only separated by a few meters. Furthermore, only those measurement days were selected where both vegetation types were inundated, to avoid differences in the measured fluxes due to oxidation of methane in the aerated part of the soil or *Sphagnum* layer.
Chamber flux measurements were performed in the summer of 2007 between July 18 and August 6 with the use of an INNOVA 1412 Photoacoustic field Gas-monitor (LumaSense Technologies A/S, Ballerup, Denmark), following the same measuring practice as described in *van Huissteden et al.* (2005). Each day the same 9 plots, situated along a boardwalk, were measured, to avoid the occurrence of variations in the measurements due to spatial differences. For each measurement point, a plastic collar of 30 cm in diameter and 10 cm in height was placed carefully in the top soil with a 14 dm^3 dark plastic chamber on top. A water lock was used in between the chamber and collar to prevent gas leakage. For 8 minutes, methane concentrations were measured 5 times with a 2-minute interval. The measurement was kept this short to make sure that the air in the chamber would not warm up too much and this was further monitored with the use of a small thermometer inside the chamber. Also, the sampled air was first passed through a tube containing soda lime and a silica gel, which removed CO_2 and reduced water vapor concentrations, to prevent cross-interference at high concentrations. Fluxes were determined by linear interpolation of the measurements, accounting for air temperature, air pressure and, if there was standing water above the surface, also for reduced air volume in the chamber. Quality control was done by calculating the root mean square error (RMSE) of the linear regression. A high RMSE would occur in the case of a non-linear increase of concentration, in which case the measurement would have to be rejected, although this did not occur for the studied period and vegetation types. In some cases the total change in concentration would be very low (< 1 ppm) and erratic in behavior, due to the measurement accuracy of the device (0.4 ppm). In these cases fluxes could not be determined accurately and because the possibility of some leakage cannot be excluded fully (although unlikely), these measurements were excluded to avoid biased means. Together with each flux measurement, the water table level, thickness of the active layer and soil temperatures at 0, 10 and 20 cm were also measured.

4.2.3 Incubation study

In July 2008, two additional sites, NS1 and NS2, with a similar vegetation distribution as the TW4 flux sites, were selected for sampling *Sphagnum*. This sampling was done outside the measurement plots to avoid disturbance, allowing for future measurements in those plots. The samples were brought back to the Netherlands in closed plastic bags and kept cool as much as possible. During transits by airplane they were no longer than 20 hours without active cooling. Incubation experiments were performed in September 2008. While flux measurements were performed in the previous year, *van Huissteden et al.* (2005) showed, by using a roving method throughout the studied area in the years preceding this study, that the difference between the studied vegetation types is quite similar between years.

Potential methane-oxidizing activity was measured by incubating whole *Sphagnum* plants, 20 grams of moist mass, in a 120 ml serum bottle sealed with airtight grey butyl rubber stoppers and aluminum caps. Before incubation, the *Sphagnum* plants were thoroughly washed 3 times with sterile demineralized water. 1 ml of methane (100% pure, Air Liquide, the Netherlands) was added to each flask and the methane concentration in the flasks was measured on a HP 5890 gas chromatograph equipped with a flame ionization detector and a Porapak Q column (100/120 mesh). The methane oxidizing activity test was performed in triplicate on ice and at 4, 10 and 20°C in the dark. Following the incubations, the *Sphagnum* mosses were dried in a vacuum stove at 70°C to determine the dry weight.
Oxidation rates were determined at three separate stages. The initial methane oxidation rate, rate 1, is measured between 0 and 18.5 hours, the second methane oxidation rate is determined between 20 and 46 hours, after adding new methane, and the last methane oxidation rate, rate 3, is determined after 46 hours when all the samples were incubated on ice. Since no peat bog water sample was available, the first wash water served as a control. Methane concentrations in the bottles were measured every hour or every day depending on the activity, while methane oxidation rates were determined by regression analysis of the data points that show a linear methane oxidation.
The obtained oxidation rates are determined in μmol CH_4 gDW^{-1} day^{-1}, while fluxes in the field are measured in mg CH_4 m^{-2} hr^{-1} and this makes it difficult to compare the two rates. Ideally, the two could be compared by multiplying with the amount of dry weight of *Sphagnum* per m^2. However, oxidation rates from the incubation study were determined under ideal conditions with an ample supply of methane and oxygen, which is unlikely to be the case for field conditions, and concentrations may vary vertically in the field. Nonetheless, by multiplying the incubation rates with the amount of dry weight of *Sphagnum* per m^2, an indication will be given whether the optimal oxidation rates from the laboratory are in the same order of magnitude as in the field. If this arguably crude translation of fluxes from the laboratory to the field shows us lower rates than the observed differences, we know that these differences must be due to other factors than oxidation alone. Notably, the reverse does not necessarily hold true but provides a picture of potential oxidation under ideal circumstances. To apply this crude method, four 0.25 m^2 plots, with the TW4 vegetation type, were selected and all *Sphagnum* was collected. This *Sphagnum* was dried in an oven for a week at 60°C and weighed afterwards. This weight was used to calculate optimal oxidation rates in mg CH_4 m^{-2} hr^{-1}.

4.2.4 Flux modeling

While fast export of plant material allowed for an incubation study, the logistics at the remote location of this research site, combined with local legislative rules, severely limited the possibilities for exporting soil samples or monoliths, performing isotope studies or inhibiting methane oxidation with CH_2F_2. To overcome these limitations and to identify which parameters would best explain the differences observed, a process model was applied to model methane fluxes of both vegetation types. Methane fluxes from the Kytalyk site have been modeled by *Petrescu et al.* (2008) and *van Huissteden et al.* (2009) using the PEATLAND-VU model that includes a version of the *Walter and Heimann* (2000) wetland CH_4 flux model (*van Huissteden et al.*, 2006).
To show how sensitive the model was to each parameter, the GLUE method (General Likelihood Uncertainty Analysis, e.g. *Beven* (2008)) by *van Huissteden et al.* (2009) was applied.

In the GLUE method, a large number of model runs are done with randomly selected values for the studied parameters. The results of each run are compared with measurement data and an objective function is calculated that indicates the model fit. Here, 2000 runs were used, which were compared with the measurement data for TW1 and TW4. The distribution of objective function values vs. parameter values shows how sensitive the model performance is to different values for each parameter. We assume that a distinct clustering of high objection function values within a certain range of parameter values represents an approximation of the true values, given the model structure.
We used the Nash-Sutcliffe efficiency for grouped site data (*Nash and Sutcliffe*, 1970), which compares the model results with site group average and standard deviation. The GLUE analysis has been compared for both vegetation types. We compared all parameters that influence the methane flux, including methane production, the oxidation of methane during plant transport and plant transport rate (*van Huissteden et al.*, 2009):

- R_0: Methane production rate factor (0.1-0.5 $\mu M hr^{-1}$), relating the methane production rate to substrate quantity from plants.
- f_{ox}: within plant oxidation factor (0-1), reducing the amount of emitted CH_4 from plants.
- V_{transp}: plant transport factor (0-15), increasing the amount of emitted CH_4 from plants.
- f_{shoots}: fraction (0-1) of net primary production (NPP) allocated to aboveground shoots.
- Z_{roots}: maximum root depth (0.1-0.6 m).
- P_{max}: maximum daily NPP (0.001-0.005 kgC m^2 day^{-1}).

4.3 Results

4.3.1 Methane flux measurements

In Figure 4.3, water level, active layer thickness and temperature for the two vegetation classes at each measurement day are shown. From the figure it becomes clear that soil temperature was very similar between the two vegetation types and active layer depth did not differ that much either. However, a significant difference was observed for water level. While water levels were above the surface for both vegetation types, the water level in TW4 was somewhat lower from July 23 to July 30. After that, water levels were more similar, although a small difference in water level remained.
In Figure 4.2, the daily fluxes of the class with, and without submerged *Sphagnum* have been plotted next to each other and the error bars represent the standard deviations of the measurements. Average daily fluxes ranged from 3.6 to 12.3 mg CH_4 m^{-2} hr^{-1} for TW1 and from 0.7 to 7.8 mg CH_4 m^{-2} hr^{-1} for TW4. The averages of the measured fluxes were 8.0 ± 4.7 mg CH_4 m^{-2} hr^{-1} and 4.1 ± 3.1 mg CH_4 m^{-2} hr^{-1} for TW1 and TW4 respectively. From the difference of the means it follows that the emissions from the vegetation type with submerged *Sphagnum* were half as much as emissions from the vegetation type without *Sphagnum*.

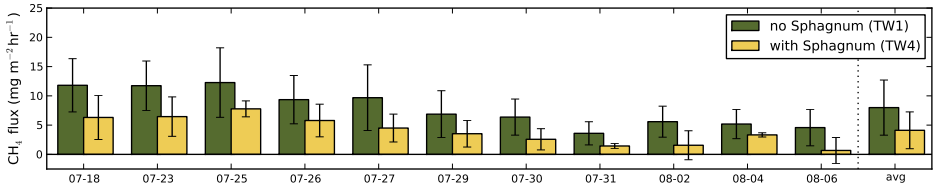

Figure 4.2: Daily fluxes for terrain types without (TW1) and with *Sphagnum* (TW4). Measurements are shown per day and on the right the average flux of the two vegetation types is shown. Error bars denote the standard deviation of the measurements.

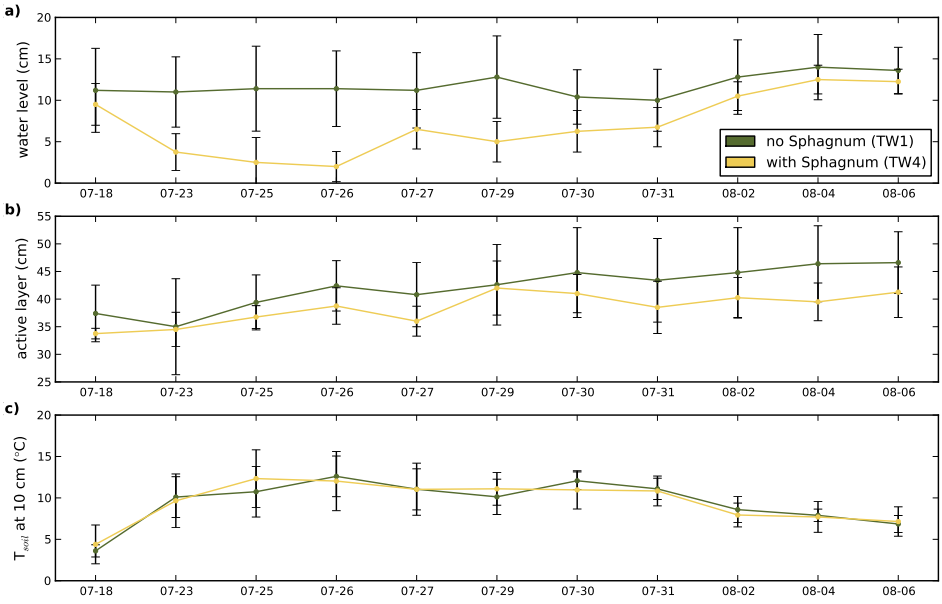

Figure 4.3: Environmental parameters during the measurement campaign for the two vegetation types. Green shows the data for the vegetation type without *Sphagnum*, TW1, while the data for the vegetation type with *Sphagnum*, TW4, is shown in yellow. Error bars denote standard deviations. a) Daily water level above the surface. b) Active layer thickness. c) Daily soil temperature at 10 cm depth.

For each measurement day, the plots without *Sphagnum* show higher fluxes than the plots with *Sphagnum*, as expected. However, since the measurements were performed manually, only a limited amount of measurements (4 to 5) could be done per vegetation class per day. This led to a high standard deviation and there is some overlap between the two vegetation types. To show statistically that the two vegetation types do show different fluxes, a linear mixed model (Type III test of fixed effects with an AR(1) covariance structure, e.g. *Littell et al.* (1998)) was performed with the use of PASW Statistics 18.0 (SPSS Inc., Chicago, IL). This method was preferred over a repeated measures ANOVA since the latter cannot handle missing data. The mixed model showed that the two vegetation types are indeed different at a 95% significancy level (p=0.046).

Table 4.2: Mean methane oxidation rates for the two analyzed *Sphagnum* samples from sites NS1 and NS2 at different incubation temperatures. The values are in μmol CH_4/g dry weight/day ± standard deviation (n=3).

Temperature (°C)	4°	10°	20°
		NS1	
Oxidation rate1	40±0.9	58±0.5	80±0.3
Oxidation rate2	30±0.7	42±0.4	75±0.6
		NS2	
Oxidation rate1	33±0.3	39±0.4	54±0.2
Oxidation rate2	32±0.6	38±0.5	62±0.5

4.3.2 Incubation study

High methane oxidation rates were found for the samples NS1 and NS2 at 4°C, 10°C and 20°C, as shown in Table 4.2. Methane oxidation rates varied between 32 and 80 μmol CH_4 gDW^{-1} day^{-1} and addition of new methane did not result in increased rates. Surprisingly, all samples showed activity between 2.7 and 7 μmol CH_4 gDW^{-1} day^{-1}, when incubations were continued on ice. Methane oxidation rates measured in the water controls were negligible since rates were 0.04 ± 0.02 μmol CH_4 gDW^{-1} day^{-1} on average. A more in-depth microbiological analysis on the bacterial community of these samples has been published previously by *Kip et al.* (2010).
The amount of dry weight of *Sphagnum* per m^2 was determined to be 415 ± 250 g, which means that an oxidation rate from the incubation study of 10 μmol CH_4 gDW^{-1} day^{-1} would equal 2.8 ± 1.7 mg CH_4 m^{-2} hr^{-1} under idealized circumstances. The observed temperature range in the field was roughly between 4 and 12°C and, according to Table 4.2, oxidation rates at these temperatures vary between 30 and 40 μmol CH_4 gDW^{-1} day^{-1} or 8.4 ± 5.0 to 11.1 ± 6.6 mg CH_4 m^{-2} hr^{-1}, which is about a factor of two larger than the observed difference between the two vegetation types. This large discrepancy between the field and the incubation study was expected, since these rates were determined under laboratory conditions, with ample O_2 and CH_4 available, and as such the two are not directly comparable. Nonetheless, these numbers indicate that a high potential for oxidation within *Sphagnum* exists.

4.3.3 Flux modeling

The results of the model runs for the two vegetation types are shown in figure 4.4. For most days the model agrees quite well, falling within the standard deviations of the observed values. Poor model performance only occurs on July 18, when observed fluxes of sites without *Sphagnum*, TW1, are clearly higher than those modeled and on July 31, when observed fluxes of both vegetation types are much lower than those modeled.

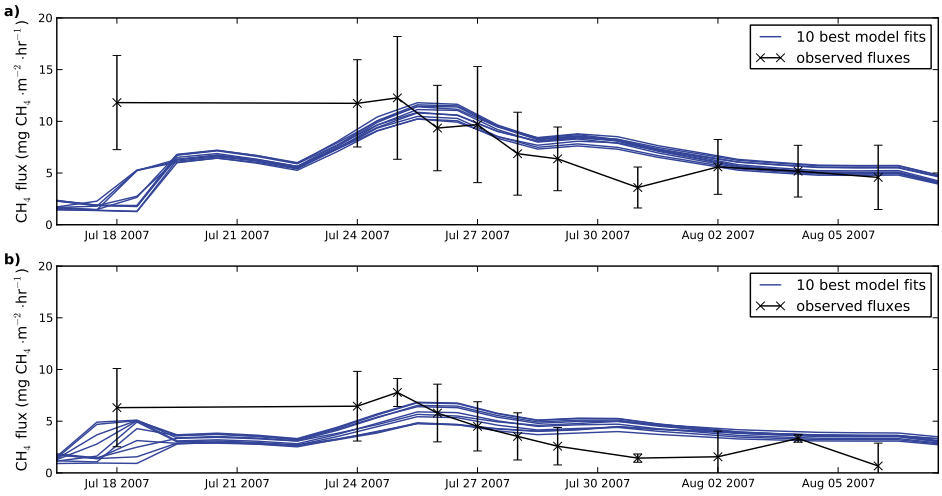

Figure 4.4: The 10 best model fits (blue) plotted together with observed data (black). Error bars denote standard deviations.

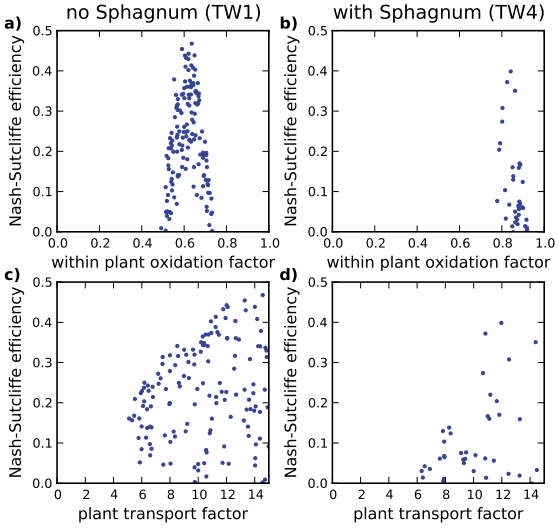

Figure 4.5: GLUE analysis of model parameters for both vegetation types, showing Nash-Sutcliffe efficiency. On the left side (a, c and e) the results for the vegetation type without *Sphagnum*, TW1, are shown, while the results for the vegetation type with *Sphagnum*, TW4, are shown on the right hand side (b, d and f). The top row (a and b) shows values for methane production, R_0. The middle row (c and d) shows values for within plant oxidation of methane, f_{ox}, and the bottom row (e and f) shows values for plant transport factor, V_{transp}.

In Figure 4.5, the results of the GLUE analysis are shown for all runs where the Nash-Sutcliffe efficiency was larger than zero, and for the three parameters that are expected to influence methane emission most strongly, methane production, R_0, within plant oxidation, f_{ox}, and plant transport, V_{transp}. Of the 2000 random model runs, fewer runs gave a positive Nash-Sutcliffe efficiency for sites with *Sphagnum* than without *Sphagnum* and therefore fewer points

are plotted for that vegetation type. The significance threshold ($p<0.1$, NS=0.551 according to an F test) was crossed for TW4 but not for TW1, but this is common for methane emission modeling (*van Huissteden et al.*, 2009); for TW1 the threshold is approached.
More importantly, the GLUE results show large differences in the identifiability of the parameters. Likely values for R_0 ranged from 0.1 to 0.35 μMhr^{-1} for TW1 and 0.1 to 0.3 μMhr^{-1} for TW4. Values of V_{transp} ranged from 2 to 15 for both vegetation types. Opposed to these largely overlapping ranges, f_{ox} showed distinctively different ranges of 0 to 0.8 and 0.4 to 0.9 for TW1 and TW4 respectively. This clearer distinction for f_{ox} becomes even more apparent when the average of these parameters is considered. Average values in TW1 and TW4 were 0.19 and 0.15 μMhr^{-1} for R_0 ($p<0.001$) and 10.1 and 9.0 for V_{transp} ($p<0.1$), while f_{ox} showed average values 0.44 and 0.73, the latter value resulting in significantly higher oxidation (tested with t-test, $p<0.001$). For the other parameters, no significant differences could be detected and are therefore not shown in Figure 4.5.
It is likely that a difference in parameter identifiability and parameter values indicate realistic factors that influence the methane fluxes. This indicates that the difference in fluxes between the two vegetation types is best explained by differences in oxidation rate during transport, and to a lesser extent by differences in CH_4 production rate and plant transport rate.

4.4 Discussion

The measurements of the methane emissions from the two inundated vegetation types show that fluxes from vegetation without submerged *Sphagnum*, TW1, was 8.0 $\pm$ 4.7 mg CH_4 m^{-2} hr^{-1} and 4.1 $\pm$ 3.1 mg CH_4 m^{-2} hr^{-1} for vegetation with submerged *Sphagnum*, TW4; a difference of a factor of two. The standard deviation on the averages is quite large since the measured plots were selected in such a way that they represent the spatial variation for that vegetation type and large variations between individual measurements are therefore to be expected. The two vegetation types were shown to have significantly different fluxes through a linear mixed model (95% confidence level, p=0.046). In previous years, the same difference between these two vegetation types was observed at the same site while using a roving measurement scheme for determining fluxes (*van Huissteden et al.*, 2005; *van der Molen et al.*, 2007; *van Huissteden et al.*, 2009), confirming these results. Furthermore, others have observed the high reduction in fluxes between these two types of vegetation as well, such as *Hines et al.* (2008), who similarly reported a 50% lower flux in a mixed vegetation of sedges and *Sphagnum*.
Apart from the difference in fluxes, the two vegetation types observed also showed a large differences in vascular plant cover. Since this type of plant is able to influence methane emissions in wetlands (*Joabsson et al.*, 1999), it would have been preferable to select sites where vascular plant cover was similar and only *Sphagnum* cover would be different. However, in the field it became clear that vascular plant cover was always higher for vegetation without *Sphagnum*, TW1, than for vegetation with *Sphagnum*, TW4. This difference in vascular plant cover could be due to competition between *Sphagnum* and vascular plants, as has been shown by *Heijmans et al.* (2002), making this difference a de facto situation that cannot be avoided, at least not in the field.
The question still remains whether the observed difference in fluxes can be attributed to vascular plant cover alone. To investigate this hypothesis, the average methane flux of all measurement sites was plotted against vascular plant cover, obtained from a vegetation mapping for each site, in Figure 4.6. This figure shows that, as expected, the TW4 sites show lower fluxes

and have a lower vascular plant cover than TW1. However, this difference in flux magnitude is not necessarily due to vascular plant cover. Alternatively, the difference in fluxes from the two classes could be explained by plotting them against *Sphagnum* cover, since TW4 has a high *Sphagnum* cover and TW1 none. Therefore, it was preferred to study the relationship between vascular plant cover and fluxes separately within each vegetation class. For each class, Figure 4.6 clearly shows that there is no pattern with vascular plant cover and no significant regression could be found. Notably, the second highest fluxes in the TW1 class were measured in a plot with a vascular plant cover close to that of the TW4 plots.

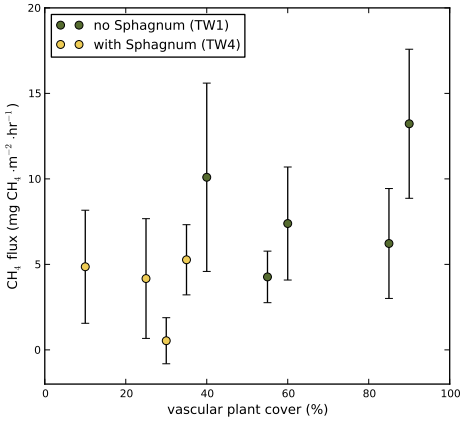

Figure 4.6: Average methane fluxes of each measurement site, plot along its vascular plant cover. The error bars denote standard errors along all measurement days. Although there is a difference in vascular plant cover and methane flux between the two vegetation types TW1 and TW4, within each vegetation class there is no significant increase with vascular plant cover.

The poor predictability of vascular plant cover on methane fluxes was confirmed by our modeling study. Average model parameters for within plant oxidation were 50% higher in areas with *Sphagnum* compared to areas without *Sphagnum*, while only a small difference was found in plant transport. So, although the two vegetation types have different vascular plant cover percentages, the measurements and model both suggest that vascular plant cover is not the most likely parameter to explain the observed differences.

When compared to previous research on plant transport (*Joabsson and Christensen*, 2001; *Tsuyuzaki et al.*, 2001; *Ström et al.*, 2003; *Christensen et al.*, 2003; *Kutzbach et al.*, 2004), this result seems counter intuitive, but it can be explained by the fact that vascular plants usually increase methane fluxes by bypassing the aerated parts of the soil, where methane would otherwise be oxidized. In this study, no aerated soil layer, associated with methane oxidation, was present, since the studied vegetation types were always inundated. This inundation made the difference between net transport to the atmosphere through aerenchyma and upward diffusion much smaller and the relative contribution of plant transport to net methane emissions was reduced.

While this inundation reduced the relative influence of plant transport, it introduces a new issue since water levels were significantly different between vegetation types. Most measurements in July were performed with a higher water table for TW1 than for TW4, as shown in Figure 4.3. Since this higher water table can lead to lower transport and higher oxidation of methane (*Sachs et al.*, 2010), this could lead to differences in oxidation not related to the

methanotrophic bacteria associated with *Sphagnum*. However, this potentially increased oxidation in TW1, the vegetation type without *Sphagnum* and exhibiting the highest emissions, would diminish both methane emissions from TW1 and the difference between the two vegetation types, not increase them. Furthermore, the relative difference between the vegetation types shows no apparent effect of water table. While a large increase in the difference in water level between the vegetation types occurred between July 18 and July 23, the relative difference in emissions did not change. Moreover, the largest relative difference in emissions between the vegetation types was observed for the last 4 measurement days when water levels in both vegetation types were very similar. The observed differences in fluxes are therefore not likely to be due to a difference in surface water level.

Although water column oxidation and plant transport were not likely to explain the differences observed, an alternative explanation to the higher emissions in TW1 than TW4 might lie in a difference in methane production. Methane production can be increased by the exudation of substrate by plants such as *Eriophorum* (*Ström et al.*, 2005). While the amount of substrate and methanogenic activity in the soil could not be assessed, due to legislative restrictions that preclude fast export of soil samples and limited analysis possibilities at the site, methane production related to substrate availability had to be modeled within the process model. In Figure 4.5, it is shown that parameter values for methane production had quite similar ranges for both TW1 and TW4, with TW1 showing slightly higher possible values (0.3 vs 0.35 μMhr^{-1}). Also, the average methane production for TW1 was 0.19 μMhr^{-1} while TW4 had a somewhat lower average of 0.15 μMhr^{-1}. These results suggest that it's likely that production of methane was higher in TW1 but the difference between the two vegetation types is not very large and possible parameter values largely overlap. This would indicate that methane production can only partly explain the difference observed between the two vegetation types.

While the measurements and model indicate that the combination of plant transport, oxidation within the water column and methane production alone is not sufficient to explain the observed differences, the model did indicate that oxidation should be 50% higher in TW4 than TW1 to explain the observed differences. Indeed, the incubation study found very high methane oxidation rates in submerged *Sphagnum*. These high rates are not atypical when compared to oxidation rates for incubations of submerged *Sphagnum* samples from around the world. For example, a site from Argentina showed similar oxidation rates at 20°C (*Kip et al.*, 2010). Most surprisingly, the samples from the studied site still showed some methane oxidation at 4°C and on ice. No methane oxidation could be measured under those circumstances for the other samples incubated by *Kip et al.* (2010), who also showed, with the use of a pmoA-based microarray and enrichment cultures, that this behavior is attributed to an unique methanotrophic bacterial community present in the Northeastern Siberian ecosystem. Apparently, this community is active over a very large temperature range, 0-20°C, which explains why oxidation rates stay high in the cold Siberian soil.

The rates obtained from the incubation study were recalculated to fluxes per m^2 by multiplying the oxidation rates by the amount of dry weight per m^2. Although differences in methane and oxygen concentrations between the lab and the field preclude a direct comparison to differences observed in the field, they do show that there is a very high potential for methane oxidation in submerged *Sphagnum* if viewed under these ideal conditions. The conversion to m^2 gave oxidation rates that were twice as high as in the field. Tthis indicates that the potential for high oxidation in *Sphagnum* is there, although caution has to be expressed to view these numbers in an absolute way since they are most likely overestimating the real field

conditions.
Thus, the results from the model and the incubation study both point towards high oxidation in the *Sphagnum* dominated vegetation type and it is less likely that the observed differences can be explained by methane production, within water column oxidation and plant transport alone. These observations make it likely that methanotrophic bacteria play a large role in the recycling of methane of the studied vegetation type.

4.5 Conclusion

In this study, methane emissions from two inundated vegetation types were compared. Areas dominated by submerged *Sphagnum* with some sedges were found to exhibit emissions that were two times lower than inundated vegetation dominated by sedges but without *Sphagnum*. An incubation study of submerged *Sphagnum* samples showed that very high oxidation rates of methane, even at 4°C and on ice, were possible in this vegetation. This suggested that below the water table oxidation in submerged *Sphagnum* is one of the key processes in clarifying the difference between the two studied vegetation types.
To assess the likelihood in which other known parameters such as plant transport and methane production could explain the observed differences, both vegetation types were modeled in detail, together with a sensitivity analysis on the parameters. While this model study showed that methane production and plant transport might be somewhat higher in the vegetation type without *Sphagnum*, possible values largely overlapped and averages were comparable. Furthermore, the model appeared to be much more sensitive to within plant oxidation, which showed average values that were 50% higher in the vegetation type with *Sphagnum*. This reaffirms the importance of the activity of these methanotrophic endophytes in submerged *Sphagnum*.
Since most methane at this tundra site is emitted from the two studied vegetation types, these results are also spatially important. Respective surface cover of the two vegetation types is 7 to 3 for TW1 and TW4 respectively (*van der Molen et al.*, 2007) and this means that the vegetation type dominated by submerged *Sphagnum* represents 30% of the methane emitting surface. If we assume a ratio of 2 to 1 in the emissions between the two vegetation types, it can be estimated that oxidation by methanotrophic endophytes plays a large role in 15% of the net methane emission from this tundra site.
We conclude, by combining flux chamber measurements, an incubation study and modeling, that this type of methanotrophic bacteria, that live in a cooperation with submerged *Sphagnum*, is an important factor in the recycling of methane within this tundra vegetation type. Although other factors such as methane production and plant transport are also important in determining emissions, the activity of these endophytic bacteria adds to a better understanding of the drivers and controls of methane emissions from tundra.

Acknowledgements
We like to acknowledge the people at the Institute for Biological Problems of the Cryolithozone SB RAS, Yakutsk for their assistance. In particular Alexander Kononov and Dimitri Suzdalov for all the help in the field in the summer of 2007 and Elena Ivanova and Lena Poryadina for the determination of the *Sphagnum* samples for the vegetation description. Furthermore we thank the people at the local WWF office in Chokurdakh who provided the logistical support and made it able for us to stay at the station throughout the season. Also, we like to thank Monique Heijmans for her helpful comments and Cinzia Berrittella for previous

work on collecting and analyzing *Sphagnum* samples, which furthered interest to pursue this research. Finally, we like to thank the Darwin Center for Biogeosciences who supported this research with a grant to F.J.W. Parmentier (142.16.1041) and N.Kip (142.16.1061).

References

Basiliko, N., R. Knowles, and T. R. Moore, Roles of moss species and habitat in methane consumption potential in a northern peatland, *Wetlands*, *24*(1), 178--185, 2004.

Beven, K., Environmental Modelling: An Uncertain Future?, *Routledge: London*, p. 328, 2008.

Bubier, J. L., The relationship of vegetation to methane emission and hydrochemical gradients in northern peatlands, *Journal of Ecology*, *83*(3), 403--420, 1995.

Christensen, T. R., N. S. Panikov, M. Mastepanov, A. Joabsson, A. Stewart, M. Oquist, M. Sommerkorn, S. Reynaud, and B. Svensson, Biotic controls on CO_2 and CH_4 exchange in wetlands - a closed environment study, *Biogeochemistry*, *64*(3), 337--354, 2003.

Corradi, C., O. Kolle, K. M. Walter, S. A. Zimov, and E.-D. Schulze, Carbon dioxide and methane exchange of a north-east Siberian tussock tundra, *Global Change Biology*, *11*(11), 1910--1925, 2005.

Fechner, E. J., and H. F. Hemond, Methane transport and oxidation in the unsaturated zone of a Sphagnum peatland, *Global Biogeochemical Cycles*, *6*(1), 33--44, 1992.

Frenzel, P., and J. Rudolph, Methane emission from a wetland plant: the role of CH_4 oxidation in Eriophorum, *Plant And Soil*, *202*(1), 27--32, 1998.

Frolking, S., N. T. Roulet, and J. Fuglestvedt, How northern peatlands influence the Earth's radiative budget: Sustained methane emission versus sustained carbon sequestration, *Journal of Geophysical Research-Biogeosciences*, *111*(G1), G01,008, 2006.

Greenup, A. L., M. A. Bradford, N. P. McNamara, P. Ineson, and J. A. Lee, The role of Eriophorum vaginatum in CH_4 flux from an ombrotrophic peatland, *Plant And Soil*, *227*(1-2), 265--272, 2000.

Heijmans, M. P. D., H. Klees, and F. Berendse, Competition between Sphagnum magellanicum and Eriophorum angustifolium as affected by raised CO_2 and increased N deposition, *Oikos*, *97*(3), 415--425, 2002.

Hines, M. E., K. N. Duddleston, J. N. Rooney-Varga, D. Fields, and J. P. Chanton, Uncoupling of acetate degradation from methane formation in Alaskan wetlands: Connections to vegetation distribution, *Global Biogeochemical Cycles*, *22*(2), GB2017, 2008.

Joabsson, A., and T. R. Christensen, Methane emissions from wetlands and their relationship with vascular plants: an Arctic example, *Global Change Biology*, *7*(8), 919--932, 2001.

Joabsson, A., T. R. Christensen, and B. Wallen, Vascular plant controls on methane emissions from northern peatforming wetlands, *Trends In Ecology & Evolution*, *14*(10), 385--388, 1999.

Kip, N., J. F. van Winden, Y. Pan, L. Bodrossy, G.-J. Reichart, A. J. P. Smolders, M. S. M. Jetten, J. S. S. Damste, and H. J. M. Op den Camp, Global prevalence of methane oxidation by symbiotic bacteria in peat-moss ecosystems, *Nature Geoscience*, *3*(9), 617--621, 2010.

Kutzbach, L., D. Wagner, and E.-M. Pfeiffer, Effect of microrelief and vegetation on methane emission from wet polygonal tundra, Lena Delta, Northern Siberia, *Biogeochemistry*, *69*(3), 341--362, 2004.

Larmola, T., E.-S. Tuittila, M. Tiirola, H. Nykänen, P. J. Martikainen, K. Yrjälä, T. Tuomivirta, and H. Fritze, The role of Sphagnum mosses in the methane cycling of a boreal mire, *Ecology*, *91*(8), 2356--2365, 2010.

Littell, R. C., P. R. Henry, and C. B. Ammerman, Statistical analysis of repeated measures data using SAS procedures, *Journal of Animal Science*, *76*(4), 1216--1231, 1998.

McGuire, A. D., et al., Sensitivity of the carbon cycle in the Arctic to climate change, *Ecological Monographs*, *79*(4), 523--555, 2009.

Minkkinen, K., and J. Laine, Vegetation heterogeneity and ditches create spatial variability in methane fluxes from peatlands drained for forestry, *Plant And Soil*, *285*(1-2), 289--304, 2006.

Nash, J. E., and J. V. Sutcliffe, River flow forecasting through conceptual models part I -A discussion of principles, *Journal of Hydrology*, *10*(3), 282--290, 1970.

Petrescu, A. M. R., J. van Huissteden, M. Jackowicz-Korczyński, A. Yurova, T. R. Christensen, P. M. Crill, K. Backstrand, and T. C. Maximov, Modelling CH_4 emissions from arctic wetlands: effects of hydrological parameterization, *Biogeosciences*, *5*(1), 111--121, 2008.

Popp, T. J., J. P. Chanton, G. J. Whiting, and N. Grant, Evaluation of methane oxidation in the rhizosphere of a Carex dominated fen in north central Alberta, Canada, *Biogeochemistry*, *51*(3), 259--281, 2000.

Post, W. M., W. R. Emanuel, P. J. Zinke, and A. G. Stangenberger, Soil carbon pools and world life zones, *Nature*, *298*(5870), 156--159, 1982.

Raghoebarsing, A. A., et al., Methanotrophic symbionts provide carbon for photosynthesis in peat bogs, *Nature*, *436*(7054), 1153--1156, 2005.

Sachs, T., M. Giebels, J. Boike, and L. Kutzbach, Environmental controls on CH_4 emission from polygonal tundra on the microsite scale in the Lena river delta, Siberia, *Global Change Biology*, *16*(11), 3096--3110, 2010.

Ström, L., A. Ekberg, M. Mastepanov, and T. R. Christensen, The effect of vascular plants on carbon turnover and methane emissions from a tundra wetland, *Global Change Biology*, *9*(8), 1185--1192, 2003.

Ström, L., M. Mastepanov, and T. R. Christensen, Species-specific effects of vascular plants on carbon turnover and methane emissions from wetlands, *Biogeochemistry*, *75*(1), 65--82, 2005.

Sundh, I., C. Mikkela, M. Nilsson, and B. H. Svensson, Potential aerobic methane oxidation in a sphagnum-dominated peatland - controlling factors and relation to methane emission, *Soil Biology & Biochemistry*, *27*(6), 829--837, 1995.

Tarnocai, C., J. G. Canadell, E. A. G. Schuur, P. Kuhry, G. Mazhitova, and S. A. Zimov, Soil organic carbon pools in the northern circumpolar permafrost region, *Global Biogeochemical Cycles*, *23*, GB2023, 2009.

Tsuyuzaki, S., T. Nakano, S. Kuniyoshi, and M. Fukuda, Methane flux in grassy marshlands near Kolyma River, north-eastern Siberia, *Soil Biology & Biochemistry*, *33*(10), 1419--1423, 2001.

van der Molen, M. K., J. van Huissteden, F. J. W. Parmentier, A. M. R. Petrescu, A. J. Dolman, T. C. Maximov, A. V. Kononov, S. V. Karsanaev, and D. A. Suzdalov, The growing season greenhouse gas balance of a continental tundra site in the Indigirka lowlands, NE Siberia, *Biogeosciences*, *4*(6), 985--1003, 2007.

van Huissteden, J., T. C. Maximov, and A. J. Dolman, High methane flux from an arctic floodplain (Indigirka lowlands, eastern Siberia), *Journal of Geophysical Research-Biogeosciences*, *110*(G2), G02,002, 2005.

van Huissteden, J., R. van den Bos, and I. M. Alvarez, Modelling the effect of water-table management on CO_2 and CH_4 fluxes from peat soils, *Netherlands Journal Of Geosciences-Geologie En Mijnbouw*, *85*(1), 3--18, 2006.

van Huissteden, J., A. M. R. Petrescu, D. M. D. Hendriks, and K. T. Rebel, Sensitivity analysis of a wetland methane emission model based on temperate and arctic wetland sites, *Biogeosciences*, *6*(12), 3035--3051, 2009.

Vecherskaya, M. S., V. F. Galchenko, E. N. Sokolova, and V. A. Samarkin, Activity and species composition of aerobic methanotrophic communities in tundra soils, *Current Microbiology*, *27*(3), 181--184, 1993.

Walker, D. A., et al., The Circumpolar Arctic vegetation map, *Journal of Vegetation Science*, *16*(3), 267--282, 2005.

Walter, B. P., and M. Heimann, A process-based, climate-sensitive model to derive methane emissions from natural wetlands: Application to five wetland sites, sensitivity to model parameters, and climate, *Global Biogeochemical Cycles*, *14*(3), 745--765, 2000.

Whalen, S. C., Biogeochemistry of methane exchange between natural wetlands and the atmosphere, *Environmental Engineering Science*, *22*(1), 73--94, 2005.

Whalen, S. C., and W. S. Reeburgh, Consumption of atmospheric methane by tundra soils, *Nature*, *346*(6280), 160--162, 1990.

Wille, C., L. Kutzbach, T. Sachs, D. Wagner, and E.-M. Pfeiffer, Methane emission from Siberian arctic polygonal tundra: eddy covariance measurements and modeling, *Global Change Biology*, *14*(6), 1395--1408, 2008.

Zhuang, Q., J. M. Melillo, D. W. Kicklighter, R. G. Prinn, A. D. McGuire, P. A. Steudler, B. S. Felzer, and S. Hu, Methane fluxes between terrestrial ecosystems and the atmosphere at northern high latitudes during the past century: A retrospective analysis with a process-based biogeochemistry model, *Global Biogeochemical Cycles*, *18*(3), GB3010, 2004.

Chapter 5

Spatial and temporal dynamics in eddy covariance observations of methane fluxes at a tundra site in Northeastern Siberia[1]

Abstract
In the past two decades, the eddy covariance technique has been used for an increasing number of methane flux studies at an ecosystem scale. Previously, most of these studies used a closed path setup with a tunable diode-laser spectrometer (TDL). Although this method worked well, the TDL has to be calibrated regularly and cooled with liquid nitrogen or a cryogenic system, which limits its use in remote areas.
Recently, a new closed path technique has been introduced that uses off-axis integrated cavity output spectroscopy that does not require regular calibration or liquid nitrogen to operate and can thus be applied in remote areas.
In the summer of 2008 and 2009, this eddy covariance technique was used to study methane fluxes from a tundra site in Northeastern Siberia. The measured emissions showed to be very dependent on the fetch area, due to a large contrast in water table between wind directions. Furthermore, the observed short and longterm variation of methane fluxes could be readily explained with a non-linear model that used relationships with atmospheric stability, soil temperature and water level. This model was subsequently extended to fieldwork periods preceding the eddy covariance setup and applied to evaluate a spatially integrated flux. The model result showed that average fluxes were 56.5, 48.7 and 30.4 nmol CH_4 m^{-2} s^{-1} for the summers of 2007 to 2009.
While previous models of the same type were only applicable to daily averages, the method described can be used on a much higher temporal resolution, making it suitable for gap-filling. Furthermore, by partitioning the measured fluxes along wind direction, this model can also be used in areas with non-uniform terrain but nonetheless provide spatially integrated fluxes.

[1]The content of this chapter has been submitted as "Spatial and temporal dynamics in eddy covariance observations of methane fluxes at a tundra site in Northeastern Siberia" to JGR-Biogeosciences

5.1 Introduction

Methane emissions from Arctic ecosystems play a special role in the global carbon cycle due to the amplified and unprecedented warming of the region (*Serreze et al.*, 2000; *Kaufman et al.*, 2009) in combination with the large expected temperature sensitivity of the carbon stores in permafrost areas (*Christensen et al.*, 2004). It has been suggested that this combination could lead to a positive feedback when higher temperatures lead to more carbon availability through increased melting of the permafrost which would lead, in turn, to higher methane emissions, resulting in increasingly higher temperatures (*Oechel et al.*, 1993; *McGuire et al.*, 2009). Therefore, to better understand the relationships of these emissions to environmental parameters, methane fluxes have been measured in the past two decades at a number of sites using chamber flux measurements (*Christensen et al.*, 1995; *van Huissteden et al.*, 2005), and, since recently, the eddy covariance technique (*Friborg et al.*, 2000; *Wille et al.*, 2008).
Most of these studies on methane emissions preferred chamber flux measurements for a number of reasons. For example, the chamber flux method has a low power requirement, which makes it applicable in remote areas where a steady power supply is absent. Also, due to the small footprint, correlations between environmental parameters such as soil temperature, water level and vegetation are more easily determined. Furthermore, chamber flux measurements are portable and therefore measurements can be readily performed at a relatively large number of locations (*Christensen et al.*, 1995; *van Huissteden et al.*, 2005).
On the other hand, chamber flux measurements are very labor intensive, have a low temporal resolution and can easily be disturbed by the person performing the measurement. Most of these concerns can be alleviated by the use of automatic flux chambers, since they perform measurements at a regular interval with much less effort (*Mastepanov et al.*, 2008). However, with automatic chambers the drawbacks that are inherent to point measurements remain. For example, when flux chamber measurements are being upscaled to an integrated flux estimate of a larger area, a significant amount of measurements are needed for each vegetation type present, together with a precise vegetation mapping (*van der Molen et al.*, 2007). The higher number of measurements involved all have their own added uncertainty, making it more complicated to establish a correctly upscaled flux. Besides, even if very precise measurements are performed and the vegetation has been mapped in close detail, the fact remains that chamber measurements decouple the surface from atmospheric influences such as wind and turbulence and they are unsuitable for registering irregular events such as ebullition, all of which can have a significant effect on the amplitude of fluxes, methane in particular (*Kellner et al.*, 2006; *Sachs et al.*, 2008).
Therefore, to be able to measure methane fluxes in a non-intrusive way, over large terrain and with a high temporal resolution, the eddy covariance method may perform better. This method has already been well established for the measurement of evaporation and CO_2 fluxes (*Aubinet et al.*, 2000; *Moncrieff et al.*, 1997) and has been successfully applied to measure methane fluxes as well. For example, one of the earliest studies on eddy covariance of methane fluxes was performed by *Fan et al.* (1992), who used a fast response flame ionization detector and a prototype fast HeNe laser methane monitor to measure methane emissions from tundra in Southwestern Alaska and found relationships with wind speed for methane emissions from lakes. Alternatively, *Verma et al.* (1992) measured methane fluxes in a Minnesota peatland with a fast response tunable diode laser spectrometer (TDL) (*Zahniser et al.*, 1995) and found the method to be satisfactory for measuring methane fluxes. Afterwards, this method was used in several other eddy covariance studies. For example, *Suyker et al.* (1996) measured

methane fluxes in a fen in central Saskatchewan and could model observed fluxes from non-linear relationships with midday temperature measurements and water level. *Friborg et al.* (2000) expanded upon this model, with measurements obtained at a high Arctic site in NE-Greenland, by using daily averages and by adding relationships with active layer depth. *Wille et al.* (2008) applied a similar non-linear model, explaining most day to day variation by relationships with soil temperature and friction velocity, to measurements obtained with a TDL from polygonal tundra on a Northeastern Siberian site in the delta of the Lena river. *Sachs et al.* (2008), with measurements at the same site but in a later year, further developed the model by adding air pressure, which significantly improved results. Also, it was shown that the model performed well over the entire growing season.

Most of these eddy covariance studies used TDL-devices that had the large drawback that they had to be cooled (either with liquid nitrogen or a cryogenic system) and required regular calibration to obtain precise measurements of methane concentrations. Recently, an off-axis integrated cavity output spectroscopy method was introduced that can measure methane concentrations at a high frequency (10 Hz) and it was shown to give good results when used for eddy covariance (*Hendriks et al.*, 2008; *Zona et al.*, 2009). Although this application requires a large pump, to pass air at sufficient speed through the system, and power requirements therefore remain high, this method does not require cooling or regular (daily or subdaily) calibration. In areas where liquid nitrogen and calibration gases are not readily available, this method opens up new measurement opportunities, given a steady power supply.

When considering new study areas, it becomes apparent that most previous studies on Arctic carbon cycling have been performed in Alaska, Canada or Scandinavia (*Whalen and Reeburgh*, 1990; *Fan et al.*, 1992; *Morrissey et al.*, 1993; *Torn and Chapin III*, 1993; *Vourlitis and Oechel*, 1997; *Oechel et al.*, 1998; *Christensen et al.*, 2004; *Schuur et al.*, 2008; *Dorrepaal et al.*, 2009) and only few in Siberia (*Christensen et al.*, 1995; *Nakano et al.*, 2000; *Corradi et al.*, 2005; *van der Molen et al.*, 2007; *Kutzbach et al.*, 2007), while the largest extent of the Arctic lies in Russian territory. Moreover, these are largely studies using flux chambers, not eddy covariance.

In 2003, to fill this gap in our knowledge of carbon cycling around the arctic, a new station was established in Northeastern Siberia to measure fluxes of CO_2 and CH_4. While CO_2 fluxes have been measured with eddy covariance from the beginning, measurements of methane fluxes had to be performed with the flux chamber method, because of the remoteness of this area and the associated logistical difficulties. As mentioned earlier, measurements with this method can be difficult to translate to a larger area and therefore the new off-axis spectroscopy method was used to determine spatially integrated methane emissions at this site in the summer of 2008 and 2009. In this paper, we show the results and analysis of these measurements with the help of the aforementioned model framework (*Suyker et al.*, 1996; *Friborg et al.*, 2000; *Wille et al.*, 2008; *Sachs et al.*, 2008). Previous studies using this framework considered non-linear relationships to daily averages, while this new study found that fluxes could be well described on a three-hour interval. This was achieved by including the attenuating effect of atmospheric stability on flux measurements, while production was related to soil temperature and water level. This result largely improves the temporal scale of the model framework, making it suitable for gap-filling. Furthermore, the relationships found were applied to simulate spatially integrated methane fluxes in the highly heterogenous terrain of the study site, a common trait of most tundra sites.

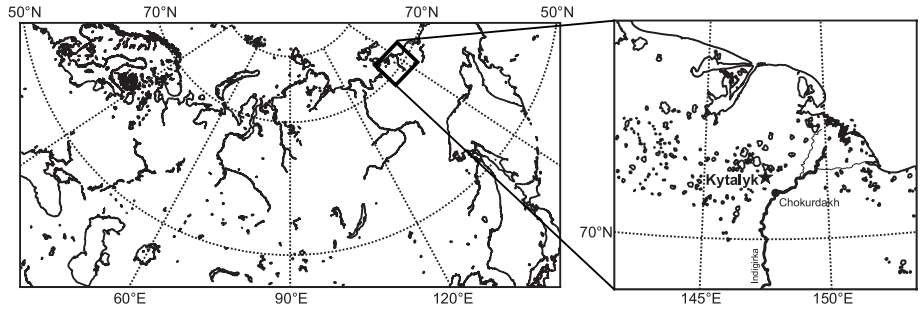

Figure 5.1: The location of the research site within Northeastern Siberia

5.2 Materials and Methods

5.2.1 Site Description

The research site (70°49'44.9" N, 147°29'39.4" E) is located approximately 30 km to the Northwest of the settlement of Chokurdakh in the nature reserve 'Kytalyk' in Northeastern Siberia, alongside the river Berelekekh (Yelon), a tributary to the Indigirka (as shown in Figure 5.1). At a considerable distance from the river, the eddy covariance tower is situated in a depression that originated as a thermokarst lake of Holocene age that has been drained by fluvial erosion.

The climate at the site is continental, with an average temperature of -10.5 °C and typical temperatures of -25 to -40 °C in winter and 5 to 25°C in summer. Normally snowmelt starts at the end of May, early June. Apart from some isolated patches, usually most of the snow is melted by the first half of June. Bud break occurs somewhat later at the end of June or start of July, together with the first truly warm days of the year. However, temperatures vary rapidly in summer when either cold winds are blowing from the Arctic Ocean to the North (± 100 km) or warm winds from the Siberian continent to the South. At the start of September, when temperatures again drop below zero, the growing season stops. By then, the growing season will have seen half of the yearly precipitation as rain while the other half falls as snow in the rest of the year. Snow cover is around 30 cm with little variation in recent years. Total precipitation is around 220 mm per year and while this is a relatively low amount compared to other parts of the world, most evaporation is limited to the short growing season and as such soil conditions remain wet.

Because of the cold climate, the area is underlain by permafrost and areas with a well developed polygonal structure as well as areas with small palsa-like hills occur. These cryogenic structures have led to shallow elevation differences in the landscape with dryer areas where ice lenses created slightly higher lying mounds and wetter, mostly flooded, areas in between these raised areas. In the wet areas, the soil is overlain by a coarse peaty organic top layer of around 10 to 15 cm, consisting of sedge roots and/or Sphagnum peat, while drier parts have a less developed organic layer. A difference also exists in active layer depth, which varies from 40 to 50 cm in the wetter parts to 20 to 30 cm in the dryer parts. Furthermore, in areas where ice wedges are actively developing, open water and small ponds occur. These ponds cover 5% in the West of the research area, locally up to 10%, while the Northeast part almost completely lacks ponds.

These small scale hydrological changes influence the vegetation composition. In dry areas, vegetation consists of *Betula nana* and *Salix pulchra* dwarf shrubs or hummocks of the sedge *Eriophorum vaginatum* with *Salix pulchra* in between. In these areas a moss and lichen ground cover is common. This dry vegetation type occurs on well drained slopes, palsas and on the rims of ice wedge polygons. In the transition zone from a dry to a wet area, mosses and lichens are replaced by *Sphagnum spp.* and shrub cover is largely reduced. In these parts, *Potentilla palustris* occurs and sedge cover increases to 50% with species such as *Arctagrostis latifolia*, *Eriophorum angustifolium* and *Carex aquatilis*. These last two species dominate the wet, flooded parts of terrain depressions and polygon centers where *Sphagnum* is absent and sedge cover is around 80 to 100%. A more detailed description of the studied area is given in (*van der Molen et al.*, 2007).

5.2.2 Instrumentation

The equipment used, measured a large set of environmental parameters. To measure wind speeds and temperature, an ultrasonic anemometer (Gill Instruments, Lymington, UK, type R3-50) was installed on top of a small mast at a height of 4.7 m. At the same height, with a separation of 20 cm, an inlet was situated where air was drawn down towards the fast methane analyser (Los Gatos Research, Mountain View, California, USA, type DLT-100). This inlet was fitted with a filter, which had a pore size of 60 μm, to prevent dust or insects from entering the system. To prevent rainwater from entering the system, a metal cap was placed over the filter and the air was first led upwards for 30 cm through a 3/8" metal tube and back downwards following an u-turn. At a height of 3 meters and below, the air was led through flexible silicon tubing, with the same internal diameter, towards the box in which the fast methane analyzer was situated. At the end of the setup, a dry vacuum scroll pump (XDS35i, BOC Edwards, Crawly, UK) was installed that drew air through the system, which was exhausted through a silencer. Although this pump is capable of speeds up to 9.72 10^{-3} m^3 s^{-1}, the pressure in the measurement cell should be maintained at 210 hPa during operation and as such the actual pumping speed was 5.5 10^{-3} m^3 s^{-1}. With a measurement cell volume of 0.55 m^3, this provided the system with an effective instrument response time of 0.1 s.
Because the vacuum scroll pump and the fast methane analyzer had a high power requirement, a diesel generator was set up 150 m south of the tower to provide power. The generator required refueling twice a day and as a consequence CH_4 measurements were constrained to the period that the research station was occupied. All other measurements, including the sonic anemometer, could run autonomously with a power supply from solar panels and a small wind generator. The data put out by the system was logged at a frequency of 10 Hz to a handheld computer (*van der Molen et al.*, 2006) and half-hourly fluxes were computed afterwards following the Euroflux methodology (*Aubinet et al.*, 2000), with the addition of an angle of attack dependent calibration (*van der Molen et al.*, 2004; *Nakai et al.*, 2006). Corrections were applied for the time lag of 0.6 s between the sonic anemometer and the measurement cell and for the damping effect caused by the instrument response time (*Moore*, 1986). Corrections for density fluctuations according to *Webb et al.* (1980) were not applied since the flow of air through the tube dampened density fluctuations and corrections for water vapor fluctuations were found to be very small, as was also found by *Zona et al.* (2009) with the a similar methane analyser. As a final check, it was found that the energy balance for the measured period showed the same closure as reported earlier by *van der Molen et al.* (2007), who found a good 1:1 agreement at the same site but for previous years. A more detailed

study on the performance of the DLT-100 methane analyser has been performed by *Hendriks et al.* (2008) for a site in the Netherlands with largely identical instrumentation.
In the summer of 2008, the fast methane analyser was set up for the first time. Due to logistical difficulties however, measurements could not start before 25 July. From that day on, measurements were performed until 9 August, when the field campaign ended. On 28 July, a generator failure caused the system to be offline for approximately 15 hours but, apart from that brief period, measurements were continuous. In 2009, the measurements were started on 5 July, at the beginning of the field campaign, after which measurements continued uninterrupted until 3 August.
In another tower, situated 5 meters away from the eddy covariance tower, a shortwave radiometer (Kipp & Zn, Delft, the Netherlands, type albedometer, CM7b), up- and down facing longwave radiometers (The Eppley Laboratory, Newport, RI, USA, type PIR) and a net radiometer (Campbell Scientific, Logan, UT, USA, type Q7) were installed. Soil temperature sensors (type Pb107, manufactured at the VU University Amsterdam) were installed in two profiles, each reaching 60 cm into the ground and measuring temperature at 10 depths each. One profile was situated in an inundated depression with vegetation dominated by sedges, while the other was situated in a higher, drier part dominated by shrubs. A pressure sensor (manufactured at the VU University Amsterdam) was used to measure barometric pressure, while a tipping bucket rain gauge (Campbell Scientific, Logan, UT, USA) was used to measure precipitation. Each day, water level was measured manually from a piezometer that was installed into the soil of the low part of the polygon, where the water level remained above the surface for the measured period. Although significant differences in water level exist throughout the area, it was found that variations in the water level at this single measurement point represented fluctuations in the water table at a larger scale. Manual measurements that were performed throughout the area showed the same day to day variation and as such water level measurements at this one point are a reasonable indication for water level changes in the area around the tower.

5.2.3 Chamber measurements and upscaling

During the field work campaigns of 2007, 2008 and 2009, independent methane flux measurements were performed with manual flux chambers that were connected to an INNOVA 1412 Photoacoustic field Gas-monitor (LumaSense Technologies A/S, Ballerup, Denmark) following the same measurement practice as described in *van Huissteden et al.* (2005). At varying dates and during daytime, measurements were performed on 20 different locations that covered the main vegetation types at the site and the variability therein. Together with each measurement, active layer depth was measured by inserting a steel rod into the ground until it hit the permafrost, noting the distance between the surface and the permafrost. This allowed for a spatially integrated value of this parameter.
To be able to compare the flux chamber measurements to the eddy covariance, these were upscaled with the use of a satellite derived vegetation map. To obtain this map, extensive ground truth on vegetation composition was collected in July 2008 and 2010. In 31 georeferenced validation plots of 20x20m, species composition was determined at 12 locations. Based on the recorded dominant species, the 31 validation plots were then grouped into 5 vegetation communities. All validation plots per vegetation community were used as training areas for a supervised classification. A maximum likelihood classification algorithm (implemented in

ENVI) was applied on an atmospherically corrected GeoEye-1 satellite image that was acquired on 19 August 2010. GeoEye-1 provides a spatial resolution of 2m for the multispectral bands (blue: 480nm, green: 545nm, red: 672.5nm, nir: 850nm). Including all classes in the confusion matrix, the overall accuracy of the resulting vegetation map was 86.79% and the kappa coefficient 0.75. This classification was then applied to a 300m diameter around the flux tower to establish a vegetation map. By multiplying the average methane flux per vegetation class with its fractional cover and summing the results, an average methane flux for the area could be determined.

5.2.4 Flux model

The model used in this study was developed from previous studies on eddy covariance measurements of methane that noted that observed fluxes could be best described by non-linear relationships with a varying set of environmental parameters (*Suyker et al.*, 1996; *Friborg et al.*, 2000; *Wille et al.*, 2008; *Sachs et al.*, 2008). Parameters such as temperature, water level and/or friction velocity were related to daily averages of fluxes and as such most variation could be explained. In this study, production of methane was related to both water level and soil temperature but it was less practical to compare these parameters to daily averages of the measured methane flux. At the study site, large differences in wetness and vegetation composition, and thus methane emissions, exist within the area (*van der Molen et al.*, 2007). As the wind direction changes, the footprint of the tower and the amplitude of the measured methane flux change. Therefore, the temporal resolution of the model has to be high enough to appreciate the contributions from different wind directions separately. A consequence of this shorter averaging period is that the diurnal variation in environmental parameters that influence the measured flux have to be captured as well. It was found that three-hourly averages would both be short enough to capture most changes in wind direction and would also capture diurnal patterns in other environmental parameters sufficiently.
One environmental parameter that shows a clear diurnal pattern, is atmospheric stability. While atmospheric stability does not affect the bacterial production of methane within the soil, stable atmospheric conditions can have a suppressing effect on the transport of trace gases (*Hollinger et al.*, 1998). During stable atmospheric conditions, usually during nighttime when air close to the ground is cooler and heavier, vertical transport of air parcels, including methane, is suppressed. During unstable atmospheric conditions, normally during daytime when air closer to the ground is warmer and thus lighter, vertical transport is stronger due to the enhanced buoyancy (*Denmead*, 2008). If merely daily averages of methane flux are considered, the effect of atmospheric stability is averaged out but in the higher temporal resolution of the model in this study, these effects have to be taken into account.
To calculate atmospheric stability, we used the stability function to the Monin-Obukhov length, L, according to (*Paulson*, 1970) for unstable ($L < 0$) and stable ($L > 0$) conditions as described in Equation 5.1.

$$\begin{aligned} \Phi(L > 0) &= (1 - 16(z/L))^{-1/2} \\ \Phi(L < 0) &= 1 - 5(z/L) \end{aligned} \tag{5.1}$$

Here, z is the observation height minus the displacement height. This function was preferred over z/L itself, since it constrains outliers in the value of L, which could otherwise easily disturb model optimization. As a consequence, unstable conditions are expressed in the range $0 < \Phi < 1$, neutral conditions occur at Φ = 1 and unstable conditions are expressed for values

of $\Phi > 1$.
In Equation 5.2 it is shown how the observed methane flux is described with the use of the atmospheric stability function, soil temperature and water level.

$$F_{CH_4,model} = p_0 \cdot p_1^{(\Phi-\overline{\Phi})} \cdot p_2^{((T_{soil}-\overline{T_{soil}})/10)} \cdot p_3^{(w_l-\overline{w_l})} \quad (5.2)$$

Here, F_{CH_4} is the methane flux expressed in nmol m^{-2} s^{-1}, Φ is the result of the atmospheric stability function, T_{soil} is the soil temperature from an inundated area dominated by sedges (averaged for depths of 2 and 4 cm) in °C, w_l is the measured water level in cm, and p_0 to p_3 are the parameters on which the model was optimized. This optimization was done with a non-linear least squares fit according to the Levenberg-Marquardt algorithm (*Levenberg*, 1944) as included in the Open Source Scientific Tools for Python (SciPy). With the use of this algorithm, the values of p_0 to p_3 were varied until the sum of squares of the difference of the model and the observed values was reduced to a minimum. After the values of these model parameters had been established, the model was also run for the fieldwork period of 2007 and the first half of the fieldwork period in 2008, before the methane eddy covariance measurements were started.

5.3 Results

5.3.1 Environmental conditions

In Figure 5.2, the environmental conditions during the fieldwork periods of 2007, 2008 and 2009 have been plotted. In 2007, the fieldwork started with several warm days with air temperatures around 25 °C on 10 July. Hereafter, temperatures dropped gradually until they reached 5 °C in mid July, which was accompanied by several days of rain. Within this period, water level rose from +5 cm above the surface until +15 cm and it stayed high for the remainder of the fieldwork. After this period, the air temperature rose to 20 to 25 °C in the last week of July. At the start of August, the air temperature dropped to 10 °C and this period was met with regular showers of a few mm. During the fieldwork period, the active layer was very deep, starting at an average of 30 cm until 40 cm at the end of the fieldwork period. In wet areas, depths up to 50 cm had been recorded. This was mainly due to a much earlier start of the growing season, with snowmelt in mid May, while in 2008 and 2009 snowmelt did not occur until June.
The field campaign in 2008 started on 9 July with air temperatures around 5 to 10 °C during the day and just above zero at night. Over the course of a week, temperatures increased gradually to a maximum of 32 °C on 18 July. After this exceptionally hot day, the wind turned North and temperatures dropped back to values of 15 °C and decreased further to 5 °C in the course of several days. At 25 July, when the eddy covariance measurements of methane were started, temperatures peaked around 15 °C. Two days later, two separate rain storms passed on 27 and 28 July with an intensity of about 10 and 25 mm, respectively. Up to that moment, the water level near the tower had been dropping steadily from +10 cm above the surface at the start of the measurements, to +5 cm just before the rain storms. After the rain storms, the water level had risen to +15 cm in just two days and would not drop below +10 cm above the surface for the remainder of the field campaign. The days following the rainstorms were cold, with temperatures around 5 °C until the beginning of August, when temperatures rose again, up to 25 degrees on 5 August, which was followed by a couple of days with temperatures around 15 °C. The depth of the active layer was shallow at the start of

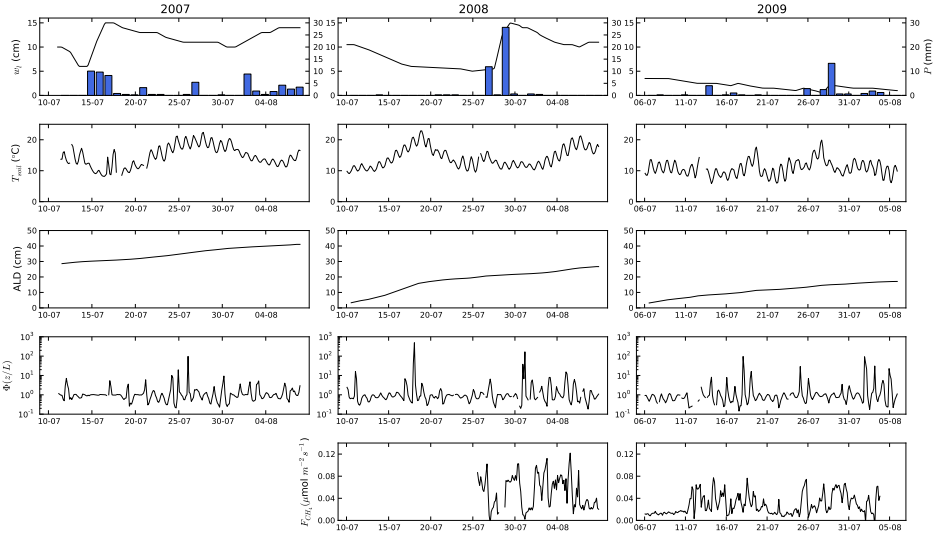

Figure 5.2: Environmental parameters measured during the 2008 and 2009 field campaigns. The top graph shows water level in the piezometer near the tower, w_l, as a continuous line, while precipitation, P, is indicated by the blue bars. Soil temperature (averaged from a depth of 2 and 4 cm), T_{soil}, is shown in the second plot. The third plot shows the average active layer depth for the study area and the fourth shows the results of the stability function, $\Phi(z/l)$. In the bottom plot, the methane flux, F_{CH_4}, has been plotted.

the fieldwork, with an average of 5 cm, although depths in the wet methane producing parts could be as deep as 10 cm. Active layer depth increased gradually during the fieldwork with a depth of 30 cm at the end and depths of 40 cm in the wetter parts of the tundra.
In 2009, measurements were started on 6 July and temperatures were varying between 5 and 15 °C for two weeks, after which temperatures rose to 20 °C on 18 and 19 July. Precipitation was low in this period (around 10 mm in total), with small showers occurring irregularly. On 20 July, temperature was down to 5 °C again and after that continued to rise steadily until approximately 25 degrees on 27 July. After this day, a couple of showers occurred and temperatures dropped and would remain around 5 to 10 °C for the rest of the period. Water level was very low during the measured period. At the start of the fieldwork, the water level was +4 cm above the surface and steadily decreased in time. Many areas in the tundra were much drier than in previous years with smaller ponds and significant areas with sedges falling dry, in areas where there was standing water in 2008. The water level as measured near the tower however, remained above the surface for the entire period. Active layer depth at the start of the fieldwork was shallow, at 5 cm, and remained low for the fieldwork period, averaging around 20 cm at the start of August. In wet areas however, this depth could be as deep as 40 cm.

5.3.2 Methane fluxes

The observed fluxes, as shown in Figure 5.2, presented great variability. Within hours, fluxes changed by an order of magnitude. These changes coincided with a change in wind direction.

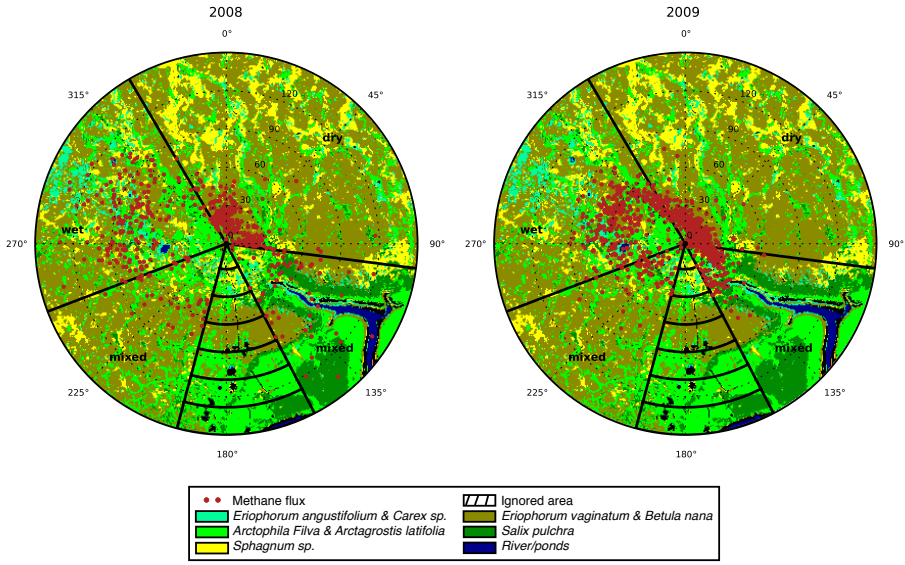

Figure 5.3: Half-hourly methane fluxes plot against the wind direction on top of the satellite derived vegetation map, which shows vegetation composition in a radius of 300 m around the tower. The tower is situated in the center, while the red points indicate the methane flux in (ϕ,r) coordinates where ϕ is wind direction and r the flux magnitude in nmol CH_4 m^{-2} s^{-1}. The measurements are plot along the wind direction and the distance from the center indicates the size of the flux. Apart from wind direction, no further calculations on the source area are used in the plot. The dashed circles indicate the scale of the flux. The striped area indicates the direction from which data was discarded due to influence on the flux from the houses and the generator to the south (which are masked black in the map).

When the wind was blowing from the Northeast, fluxes were low. When the wind came from from the South and West, fluxes were high. This partitioning can be explained by changes in the source area (*Jackowicz-Korczyński et al.*, 2010). Figure 5.3 shows the area around the tower together with the satellite derived vegetation map around the tower. In the center, the tower is shown while radially away from the tower the methane fluxes have been plotted in polar coordinates as a function of wind direction. This picture clearly shows that when the wind is coming from the Northeast, fluxes are much lower.

These different amplitudes can be explained by a difference in vegetation (*Bubier*, 1995). In the background of Figure 5.3, the satellite derived vegetation map is shown and for each sector the fractional vegetation cover is described in Table 5.1. Here it is shown that 63% of the 'Dry' sector is covered by a vegetation type that is associated with low to no methane fluxes, while 19% and 18% of the surface is covered by vegetation that emits average or high amounts of methane. Although the 'Mixed' sector is covered for 59% by dry vegetation types, the amount of vegetation that emits high to very high amounts of methane is much larger, up to 30%. In the 'Wet' sector, the amount of dry vegetation is clearly lower at 51% and the amount of vegetation emitting high amounts of methane is up to 32%, with a clear shift towards the vegetation type dominated by *Eriophorum angustifolium* and *Carex sp*, which show the highest emissions of all vegetation types.

The amount of open water in the various sectors seems low but since most small ponds in the

Table 5.1: Vegetation composition for three wind sectors according to wetness, as shown in Figure 5.3. Percentages are rounded. In the right column, it is shown how the different vegetation types compare relatively in terms of methane emission. Fluxes for the river are unknown, for ponds they are high. For the water cover, a second assessment was made with the use of a high resolution (0.5 m) satellite image, which was able to capture small ponds better.

Sector	Dry	Mixed	Wet	Methane flux
Eriophorum angustifolium & Carex sp.	4%	4%	12%	High to very High
Arctophila fulva & Arctagrostis latifolia	14%	26%	20%	Average to High
Sphagnum sp.	19%	8%	14%	Average
Eriophorum vaginatum & Betula nana	61%	41%	51%	Low to none
Salix pulchra	2%	18%	3%	Low to none
River/Ponds	0%	3%	<1%	Unknown/High
High-res image water cover	<1%	<1%	5%	Unknown/High

area have a similar size as the 2 m resolution of the multispectral satellite image, they are not always classified correctly. The same satellite picture was also available in the monochrome band, with a higher resolution of 0.5 m. From this picture a better assessment of the amount of small ponds (while ignoring the river) could be made and it was found that the dry and the mixed sector had 0.5% open water and the wet area 5%. This has been indicated in Table 5.1. To ascertain whether the size of the obtained vegetation map agreed with the source area of the tower, a footprint analysis was performed for the observed period according to the model presented by *Kormann and Meixner* (2001). Typical dimensions of the footprint would be 100 to 200 m in width and 300 to 500 m in length, for an area that contributes 90% to the flux. Within this area, the highest relative contribution to the measured flux typically comes from an area around 30 to 50 meters away from the tower. When calculated for the radius of Figure 5.3, it was found that this area would contribute 75% to 90% of the flux. The size of the fetch did not show any relationship with wind direction and therefore these values are typical for all three sectors.

5.3.3 Diurnal pattern

In Figure 5.4, the diurnal pattern of methane flux, atmospheric stability and soil temperature are shown for 2008 and 2009, for the duration that the methane eddy covariance was run. Because of the large variation in amplitude between the three sectors, half-hourly measurements have been split up to show diurnal patterns for each sector separately. For each time of day, the average for the methane flux, atmospheric stability and soil temperature was determined for those measurements that were measured at that time and for the same sector. From this, the diurnal pattern of the various model parameters could be determined. Because of its low variation, water level was measured once a day and therefore not included in this graph.
The data for the mixed sector in 2008 shows a large scatter since only a few data points were available for each time step, but for the other sectors enough data points were available to obtain a well averaged diurnal pattern. In all sectors and for all years, the methane flux shows a diurnal pattern, where methane fluxes are low during the night and peak around 3 PM. When compared to the atmospheric stability, we see unstable conditions ($\Phi < 1$) during the day from 6 AM until 9 or 11 PM, followed by stable conditions ($\Phi > 1$) until 6 AM the next

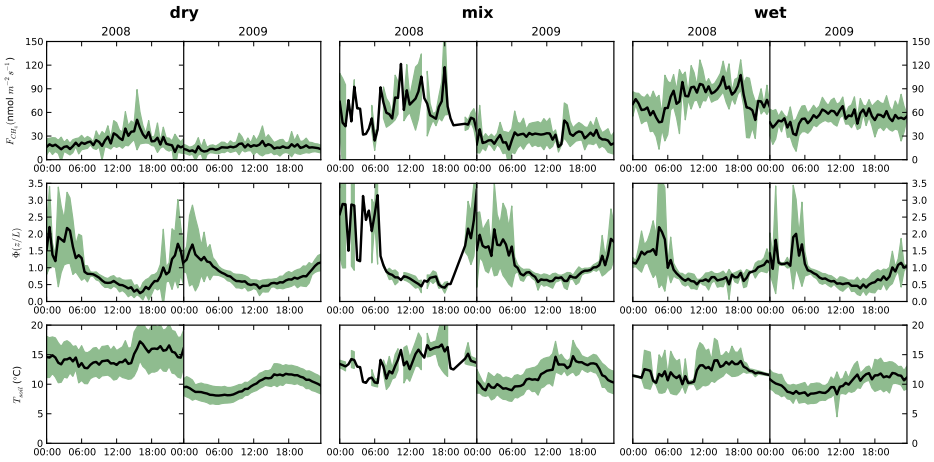

Figure 5.4: Diurnal patterns of methane flux, atmospheric stability and soil temperature. The black line shows the average of half-hourly values while the green shaded area shows standard deviations on these averages.

morning. The atmosphere is most unstable together with the peak in methane flux, around 3 PM, and methane fluxes are lower during stable atmospheric conditions. When compared to soil temperature, we see that it shows a very smooth diurnal pattern with a peak in temperature at the end of the afternoon, around 5 PM, and the lowest temperatures in the morning around 6 AM. In general, atmospheric stability shows an inverse relation to the methane flux while soil temperature lags behind on the peaks in methane flux.

5.3.4 Flux model

To prepare the data for model optimization, all observations under stable conditions where the stability function gave values higher than 5 were discarded, since the upwind area that contributes to the flux approaches infinite in these cases, which makes the eddy covariance method less representative (*Aubinet*, 2008). Also, measurements where the wind was in the direction of the generator and the research station ($155° > \alpha < 195°$), were discarded since these observations were possibly disturbed. In 2008 this concerned 13% of the measurements while only 3% had to be discarded in 2009. Finally, to remove variations in the flux due to short term changes in the footprint, all data for 2008 and 2009 was averaged over three hour periods.

After applying this data selection, the model was optimized separately for the three wind directions that showed distinctively different flux magnitudes as shown in Figure 5.3, due to their different compositions. Furthermore, the model was optimized with both the data of 2008 and 2009, to try to find parameter values that are applicable to both years. To allow for an unbiased calibration and validation, even days were used to calibrate the data and uneven days were used for validation. Scatterplots of stability, Φ, soil temperature, T_{soil}, and water level, w_l, against the observed fluxes are shown in Figure 5.5 and are split out according to the wind direction for the dry, mixed and wet sectors.

The model did not significantly improve by adding additional non-linear relationships from

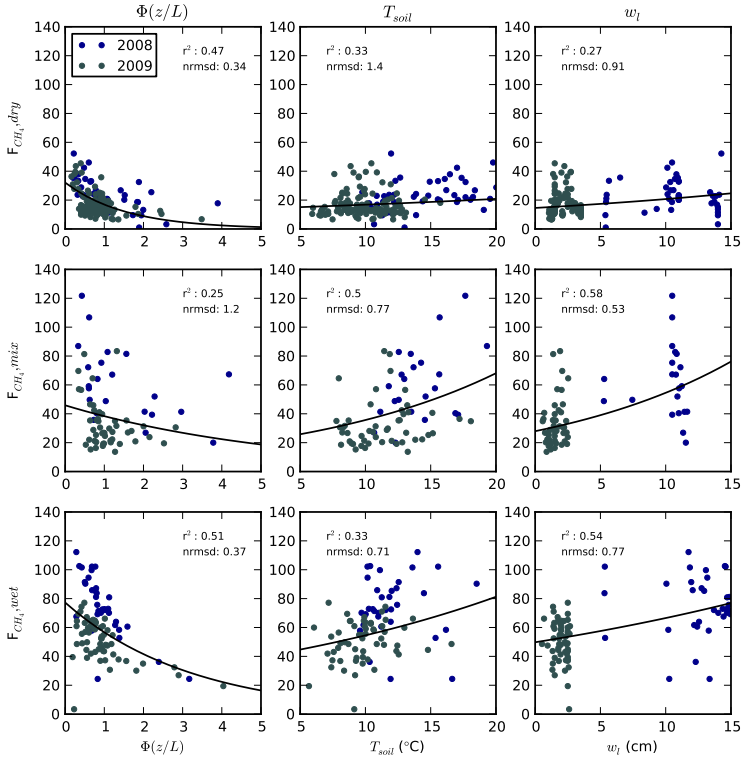

Figure 5.5: Environmental parameters plot against observed methane fluxes. The columns show the parameters, $\Phi(z/L)$, T_{soil} and w_l, while the rows indicate the relationships for the three sectors that the model was optimized for (dry, mixed and wet). Values for 2008 are shown in blue, while the measurements for 2009 are shown in grey. Methane fluxes are in nmol CH_4 m^{-2} s^{-1}

Table 5.2: Values of the model parameters p0 to p4 of Equation 5.2 for the three sub models.

Sector	p_0	p_1	p_2	p_3
Dry	17.3	0.53	1.24	1.04
Mixed	38.6	0.84	1.91	1.07
Wet	57.3	0.73	1.49	1.03

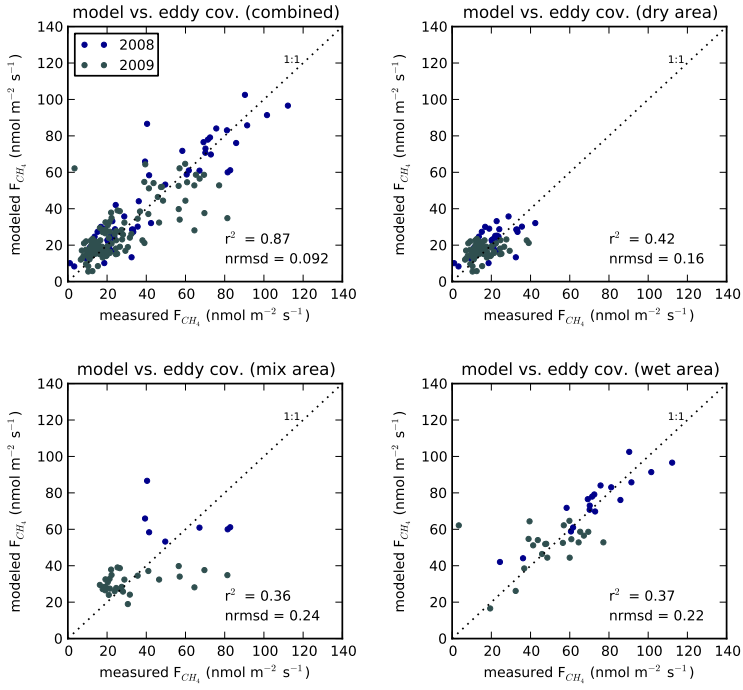

Figure 5.6: Observed vs. measured fluxes. Model calibration has been performed on even days and here model performances for uneven days are shown. The data has been split out to the dry, mixed and wet sectors.

Equation 5.2 with parameters such as wind speed, friction velocity or air pressure. Also, model performance did not change when soil temperature was replaced with air temperature or surface temperature calculated from long wave outgoing radiation. With the chosen parameters, the model performed well (r^2 = 0.87, NRMSD = 0.09) over the two years as shown in Figure 5.6. Here model performance is plot against the independent data set of the uneven days. Split out into the two years, the model and the data from 2008 showed a slightly better fit when compared to 2009 (r^2=0.91, NRMSD=0.11 for 2008 and r^2 = 0.72, NRMSD = 0.14 for 2009). Figure 5.6 also shows the performance of the three sub models for the dry, mixed and wet sectors, which had a r^2 of 0.42, 0.36 and 0.37, respectively. The NRMSD was 0.16, 0.24 and 0.22 for the wet, mixed and dry sectors. Furthermore, a 1:1 line is plotted in the figure to show the departure of the modeled values from the data.

In Figure 5.7, the time series of fluxes and the model are shown as they changed throughout the season. This figure shows that the model describes the temporal variation of the observed fluxes very well. In this figure, the model has also been run for the field campaign in 2007 and the period preceding the start of the eddy covariance in 2008. To validate the model for these periods, the modeled result has also been compared to flux chamber measurements that were performed in the vicinity of the tower in 2007, 2008 and 2009. This data was upscaled with the vegetation distribution of Table 5.1, along the dominant wind direction at the time of the flux measurement. Apart from the period following 26 July 2007, the chamber fluxes and the model show good agreement.

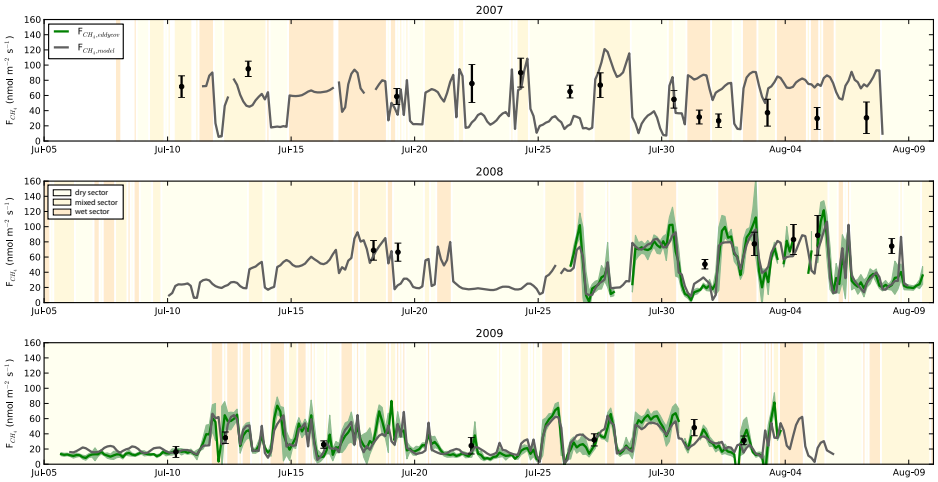

Figure 5.7: Methane fluxes as calculated with the chamber method (black errorbars), eddy covariance (green line) and the model (grey line). The model and the eddy covariance are plot in three-hourly intervals. The green shaded region indicates the standard deviation of the measured flux within that period. The yellow background indicates the predominant wind direction for that period. Light yellow represents the dry sector, medium yellow represents the mixed sector and the darker yellow represents the wet sector.

While the model performs well to reproduce the observed fluxes, it has been constructed from the combined output of three sub models, as shown in Figure 5.7, and this provides a fragmented view of the emissions from the dry, mixed and wet sectors. To show the absolute difference in emissions from these areas, the cumulative methane fluxes of the combined model and its sub models are shown in Figure 5.8. From this figure it becomes clear that the total emission of the wet sector is around 3 times higher than the emission of the dry sector, while the mixed sector shows around 2 to 2.5 times higher fluxes than the dry sector. This also follows from the values of the parameter p_0 in Table 5.2, which is 17.3, 38.6 and 57.3 for the dry, mixed and wet sectors, respectively. With an emission that is slightly below the average of the three sectors, the combined model fits in between. It is also suggested from Figure 5.8 that methane emissions were highest in 2007, somewhat lower in 2008 and at its lowest in 2009.

However, the outcome of the model is tuned to data measured by the eddy covariance system, which varies with the wind direction. This means that chance determines how often a sector contributes to the overall flux and the model does not show the spatially averaged methane emission. To obtain a better estimate of the average methane flux emitted by the area within the footprint of the tower, the sub models for the three sectors have been averaged and weighted according to the radial size of the sector. Average fluxes are estimated to be 56.5, 48.7 and 30.4 nmol CH_4 m^{-2} s^{-1} for 2007, 2008 and 2009. The cumulative sum for one month (30 days), which is approximately the timescale depicted in Figure 5.8, was found to be 2.2 g CH_4 m^{-2} $month^{-1}$, 2.0 g CH_4 m^{-2} $month^{-1}$, and 1.3 g CH_4 m^{-2} $month^{-1}$ for the three years.

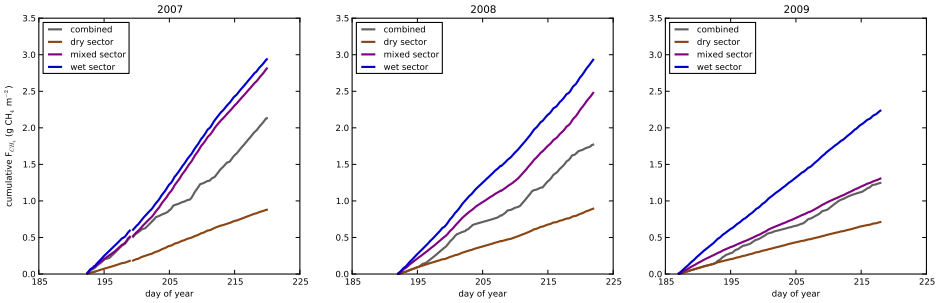

Figure 5.8: Cumulative plots of the model vs the day of year for 2007, 2008 and 2009. The grey line shows the cumulative flux of the model as it was plot in figure 6, with different model parameters with varying wind direction. The other lines show the cumulative plots of the sub models for the dry (=brown), mixed (=purple) and wet (=blue) sectors.

5.4 Discussion

5.4.1 Eddy covariance measurements

In this study, the methane fluxes measured by the eddy covariance setup were shown to be highly variable and exhibited distinctively different magnitudes between years. In Figure 5.2, the conditions for all measurement years are shown and it is obvious that water level, temperature and, as a result, methane fluxes were higher in 2008, compared to 2009. Also, because of the higher temperatures, active layer depth was larger in 2008 than in 2009. Contrary to these long-term differences, the underlying causes of the short-term changes in methane fluxes aren't immediately clear from Figure 5.2. However, Figure 5.3 clearly shows that methane fluxes differed with a change in wind direction and thus in source area. The area to the South and the West was wetter and had a vegetation composition with a higher sedge vegetation cover. Since this vegetation type shows the highest methane fluxes (*van Huissteden et al.*, 2005), it is not surprising that fluxes measured at the eddy covariance tower were higher when the predominant wind was blowing from these directions. From these two directions, fluxes were even higher for Westerly winds, since that sector included a higher number of ponds, associated with high methane fluxes (*Bastviken et al.*, 2004; *Walter et al.*, 2006) and higher amounts of wet vegetation as shown in Table 5.1. The area to the Northwest was much dryer with less sedge vegetation and almost no ponds, resulting in much lower fluxes compared to the other wind directions.

These changes in fetch made it difficult to ascertain whether fluxes showed a diurnal pattern but by splitting the data up in the three sectors and arranging them according to the time of day, a plot of diurnal patterns could be made as shown in Figure 5.4. In this figure, it was shown that atmospheric stability and methane flux showed an inverse relation, with higher fluxes under unstable conditions during daytime, and lower fluxes under stable conditions during nighttime. At the same time, soil temperature also showed a clear diurnal pattern but peaks in soil temperature were mostly seen after the peak in methane flux occurred. This would suggest that the effect of soil temperature on methane fluxes is obscured by the effect of atmospheric stability, which has been observed before for eddy covariance measurements of CO_2 (*Hollinger et al.*, 1998). Under unstable conditions, air parcels close to the ground are warmer and this increases buoyancy and vertical transport of air, including methane. During stable

conditions, air parcels close to the ground are colder and vertical transport is constrained, damping methane fluxes. In these periods, higher methane concentrations were observed regularly at the tower, indicating a buildup of methane. While previous studies considered mostly daily values, this study uses smaller timescales and as such the diurnal effect of atmospheric stability on vertical transport has to be taken into account.

5.4.2 Flux model performance

Following the interpretation of the measurements, atmospheric stability, soil temperature and water level were used as parameters to the model. In Figure 5.6, the model results have been plotted against the eddy covariance measurements, along with the correlation and NRMSD. From the correlations and the NRMSD, we see that the combined model simulated the observed fluxes well (r^2 = 0.87, NRMSD = 0.09) and they show a good 1:1 linear agreement. For the components of the model, the dry sector is modeled best (r^2 = 0.42, NRMSD = 0.16), while the mixed and wet sector are modeled less well (r^2 = 0.36 and 0.37, NRMSD = 0.24 and 0.22 respectively). These model performances are reasonable, considering that each sector holds many different vegetation types that are not uniformly distributed, which causes variation in the signal when the fetch within a sector changes. This perhaps explains the larger spread between model and data for the mixed sector. This variability in the data is not explained by the model and is possibly due to footprint changes. Arguably, this scatter could be addressed by calculating the different contributions of each vegetation type with the use of the footprint model and the satellite derived vegetation map. However, footprint calculations have a high uncertainty of their own and it is not ensured that their application would improve model accuracy. Also, by splitting up the model in even smaller footprint areas, the amount of data available for calibration would be reduced, which would complicate robust model optimization. By dividing the area in a limited number of sectors, it is ensured that the model remains simple, while achieving acceptable performance.
The correlations and the NRMSD show that atmospheric stability explained most of the variation observed in the dry and wet sector (r^2 = 0.47 and 0.51, NRMSD=0.34 and 0.37, respectively) while it was a poor predictor in the mixed sector (r^2=0.25, NRMSD=1.2). Soil temperature was a poor predictor in the dry sector but explained part of the variation in the mixed and wet sector (r^2=0.5 and 0.33, NRSMD=0.77 and 0.71). Finally, water level was the best predictor to observed variations in the mixed sector (r^2=0.58, NRMSD=0.53), while only part of the variation in the dry and wet sector was explained by water level (r^2=0.27 and 0.54, NRSMD=0.91 and 0.77). The strong relation with water level in the mixed sector can be explained by its vegetation distribution and topography. This area shows gentle small-scale topographic differences and as such, a small increase in the water level leads to a large increase in flooded areas and thus in methane fluxes. This has also been observed in the field: the extent of inundated areas was much lower in 2009 than in 2008, which is also represented by the partitioning of the fluxes for these years along water level. Water level also partly explained the variation in the wet sector, but due to the higher amount of ponds, whose areal size is less sensitive to water level changes, the residuals from fitting this parameter were higher. In the dry sector, it seems that no strong relationship with water level exists, which can be explained by the already low amount of wet areas in this sector.

5.4.3 Alternative parameter selection

Previous studies on eddy covariance measurements of methane fluxes have found relationships with various parameters such as mean windspeed (*Fan et al.*, 1992), temperature, water level (*Suyker et al.*, 1996), active layer depth (*Friborg et al.*, 2000), friction velocity (*Wille et al.*, 2008) and air pressure (*Sachs et al.*, 2008). Not all of the these relationships were found in the current study, which is possibly due to the use of three hour averages. Although some have sought to explain the diurnal variation (*Zona et al.*, 2009), most previous studies sought relationships with daily averaged values. This study provides a framework for a higher temporal resolution but this may lead to different relationships with environmental parameters.
In some of the previous studies wind speed and friction velocity were shown to increase methane emissions from open water and therefore we tested model performance when wind speed or friction velocity were used, while leaving atmospheric stability out of the equation. The resulting fits of friction velocity and wind speed against methane fluxes showed low correlations (typically around 0.2) and a high NRMSD of 2 or 3. Also, optimizations for the three sectors differed where some fits showed an increase in fluxes with higher friction velocity or wind speed, while others showed opposite fits. Actually, the model performed better when friction velocity and wind speed were left out of the equation, which was also indicated by the high NRMSD values. Apparently, friction velocity and wind speed were not suitable to explain fluxes on this high resolution and they were therefore not used in the model equation.
Also, model results did not improve when air pressure was added. It has been established that air pressure has a direct effect on ebullition from peatlands (*Kellner et al.*, 2006) and it has since been used to explain variations in tundra methane fluxes as measured by eddy covariance (*Sachs et al.*, 2008). However, in this model the effect of air pressure was not pronounced. By adding air pressure, the r^2 of the model improved slightly by 0.01 points, mostly because of a slightly better fit for the dry sector. On the other hand, model performance became much worse for the mixed sector. The optimization with air pressure resulted in a poor fit for temperature with a slope near to zero. For the wet sector, a marginal relationship was found with air pressure, which did not influence the model result. Because of these varying responses to air pressure and its low contribution to improving the model, it was decided to exclude air pressure from the model.
This lack of a relationship with air pressure might be explained by the soil conditions at the site. Air pressure effects ebullition but for large pulses to occur, a lot of methane has to be built up in the soil. This would require a large reservoir for methane while at this site the peat layer is only 15 cm thick, underlain by compact silt and the active layer reaches a maximum of just 30 to 50 cm. This provides for limited space where methane can accumulate, which is required to see significant pulses of methane when air pressure drops. Also, the division of fluxes into the three wind directions could further explain the poor fit with air pressure. Air pressure changes occur at timescales of several days, while a limited amount of measurement days were available per sector. More measurements, with a larger variation in air pressure for all wind directions, might lead to an improved understanding of air pressure effects on the measured fluxes.
Apart from wind speed, turbulence and air pressure, another parameter that was not included in the parameter set, was active layer depth. Active layer depth can be used to model methane fluxes as shown by *Friborg et al.* (2000) and fluxes at a small plot scale showed differences along active layer depth at this site (*van Huissteden et al.*, 2005). As can be seen in Figure 5.2, the temporal variation of the active layer was quite low, with a slow increase during the season. The largest difference in active layer was between the two measurement years, similar

to the relationship with water level and a good model fit for active layer depth would thus result in a poor fit with water level, or vice versa. Besides, a deeper active layer would lead to higher fluxes in the model and the very deep active layer in 2007 would thus translate into a higher amplitude of the modeled flux for that year. Since the model already simulated fluxes for August 2007 that were higher than measurements performed with the independent flux chambers, this overestimation would only be increased by adding active layer depth. Therefore, active layer depth was not included in the model.

5.4.4 Comparison with chamber fluxes and extension of the model

To compare the eddy covariance and the model with an independent technique, measured and modeled fluxes were also plotted with simultaneously performed flux chamber measurements in Figure 5.7. These flux measurements were upscaled according to the vegetation composition of the sector for the wind direction at the time of measurement. For both 2008 and 2009, chamber fluxes mostly agree with the eddy covariance measurements. Figure 5.7 shows the results from the model, which in 2008 and 2009 shows good agreement with the chamber measurements and the eddy covariance.
Because of the good agreement between the model and the chamber flux measurements, it was decided to apply the model to the fieldwork period of 2007. In that year methane fluxes were measured just with the chamber flux technique but the number of flux measurements was higher than in 2008 and 2009, allowing for good comparison. Figure 5.7 shows that the model and the chamber fluxes agree quite well for the month of July but that in August modeled fluxes are much higher than the upscaled chamber fluxes. As can be seen from Figure 5.2, soil temperatures lowered at the start of August, which led to lower methane fluxes. Apparently the measured chamber fluxes in 2007 were more sensitive to a lowering of soil temperature than the model would suggest. In 2007, the soil thermal regime was very different from the other years, since the start of the growing season was much earlier and this led to a much thicker active layer. Because the model was calibrated to years with a shallower active layer depth, the different soil conditions could provide an explanation for the poor agreement between the chamber flux measurements and the model. Although care has to be taken when the model is applied to years with highly different environmental conditions, the model agreed well for the majority of the measurements in 2007.
With the addition of the model runs for the periods without eddy covariance measurements, estimates of average fluxes for the summer fieldwork seasons of 2007, 2008 and 2009 can be made. By using the average of the three sub models, in proportion to the size of each sector, average methane fluxes were estimated at 56.5, 48.7 and 30.4 nmol CH_4 m^{-2} s^{-1} for 2007, 2008 and 2009, respectively. Compared to other eddy covariance studies on methane from around the Arctic, as shown in Table 5.3, this site exhibits methane emission rates amongst the highest reported.

5.5 Conclusion

In this study, the eddy covariance technique was used to measure methane fluxes at a tundra site in Northeastern Siberia. These fluxes showed to be highly variable, with large changes occurring within hours. From a careful data analysis, most of these variations could be explained

Table 5.3: Comparison of summer eddy covariance measurements of methane from various (sub) Arctic sites

Region	Site	Vegetation	Average flux (nmol CH_4 m^{-2} s^{-1})	Reference
Alaska	Bethel	Dry upland tundra	7.9±2	*Fan et al.* (1992)
Alaska	Bethel	Wet meadow tundra	20.9±2	*Fan et al.* (1992)
Alaska	Barrow	Wet sedge tundra	17.7	*Zona et al.* (2009)
Greenland	Zackenberg	High Arctic fen	7.2-86.6	*Friborg et al.* (2000)
Sweden	Stordalen	Subarctic mire	107.4±45.0	*Jackowicz-Korczyński et al.* (2010)
Siberia	Lena Delta	Wet polygonal tundra	11.0-16.1	*Wille et al.* (2008); *Sachs et al.* (2008)
Siberia	Chokurdakh	Mixed moist tundra	30.4-56.5	This study

by a change in fetch, atmospheric stability, soil temperature and water level. After splitting the data into three sectors, according to their degree of wetness, these parameters were used to calibrate a non-linear model, which successfully reproduced the observed fluxes. Model performance did not significantly improve by the addition of air pressure, active layer depth, wind speed or friction velocity. This is possibly due to the higher temporal resolution and the limited amount of measurement days per sector.

Since the model was optimized on measurements from two separate years, the underlying causes of the inter-annual variation in fluxes could be well defined. These differences were explained mostly by water level, followed by soil temperature. Following these relationships, the model was extended outside of the calibrated period and compared to independent flux chamber measurements. Although some discrepancies were noted between the flux chamber measurements and the model, overall the two methods compared well. From the output of the model, it was derived that the average summer fluxes for 2007, 2008 and 2009 were 56.5, 48.7 and 30.4 nmol CH_4 m^{-2} s^{-1}, respectively. These values are amongst the highest reported when compared to other sites across the Arctic.

Although previous studies have measured within-day variation in methane fluxes as measured by eddy covariance, to our knowledge there are currently no studies that have provided a method to model fluxes at such short time steps. Because of the short time step of the presented method, it makes it ideal for gap-filling methane flux data, of which currently few alternatives are available. Also, if the model parameterization has been performed on a dataset that shows enough spread in variation between and within years, the model can be used to estimate methane fluxes for other years as well.

This study also showed that the measurements performed with the eddy covariance method were very dependent on changes in the wind direction and the associated source area. These changes in fetch led to a fragmented measurement of methane fluxes of the area. This problem could successfully be accounted for by tuning the model separately for each source area. Subsequently, these sub models could be used to determine the spatially averaged emissions despite the highly heterogenous terrain. However, when performing eddy covariance measurements of methane within an area that shows these kinds of large differences in water level and areal extent of ponds, preferably the use of more than one tower is needed to determine spatially integrated methane emissions more accurately.

Acknowledgements

We like to acknowledge the people at the Institute for Biological Problems of the Cryolithozone SB RAS in Yakutsk for their assistance in and outside the field, especially Alexander V. Kononov for all the help with the import of equipment in 2008. Also, we like to thank T.G.

Strukova and the rangers of the Kytalyk Resource Reserve for their logistical support to and from the site and other assistance. Furthermore, we like to acknowledge the people from the engineering and electronics workshop at the VU University Amsterdam, especially Rob Stoevelaar and Ron Lootens, without whom the successful installation of the eddy covariance equipment would not have been possible. We want to acknowledge the Darwin Center for Biogeosciences who supported this research with a grant to F.J.W. Parmentier (142.16.1041). Additional funding for successful completion of this research was provided by the NWO Dutch Russian research cooperation programme entitled "Long term observation of soil carbon and methane fluxes in Siberian tundra" (047.017.037) and the GreenCyclesII training network (7th Framework programme reference 238366).

References

Aubinet, M., Eddy covariance CO_2 flux measurements in nocturnal conditions: An analysis of the problem, *Ecological Applications*, *18*(6), 1368--1378, 2008.

Aubinet, M., et al., Estimates of the annual net carbon and water exchange of forests: The EUROFLUX methodology, *Advances In Ecological Research, Vol 30*, *30*, 113--175, 2000.

Bastviken, D., J. Cole, M. Pace, and L. Tranvik, Methane emissions from lakes: Dependence of lake characteristics, two regional assessments, and a global estimate, *Global Biogeochemical Cycles*, *18*(4), GB4009, 2004.

Bubier, J. L., The relationship of vegetation to methane emission and hydrochemical gradients in northern peatlands, *Journal of Ecology*, *83*(3), 403--420, 1995.

Christensen, T. R., S. Jonasson, T. V. Callaghan, and M. Havstrom, Spatial variation in high-latitude methane flux along a transect across siberian and european tundra environments, *Journal Of Geophysical Research-Atmospheres*, *100*(D10), 21,035--21,045, 1995.

Christensen, T. R., T. R. Johansson, H. J. Akerman, M. Mastepanov, N. Malmer, T. Friborg, P. M. Crill, and B. H. Svensson, Thawing sub-arctic permafrost: Effects on vegetation and methane emissions, *Geophysical Research Letters*, *31*(4), L04,501, 2004.

Corradi, C., O. Kolle, K. M. Walter, S. A. Zimov, and E.-D. Schulze, Carbon dioxide and methane exchange of a north-east Siberian tussock tundra, *Global Change Biology*, *11*(11), 1910--1925, 2005.

Denmead, O. T., Approaches to measuring fluxes of methane and nitrous oxide between landscapes and the atmosphere, *Plant And Soil*, *309*(1-2), 5--24, 2008.

Dorrepaal, E., S. Toet, R. S. P. van Logtestijn, E. Swart, M. J. van de Weg, T. V. Callaghan, and R. Aerts, Carbon respiration from subsurface peat accelerated by climate warming in the subarctic, *Nature*, *460*(7255), 616--U79, 2009.

Fan, S. M., S. C. Wofsy, P. S. Bakwin, D. J. Jacob, S. M. Anderson, P. L. Kebabian, J. B. McManus, C. E. Kolb, and D. R. Fitzjarrald, Micrometeorological measurements of CH_4 and CO_2 exchange between the atmosphere and sub-arctic tundra, *Journal Of Geophysical Research-Atmospheres*, *97*(D15), 16,627--16,643, 1992.

Friborg, T., T. R. Christensen, B. U. Hansen, C. Nordstroem, and H. Soegaard, Trace gas exchange in a high-arctic valley 2. Landscape CH_4 fluxes measured and modeled using eddy correlation data, *Global Biogeochemical Cycles*, *14*(3), 715--723, 2000.

Hendriks, D. M. D., A. J. Dolman, M. K. van der Molen, and J. van Huissteden, A compact and stable eddy covariance set-up for methane measurements using off-axis integrated cavity output spectroscopy, *Atmospheric Chemistry And Physics*, *8*(2), 431--443, 2008.

Hollinger, D., et al., Forest-atmosphere carbon dioxide exchange in eastern Siberia, *Agricultural and Forest Meteorology*, *90*(4), 291--306, 1998.

Jackowicz-Korczyński, M., T. R. Christensen, K. Backstrand, P. M. Crill, T. Friborg, M. Mastepanov, and L. Ström, Annual cycle of methane emission from a subarctic peatland, *Journal of Geophysical Research-Biogeosciences*, *115*, G02,009, 2010.

Kaufman, D. S., et al., Recent Warming Reverses Long-Term Arctic Cooling, *Science*, *325*(5945), 1236--1239, 2009.

Kellner, E., A. J. Baird, M. Oosterwoud, K. Harrison, and J. M. Waddington, Effect of temperature and atmospheric pressure on methane (CH_4) ebullition from near-surface peats, *Geophysical Research Letters*, *33*(18), L18,405, 2006.

Kormann, R., and F. X. Meixner, An analytical footprint model for non-neutral stratification, *Boundary-Layer Meteorology*, *99*(2), 207--224, 2001.

Kutzbach, L., C. Wille, and E.-M. Pfeiffer, The exchange of carbon dioxide between wet arctic tundra and the atmosphere at the Lena River Delta, Northern Siberia, *Biogeosciences*, *4*(5), 869--890, 2007.

Levenberg, K., A Method for the Solution of Certain Non-Linear Problems in Least Squares, *Quarterly of applied mathematics*, *2*, 164--168, 1944.

Mastepanov, M., C. Sigsgaard, E. J. Dlugokencky, S. Houweling, L. Ström, M. P. Tamstorf, and T. R. Christensen, Large tundra methane burst during onset of freezing, *Nature*, *456*(7222), 628--U58, 2008.

McGuire, A. D., et al., Sensitivity of the carbon cycle in the Arctic to climate change, *Ecological Monographs*, *79*(4), 523--555, 2009.

Moncrieff, J. B., et al., A system to measure surface fluxes of momentum, sensible heat, water vapour and carbon dioxide, *Journal of Hydrology*, *189*(1-4), 589--611, 1997.

Moore, C. J., Frequency-response corrections for eddy-correlation systems, *Boundary-Layer Meteorology*, *37*(1-2), 17--35, 1986.

Morrissey, L. A., D. B. Zobel, and G. P. Livingston, Significance of stomatal control on methane release from carex-dominated wetlands, *Chemosphere*, *26*(1-4), 339--355, 1993.

Nakai, T., M. K. van der Molen, J. H. C. Gash, and Y. Kodama, Correction of sonic anemometer angle of attack errors, *Agricultural and Forest Meteorology*, *136*(1-2), 19--30, 2006.

Nakano, T., S. Kuniyoshi, and M. Fukuda, Temporal variation in methane emission from tundra wetlands in a permafrost area, northeastern Siberia, *Atmospheric Environment*, *34*(8), 1205--1213, 2000.

Oechel, W. C., S. J. Hastings, G. L. Vourlitis, M. Jenkins, G. Riechers, and N. Grulke, Recent change of arctic tundra ecosystems from a net carbon-dioxide sink to a source, *Nature*, *361*(6412), 520--523, 1993.

Oechel, W. C., G. L. Vourlitis, S. Brooks, T. L. Crawford, and E. Dumas, Intercomparison among chamber, tower, and aircraft net CO_2 and energy fluxes measured during the Arctic System Science Land-Atmosphere-Ice Interactions (ARCSS-LAII) Flux Study, *Journal Of Geophysical Research-Atmospheres*, *103*(D22), 28,993--29,003, 1998.

Paulson, C. A., The mathematical representation of wind speed and temperature profiles in the unstable atmospheric surface layer, *Journal Of Applied Meteorology*, *9*(6), 857--861, 1970.

Sachs, T., C. Wille, J. Boike, and L. Kutzbach, Environmental controls on ecosystem-scale CH_4 emission from polygonal tundra in the Lena River Delta, Siberia, *Journal of Geophysical Research-Biogeosciences*, *113*, G00A03, 2008.

Schuur, E. A. G., et al., Vulnerability of permafrost carbon to climate change: Implications for the global carbon cycle, *Bioscience*, *58*(8), 701--714, 2008.

Serreze, M. C., et al., Observational evidence of recent change in the northern high-latitude environment, *Climatic Change*, *46*(1-2), 159--207, 2000.

Suyker, A. E., S. B. Verma, R. J. Clement, and D. P. Billesbach, Methane flux in a boreal fen: Season-long measurement by eddy correlation, *Journal Of Geophysical Research-Atmospheres*, *101*(D22), 28,637--28,647, 1996.

Torn, M. S., and F. S. Chapin III, Environmental and biotic controls over methane flux from arctic tundra, *Chemosphere*, *26*(1-4), 357--368, 1993.

van der Molen, M. K., J. H. C. Gash, and J. A. Elbers, Sonic anemometer (co)sine response and flux measurement - II. The effect of introducing an angle of attack dependent calibration, *Agricultural and Forest Meteorology*, *122*(1-2), 95--109, 2004.

van der Molen, M. K., M. J. Zeeman, J. Lebis, and A. J. Dolman, EClog: A handheld eddy covariance logging system, *Computers and Electronics in Agriculture*, *51*(1-2), 110--114, 2006.

van der Molen, M. K., J. van Huissteden, F. J. W. Parmentier, A. M. R. Petrescu, A. J. Dolman, T. C. Maximov, A. V. Kononov, S. V. Karsanaev, and D. A. Suzdalov, The growing season greenhouse gas balance of a continental tundra site in the Indigirka lowlands, NE Siberia, *Biogeosciences*, *4*(6), 985--1003, 2007.

van Huissteden, J., T. C. Maximov, and A. J. Dolman, High methane flux from an arctic floodplain (Indigirka lowlands, eastern Siberia), *Journal of Geophysical Research-Biogeosciences*, *110*(G2), G02,002, 2005.

Verma, S. B., F. G. Ullman, D. Billesbach, R. J. Clement, J. Kim, and E. S. Verry, Eddy-correlation measurements of methane flux in a northern peatland ecosystem, *Boundary-Layer Meteorology*, *58*(3), 289--304, 1992.

Vourlitis, G. L., and W. C. Oechel, Landscape-scale CO_2, H_2O vapour and energy flux of moist-wet coastal tundra ecosystems over two growing seasons, *Journal of Ecology*, *85*(5), 575--590, 1997.

Walter, K. M., S. A. Zimov, J. P. Chanton, D. Verbyla, and F. S. Chapin III, Methane bubbling from Siberian thaw lakes as a positive feedback to climate warming, *Nature*, *443*(7107), 71--75, 2006.

Webb, E. K., G. I. Pearman, and R. Leuning, Correction of flux measurements for density effects due to heat and water vapour transfer, *Quarterly Journal Of The Royal Meteorological Society*, *106*(447), 85--100, 1980.

Whalen, S. C., and W. S. Reeburgh, Consumption of atmospheric methane by tundra soils, *Nature*, *346*(6280), 160--162, 1990.

Wille, C., L. Kutzbach, T. Sachs, D. Wagner, and E.-M. Pfeiffer, Methane emission from Siberian arctic polygonal tundra: eddy covariance measurements and modeling, *Global Change Biology*, *14*(6), 1395--1408, 2008.

Zahniser, M. S., D. D. Nelson, J. B. McManus, and P. L. Kebabian, Measurement of trace gas fluxes using tunable diode-laser spectroscopy, *Philosophical Transactions of The Royal Society Of London Series A*, *351*(1696), 371--381, 1995.

Zona, D., W. C. Oechel, J. Kochendorfer, K. T. P. U, A. N. Salyuk, P. C. Olivas, S. F. Oberbauer, and D. A. Lipson, Methane fluxes during the initiation of a large-scale water table manipulation experiment in the Alaskan Arctic tundra, *Global Biogeochemical Cycles*, *23*, GB2013, 2009.

Chapter 6

Longer growing seasons do not appear to increase net carbon uptake in Northeastern Siberian tundra[1]

Abstract
With global warming, snowmelt is occurring earlier and growing seasons are becoming longer around the Arctic. It has been suggested that this would lead to more uptake of carbon due to a lengthening of the period in which plants photosynthesize. To investigate this suggestion, 8 consecutive years of eddy covariance measurements at a Northeastern Siberian tundra site were investigated for patterns in net ecosystem exchange, photosynthesis and ecosystem respiration.
While photosynthesis showed no clear increase with longer growing seasons, it was clearly increased by warmer summers. Due to these warmer temperatures however, the increase in uptake was mostly offset by an increase in respiration. Therefore, overall variability in net carbon uptake was low and no relationship with growing season length was found. Furthermore, the highest net uptake of carbon occurred with the shortest and the coldest growing season. Low uptake of carbon mostly occurred with longer or warmer growing seasons. We thus conclude that the net carbon uptake of this ecosystem is more likely to decrease rather than to increase under a warmer climate. Furthermore, a longer growing season will also lead to more methane emissions. A lengthening of the growing season is therefore very likely to reduce the greenhouse gas sink of this ecosystem.

6.1 Introduction

The stability of the net carbon exchange of tundra under a changing climate depends on the combined response of respiration and photosynthesis. A longer growing season, caused by

[1] The contents of this chapter has been submitted as "Longer growing seasons do not appear to increase net carbon uptake in Northeastern Siberian tundra" to JGR-Biogeosciences

earlier snowmelt, may increase net photosynthesis. It has been suggested that this would result in an increase in biomass and carbon sink (*Churkina et al.*, 2005). However, respiration may also increase due to the the longer snow free periods, stimulated by overall higher temperatures, and in turn this would reduce the magnitude of the carbon sink. Since the Arctic contains large amounts of carbon in its cold, frozen soils (*Tarnocai et al.*, 2009), the specific way in which photosynthesis and respiration in Arctic ecosystems react, can have large impacts on the global carbon cycle (*McGuire et al.*, 2009).

Changes in the Arctic are not only expected but some have already been observed. Arctic temperatures are rising faster than the global average (*Serreze et al.*, 2000; *Chapin III et al.*, 2005; *Kaufman et al.*, 2009) and it has been shown that snowmelt in the Arctic is occurring earlier from several days up to two weeks per decade (*Dye*, 2002; *Smith et al.*, 2004; *Høye et al.*, 2007). While these changes in snowmelt seem small in absolute terms, they are large relative to the short Arctic growing season. This has already led to an earlier flowering of plants and a higher primary productivity (*Myneni et al.*, 1997; *Zhou et al.*, 2001; *Høye et al.*, 2007; *Post et al.*, 2009). In contrast to this increase in the uptake of carbon, respiration is also likely to increase with higher temperatures (*Lloyd and Taylor*, 1994). Recently it has been shown that increases in respiration can also originate from deeper soil layers that have become available for respiration after permafrost degradation (*Schuur et al.*, 2008; *Dorrepaal et al.*, 2009). Since photosynthesis and respiration fluxes act in opposite directions, their relative change will determine the future sink function of these ecosystems (*Welker et al.*, 2004).

Although estimated future changes in photosynthesis and respiration have been simulated in models, at the moment more, especially long term, measurements are required to determine realistic responses (*Piao et al.*, 2007; *Sitch et al.*, 2007; *Euskirchen et al.*, 2009). In the past, a number of eddy covariance studies of carbon cycling in the Arctic have been established that provide more insight in the dynamics of this ecosystem. However, most of these studies have been performed in Scandinavia or Alaska because of the difficult logistic conditions in the rest of the Arctic (*Fan et al.*, 1992; *Oechel et al.*, 2000; *Williams et al.*, 2000; *Hargreaves et al.*, 2001; *Harazono et al.*, 2003; *Aurela et al.*, 2004; *Beringer et al.*, 2005; *Kwon et al.*, 2006; *Lund et al.*, 2010). And although the Siberian part of the Arctic has been studied in several eddy covariance studies (*Corradi et al.*, 2005; *Kutzbach et al.*, 2007; *van der Molen et al.*, 2007), stations with long term measurements of 5 years or more, that are required to observe the inter annual variation of carbon fluxes, still remain preciously scarce outside of Alaska and Scandinavia (*Groendahl et al.*, 2007).

This paper presents the first long term ($>$ 5 years) dataset from a Northeastern Siberian tundra site, spanning the period 2003 to 2010. To our knowledge, there are no other stations in the region that have a measurement record of similar length, and these measurements fill a large gap in our knowledge of the carbon cycling of this region. By breaking down the measurements of net ecosystem exchange to its components, ecosystem respiration and photosynthesis, we will show how these carbon fluxes change along a large range of summer temperatures and different growing season lengths. We will then use these relationships to analyze the stability of the carbon uptake by this ecosystem in a changing climate.

6.2 Materials and Methods

6.2.1 Site Description

Climate

The study site (70°49'44.9" N, 147°29'39.4" E) lies in the nature reserve 'Kytalyk', 30 km Northwest of the town of Chokurdakh in the republic of Yakutia (Sacha) in Northeastern Siberia, as indicated in Figure 6.1. The climate of this region is continental with temperatures as low as -25 to -40 °C in winter, 5 to 25 °C in summer and an annual average of -10.5 °C. The large variation in summer temperatures is due to the close proximity of the Arctic Ocean, 100 km to the North. When the wind is coming from this direction, temperatures are low and when the wind is coming from the warm Siberian continent to the South, temperatures are high. During the summer, 50% of the yearly precipitation falls as rain, while the other half falls as snow during the rest of the year. The total yearly precipitation is low with an average of approximately 220 mm.

Snowmelt usually occurs at the end of May or the start of June. While the snow disappears quickly, the vegetation response to snowmelt lags a significant amount of time. Shrubs don't show bud break until after approximately 4 weeks, when a significant amount of heat has been accumulated in the soil, leading to the establishment of a thawing layer, and air temperatures have risen high enough. After bud break, photosynthesis rates are highly variable from day to day but show rather stable long-term trends. The growing season usually stops again at the end of August or the start of September, when daylight quickly diminishes and temperatures are rapidly dropping.

Figure 6.1: Location of the research site, indicated with the red star.

Soil and vegetation

The research area is located in a depression that originally formed the lakebed of a thaw lake of probably Early Holocene age, that was drained in the past by fluvial erosion. The topsoil consists of an organic layer of 10 to 15 cm, underlain by silt deposits. Although the area has no significant slope, apart from some isolated hills, cryogenic processes have led to micro topographical differences within the landscape, where ice lenses have created small mounds or palsa-like features which cause elevation differences of at most a metre. In between these higher areas, depressions occur where standing water remains during summer, especially in areas where ice wedges are actively expanding, and in some areas small ponds are created. Ice-wedge polygons also occur within the area, although less clearly visible near the measurement tower.

Vegetation in the drier areas consists of *Betula nana* and *Salix pulchra* shrubs, *Eriophorum vaginatum* sedges and mosses. Towards the wetter areas, shrub cover diminishes and *Sphagnum* mosses, *Caluna palustris* and the sedges *Eriophorum angustifolium* and *Carex aquatilis* are more common, with the latter two dominating the wettest parts. Vegetation height varies from 20 to 30 cm in the shrub dominated areas to 40 or 50 cm in the sedge dominated areas.

6.2.2 Instrumentation

Starting in April 2003, wind speed and temperature were measured with the use of a sonic anemometer (Gill Instruments, Lymington, UK, type R3-50) and concentrations of CO_2 and water vapor were measured with an open path infrared gas analyzer (Licor, Lincoln, NE, USA, type Li-7500), both installed at the top of a small mast at 4.7 m. The data was logged to a handheld computer (*van der Molen et al.*, 2006) at a rate of 5 to 10 Hz in the first few years, depending storage capacity and time between field visits. Since 2007, measurements have been performed consistently at 10 Hz after storage capacity was upgraded and it has been shown that these results were not significantly different from the measurements at a lower rate (*van der Molen et al.*, 2007). Fluxes were calculated according to the Euroflux methodology (*Aubinet et al.*, 2000), with the addition of the angle of attack calibration (*van der Molen et al.*, 2004; *Nakai et al.*, 2006). Afterwards, these measurements were gapfilled according to the standard gapfilling method in the Fluxnet community (*Reichstein et al.*, 2005; *Moffat et al.*, 2007).
To check for vertical stratification of CO_2 during nights with stable atmospheric conditions, a vertical CO_2 profile (*de Araújo et al.*, 2008) was used that measured CO_2 concentrations at 5 heights. These 5 heights were installed along a non-linear spacing from 15 cm above the ground to the measurement height. Measurements of CO_2 concentrations were performed in the summer of 2008 and 2009 in varying conditions. Even under very stable nighttime conditions with high increases of CO_2 concentrations, no significant vertical concentration gradient was found. It is therefore unlikely that storage effects pose a problem at this site.
In a second tower, additional measurements were performed of incoming and outgoing short wave radiation (Kipp & Zn, Delft, the Netherlands, type albedometer, CM7b), up- and down facing longwave radiometers (The Eppley Laboratory, Newport, RI, USA, type PIR) and a net radiometer (Campbell Scientific, Logan, UT, USA, type Q7). Soil heat flux was measured with the use of soil heat flux plates (Middleton, Melbourne, Australia). Soil temperature was recorded from two locations at 10 depths along a 60 cm profile with soil temperature sensors (manufactured at the VU University Amsterdam, type Pb107). One of these profiles was placed in a higher lain and dry area with shrubs, while the second profile was installed in an inundated depression dominated by sedges. Furthermore, an air pressure sensor (manufactured at the VU University Amsterdam) recorded barometric air pressure and precipitation was measured with a tipping bucket rain gauge (Campbell Scientific, Logan, UT, USA).

6.2.3 Flux partitioning

The dynamics of net ecosystem exchange (NEE) are governed by two processes: photosynthesis and respiration. These components need to be extracted from the eddy covariance signal, which only measures NEE. The standard procedure is to determine the flux of ecosystem respiration (R_{eco}) first and then extract gross primary production (GPP) from the remaining signal, following the equation GPP = NEE - R_{eco}. This was previously done by *Reichstein*

et al. (2005), who used the respiration model established by *Lloyd and Taylor* (1994) to estimate relationships between R_{eco} and air temperature from nighttime measurements of NEE. During Arctic summers however, it is problematic to derive R_{eco} from nighttime data since nights are very short. This problem can be alleviated by using the model presented by *Lasslop et al.* (2010), who combined the same respiration model with a hyperbolic light-response curve (*Falge et al.*, 2001), to use daytime data to estimate both R_{eco} and GPP as described in Equation 6.1.

$$\text{NEE} = -\frac{\alpha\beta R_g}{\alpha R_g + \beta} + R_{ref}\, exp\left(E_0\left(\frac{1}{T_{ref} - T_0} - \frac{1}{T_{air} - T_0}\right)\right) \tag{6.1}$$

The lefthand side of this equation describes the light-response curve and represents GPP (which is negative by definition). Here, α is the canopy light utilization efficiency in µmol C J^{-1} and describes the initial slope of the light-response curve. β is the maximum CO_2 uptake rate of the canopy at light saturation in µmol C m^{-2} s^{-1} and R_g is the incoming shortwave radiation in W m^{-2}. The righthand term describes ecosystem respiration and follows the model established by *Lloyd and Taylor* (1994). Here, R_{ref} is the reference respiration in µmol C m^{-2} s^{-1} at the base temperature T_{ref} (set to 15°C), E_0 is the temperature sensitivity, T_{air} is the air temperature in °C and T_0 is a constant parameter set at -46.02 °C.
Furthermore, *Lasslop et al.* (2010) adjusted the light-response curve in Equation 6.1 to account for changes in VPD. By adding a relationship with VPD, the model correctly attributes a drop in NEE to a decrease in GPP instead of an increase in respiration in summer afternoons with a high VPD. This effect of VPD on photosynthesis was incorporated by adjusting the value of β for periods where VPD reached values higher than 10 hPa according to Equation 6.2.

$$\beta \quad = \quad \begin{cases} \beta_0\, exp(-k(\text{VPD} - \text{VPD}_0)) & (\text{VPD} > \text{VPD}_0) \\ \beta = \beta_0 & (\text{VPD} \leq \text{VPD}_0) \end{cases} \tag{6.2}$$

Here, k is a dimensionless parameter that tunes the decay with VPD. VPD_0 is the threshold of 10 hPa and β_0 is the original value of β before the VPD adjustment.
To use this set of equations to obtain a good estimate for GPP and R_{eco}, first the value of E_0 was obtained from for a moving window of 12 days over the nighttime data, using the righthand side of Equation 6.1. This value for E_0 was then fixed and the rest of the parameters were estimated every two days, with the full equation, from daytime data on a window of 4 days. The procedure described here mostly follows *Lasslop et al.* (2010), however in this study the radiation limit to separate between daytime and nighttime was set to 20 W m^{-2} instead of 4 W m^{-2}. This is the same limit as used in the flux partitioning method by *Reichstein et al.* (2005) and this was done to make sure that in the period of the year close to summer solstice, enough nighttime data points were available to obtain an estimate of E_0. Otherwise, due to the short nights in this period of the year, the availability of data was significantly reduced and no optimization could be achieved for E_0.

6.2.4 Growing season length

In the years 2003, 2008, 2009 and 2010, eddy covariance measurements were started several weeks before snowmelt and fluxes were measured until after the end of the growing season (from now on referred to as 'continuous years'). Although measurements are lacking from springtime in the years 2004 to 2007 due to power failures combined with the inaccessibility of the site in that period (referred to as 'discontinuous years'), most of these years (2004 to

2006) were started within days from bud break, which occurs around 4 weeks after snowmelt. This period before bud break usually shows some respiration and photosynthesis (i.e. from grasses and sedges) which totals to approximately 10 g C m^{-2}. However, these amounts are very small compared to fluxes during the growing season when these amounts of carbon can be exchanged within 2 or 3 days, instead of 4 weeks. Therefore, although these springtime fluxes are missing in 4 measurement years, comparisons that are limited to the growing season will still capture most of the inter-annual variability.

To compare these growing seasons with each other, cumulative fluxes of NEE, GPP and R_{eco} need to be established. However, to be able to make these estimates, the length of the growing season has to be defined. Since the exact start of the growing season is unknown for the discontinuous years, the continuous years were studied for relationships that could predict bud break for each year, preferably with temperature. Continuous temperature measurements of this region are available for all years from the weather station of the nearby town of Chokurdakh ($\pm$ 30 km). These temperature readings and the onset of snowmelt at this weather station were highly comparable to the studied site and could therefore be used to predict the start of the growing season of the discontinuous years.

The required relationship between temperature and bud break was previously found by *Pop et al.* (2000). In their work, it was shown that a certain buildup of temperature, expressed as forcing units (FU), was needed for the shrubs *Betula nana* and *Salix pulchra* to achieve bud break. Since these shrubs are the dominant shrub species in the study area of this research, we could use the same relationship, as shown in Equation 6.3, to predict bud break at our site.

$$\text{FU day}^{-1} \quad = \quad \begin{cases} 0 & (T_{air} \leq 0°C) \\ 10/(1 + exp[–0.08(T_{air} - 18.0)]) & (T_{air} > 0°C) \end{cases} \tag{6.3}$$

Here T_{air} is the air temperature in °C. The outcome of this equation was used to calculate the cumulative amount of these forcing units since snowmelt. These values were plot against the cumulative amount of GPP as shown in Figure 6.2. From this Figure it is clear that photosynthesis picks up much more strongly when the cumulative forcing units hit a value of 70 FU, also known as $\text{FU}_{critical}$. This relationship with FU was then applied to the discontinuous years to estimate the start of the growing season (GS_{start}).

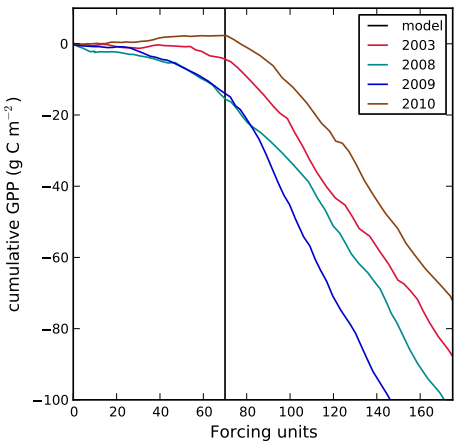

Figure 6.2: Relationship of cumulative GPP along the cumulative of forcing units (FU) for the continuous years. At a value of 70 ($\text{FU}_{critical}$), bud break of *Betula nana* and *Salix pulchra* occurs. This is indicated by the vertical black line.

While the start of the growing season showed a high variability between years, due to differences in spring temperatures, each year photosynthesis ceased in early September. Around this time, daylight quickly diminishes and temperatures start to drop. This is confirmed by the eddy covariance data, where the NEE switches from a net uptake to a net emission of carbon at the end of August. Since this happens in a very predictable way each year and closely around the same

date, it was chosen to define the end of the growing season a few days after this switch at September 7 (DOY=250). The difference between this date and GS_{start} provided the length of the growing season.

6.2.5 Gapfilling

While this provided an objective method to determine the length of the growing season, it was noticed that for the discontinuous years some days were still lacking. To fill up these gaps in R_{eco} and GPP, the daily averages of the continuous years were examined to establish relationships that could be used to fill these gaps. In the case of respiration, estimates of E_0 and R_{ref} were obtained by averaging these parameters for all years. This averaging was not done along the day of year (DOY) because snowmelt does not occur at the same day each year, which leads to large inter-annual differences along day of year. Instead, to obtain a more realistic average of R_{ref} and E_0 in relation to snowmelt, these parameters were averaged along the number of days since snow melt (DSM). The air temperature from the weather station in Chokurdakh, together with the average of the respiration parameters, could then be used to estimate respiration for the discontinuous years. These estimates were also extended into the period between snowmelt and bud break, to obtain an estimate of respiration during this period.
The amount of photosynthesis in the pre-growing season period was estimated from Figure 6.2. As can be seen here, the fluxes before bud break show a similar pattern with FU and average values of GPP with FU were used to estimate GPP in this period. Thereafter, to fill the gap in GPP within the growing season, an average of the parameters from Equation 6.1 could not be used, since no measurements for radiation were available from the local weather station. As an alternative, the data was filled with the average of the GPP flux from July. Although a rough estimate, average photosynthesis rates are rather stable at this site when compared to long time periods.
Since both these gapfilling methods have their limitations, it had to be estimated what their uncertainty range was. Therefore, the same filling technique was used on the continuous years but with artificial gaps of the same length as in each discontinuous year. The highest departure from the measurements due to these gaps, was used as the uncertainty range of the estimate for the discontinuous year that corresponded to that particular gap. By defining the uncertainty range in this way, the range represents a likely maximum uncertainty.

6.3 Results

6.3.1 Environmental conditions

In Figure 6.3, we indicated the starting day of the eddy covariance measurements (EC_{start}), the ending day of the eddy covariance measurements (EC_{end}), snowmelt (SM), the starting day of the growing season (GS_{start}) and the average daily temperatures for the measured years. Here it can be seen that the eddy covariance setup failed to measure the springtime fluxes from 2004 to 2007, due to power failures. In those years, the measurements could not be started again until after snowmelt, since the site is inaccessible during that period. However, apart from 2007, in most years the measurements were started soon after the start of the growing

season (1 to 6 days) and most of the carbon exchange was measured.
Furthermore, Figure 6.3 also shows a wide range in the timing of snowmelt. 2005 and 2007 saw a very early snowmelt, already on May 25 and May 18, respectively. In other years, snowmelt usually occurred somewhere between May 30 and June 10. Snowmelt was furthermore closely linked to the start of the growing season, which usually followed within 4 weeks ($\pm$ 4 days). The years with earlier snowmelt therefore also had an earlier start of the growing season.

These changes in snowmelt and start of the growing season are also reflected in the temperatures in Figure 6.3. Obviously, years with earlier snowmelt show higher temperatures earlier in the year. Notably, the highest average temperature for any year was also observed for the year with the earliest snowmelt, 2007. The year with the highest monthly average however is 2010, when the average July temperature reached 15 °C. During that month, record temperatures above 30°C were measured at the site and at the Chokurdakh weather station. On the other hand, the preceding year showed the lowest average temperatures for July and August and this stresses the high inter-annual variability in weather at this site.

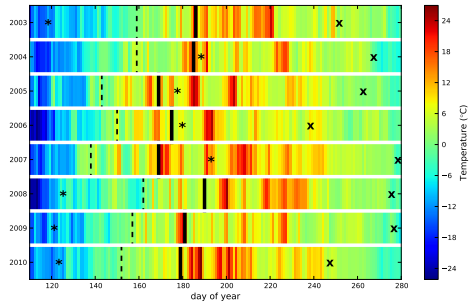

Figure 6.3: Inter-annual differences in the starting day of snowmelt (SM, indicated with a dashed line), the starting day of the growing season (GS_{start}, indicated with the thick line), the starting day of the eddy covariance (EC_{start}, indicated with an asterisk) and the ending day of the eddy covariance (EC_{end}, indicated with x). The colors indicate the temperature observed in these years (in degrees Celcius).

Opposed to these large inter-annual differences in the spring and summer, autumn temperatures are much more comparable in between years. In the weeks following DOY=250, temperatures are low, mostly < 5 °C and sometimes below freezing, and show little variation in between years due to the shorter and darker days in this period.

6.3.2 Fluxes

The large differences in the onset of snowmelt and summer temperatures between years is reflected in GPP, R_{eco} and NEE. In Figure 6.4, the cumulative totals of GPP, R_{eco} and NEE are plotted against the day of year, starting at the day of snowmelt. The estimates of springtime fluxes for the discontinuous years have also been plotted (the dotted lines in the figure), to show how these estimates fit alongside the fluxes measured in other years. From these cumulative plots, an estimate of the total fluxes of each growing season are given in Table 6.1.
From Figure 6.4 and Table 6.1, it becomes apparent that growing season photosynthesis and respiration are quite variable between years. GPP varied between -158.2 to -184 g C m^{-2}, while R_{eco} varied between 73.6 and 103.7 g C m^{-2}. These ranges are without the estimate for 2007, which showed exceptionally high photosynthesis and respiration rates (-211.3 and 129.3 g C m^{-2}, respectively). Surprisingly, the estimate of NEE of 2007 (-82.0 $\pm$ 27.5 g C

Table 6.1: Estimates of total GPP, R_{eco} and NEE during the growing season (gs) and during the snowfree period (sf) for all years. All totals are in g C m^{-2}

Year	GPP_{gs}	$R_{eco,gs}$	NEE_{gs}	GPP_{sf}	$R_{eco,sf}$	NEE_{sf}
2003	-166. 2	79. 1	-87. 1	-171. 2	94. 5	-76. 7
2004	-158.2 ± 2.4	84.0 ± 1.0	-74.2 ± 2.6	-168.1 ± 10.9	99.2 ± 3.7	-68.8 ± 11.5
2005	-184.0 ± 11.0	100.8 ± 3.0	-83.2 ± 11.4	-193.5 ± 16.5	116.8 ± 6.6	-76.7 ± 17.8
2006	-161.4 ± 5.9	92.5 ± 1.0	-69.0 ± 6.0	-170.8 ± 14.8	108.2 ± 4.2	-62.6 ± 15.4
2007	-211.3 ± 26.6	129.3 ± 7.0	-82.0 ± 27.5	-220.9 ± 28.8	147.2 ± 9.3	-73.7 ± 30.2
2008	-175. 7	87. 1	-88. 6	-191. 0	102. 3	-88. 7
2009	-168. 5	73. 6	-94. 9	-183. 2	93. 2	-90. 0
2010	-179. 6	103. 7	-75. 9	-177. 4	116. 0	-61. 4

m^{-2}) was very typical. NEE of all years varied between -74.2 and -94.9 g C m^{-2}.
These totals of GPP, R_{eco} and NEE are plot in Figure 6.5 against the length of the growing season (GS_{length}) and the growing season temperature sum (ΣT_{gs}). From this picture it becomes clear that GPP and R_{eco} show a strong relationship with ΣT_{gs} while the relationship between GS_{length} and GPP is less clear. Most importantly, while GPP and R_{eco} clearly vary with changes in either ΣT_{gs} or GS_{length}, there is no large variation in NEE. Apparently the increase in respiration is mostly offset by an increase in photosynthesis due to the longer growing season. Nonetheless, the highest NEE occurred in 2008 and 2009, years which showed the shortest growing season and the coldest summer, respectively. This suggests that respiration increases more than photosynthesis with warmer and longer growing seasons.

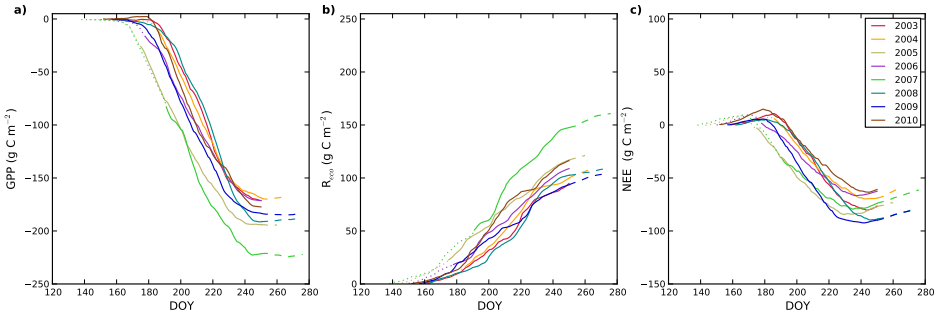

Figure 6.4: Cumulative fluxes of a) GPP, b) R_{eco} and c) NEE from snowmelt onwards plot against the day of year. The discontinuous years that have been filled with averages are plotted with a dotted line. The data measured after the end of the growing season (DOY=250) is plotted with a dashed line.

6.4 Discussion

6.4.1 Uncertainty assessment

Although the studied years showed a varying range in total amounts of GPP and R_{eco} of the growing season, some measurements were missing for the years 2004 to 2007 due to power failures (discontinuous years). This was compensated for by filling with relationships derived from the other years (continuous years) and the average photosynthesis rate during the growing season. These estimates were found to show some deviations from the actual measurements, which gave uncertainty ranges that varied between ± 2.4 to 26.6 g C m^{-2} for

GPP and ± 1 to 7 g C m^{-2} for R_{eco} as shown in Table 6.1. Expressed in percentages, these ranges equate to ± 1.5 to 12.5% for GPP and ± 1.1 to 5.5% for R_{eco}. In NEE these ranges equate to ± 3.5 to 15% for the years 2004 to 2006 and ± 33.5% for 2007. This is mostly because NEE for these years is derived as the difference of the two fluxes and therefore the same absolute ranges become larger when compared to this smaller number.

The large uncertainty range in total GPP of 2007 is due to the large gap in the measurements. The years 2004 to 2006 have small gaps from 1 to 6 days while 2007 has a gap of 22 days in the growing season and the associated uncertainty is therefore much larger. This particularly large gap occurred because the growing season started exceptionally early and the measurements were started later than usual due to power failures. However, although this range in GPP is large, it is likely that the estimate of total GPP is somewhat overestimated during that season. The gap in this total was filled with an average GPP that was established from measurements in a period that saw exceptionally high photosynthesis rates. These high rates make it likely that the estimate of GPP for 2007 is somewhat too high and unlikely to be even higher. Therefore, if we do not see an increase in NEE, even with these (possibly) overestimated GPP totals, it is likely that an earlier onset of the growing season will not lead to more uptake of carbon.

For the estimate of the uncertainty range of total respiration, the model used was more straight forward. Temperature measurements from the weather station in Chokurdakh could be used together with the respiration model by *Lloyd and Taylor* (1994) to estimate respiration. The parameters R_{ref} and E_0 of this equation were estimated by using averages from other years. This method led to much smaller uncertainty ranges than for the gapfilling of GPP since temperature differences of that year were incorporated. However, the estimate for 2007, due to the large gap in that year, is more uncertain but the relative amount of this range is much smaller for the estimate of R_{eco} than for GPP.

Arguably, an additional error is introduced by comparing the totals of GPP, R_{eco} and NEE within the growing season instead of exactly the same window for each year. The difference in growing season length shows a spread of three weeks and fluxes that are measured before the start of the growing season are not accounted for. Unfortunately, the amount of photosynthesis of the period before the start of the growing season was unknown for the discontinuous years. An estimate for these years can be made from the available data in the continuous years. This data showed that photosynthesis was near to zero before snowmelt, as expected. After snowmelt it picked up slowly until the start of the growing season. At that date, the cumulative amount of GPP ranged from close to zero to 16 g C m^{-2} as shown in Figure 6.2. Similar values were found for respiration. The cumulative exchange of carbon until snowmelt was in the order of 1 to 2 g C m^{-2}. After snowmelt, the total respiration amounted to 12 to 20 g C m^{-2}.

Since these extra amounts of total GPP and R_{eco} are of similar size, the total amount of NEE was not affected much since they largely cancel each other out, with respiration being slightly larger. By incorporating measured or estimated springtime fluxes, the patterns from Figure 6.5 were not significantly altered. Nonetheless, to provide a complete picture, the fluxes of GPP, R_{eco} and NEE from snowmelt until the end of the growing season have also been included in Table 6.1. Fluxes before snowmelt were omitted, since they were found to be close to zero. While the variable start of the growing season had a limited effect on NEE, the selection criterium for establishing the end of the growing season possibly introduces another error since respiration after the end of the growing season is also ignored. However, as can clearly be seen from Figure 6.3, autumn temperatures are much more comparable in between years than springtime temperatures. Subsequently, the cumulative amount of carbon fluxes of the years

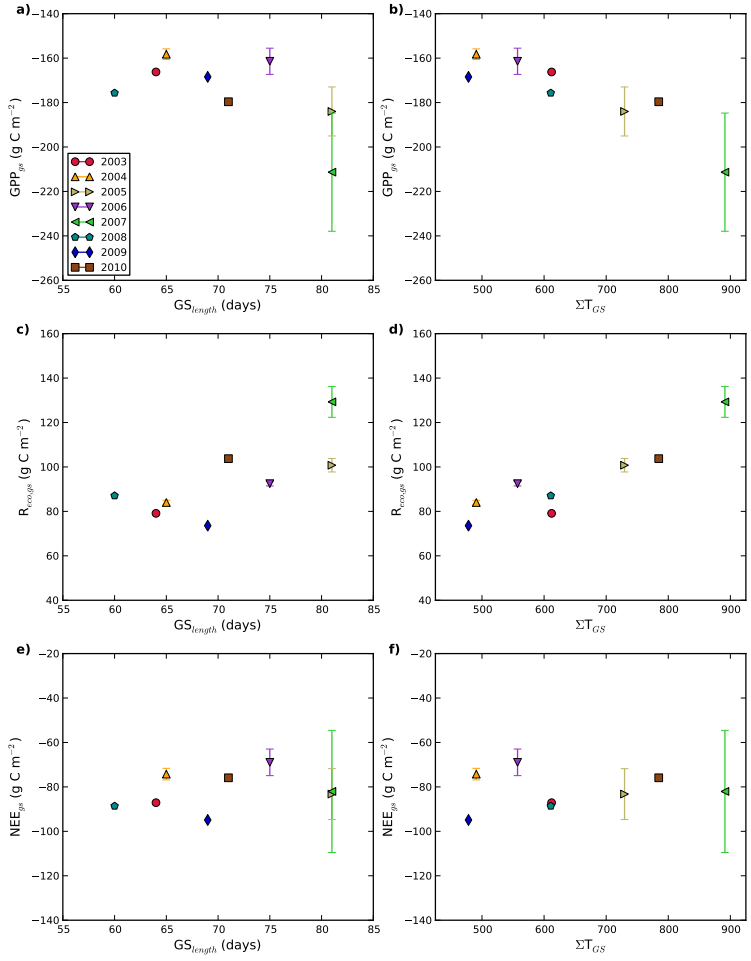

Figure 6.5: Total fluxes of a,b) GPP, c,d) R_{eco} and e,f) NEE plot against the day of snowmelt and the average temperature during the snow free period. The discontinuous years where parts of the data has been gapfilled with averages are plot with errorbars that indicates the possible range of the fluxes.

where autumn fluxes were measured, showed very similar slopes after the end of the growing season as shown in Figure 5.8. Although autumn fluxes were not measured every year, due to power failures, it can be seen that the difference in respiration between these years is low and the relative difference in NEE between years does not diverge much due to respiration from this period. Even for the year 2007, which had the highest temperatures for September, the pattern is not very different. We therefore conclude that fluxes measured after the end of the growing season until the start of snowmelt in the following year, show much more similar patterns in between years and are not expected to significantly change the relative differences in carbon fluxes between years. The comparison of fluxes between growing seasons provides us with an accurate estimate of the relative difference between years.

6.4.2 Relationship with growing season length and summer temperatures

With the uncertainties constrained, we are confident that most of the relative inter-annual differences will be governed by variations in GPP and R_{eco} during the growing season. Therefore, total amounts of growing season GPP, R_{eco} and NEE were plotted in Figure 6.5 against growing season length (GS_{length}) and the growing season temperature sum (ΣT_{gs}).
With the exception of the (possibly too high) estimate of 2007, it appears that the total amount of photosynthesis does not vary much with a change in the length of the growing season. This weak relationship with a longer growing season is supported by the fact that the year that showed the latest onset of snowmelt and start of the growing season, 2008, also showed one of the highest totals of GPP. While this makes the relationship with growing season length somewhat unclear, it does appear that GPP shows a relationship with the growing season temperature sum. In Figure 6.5b, the coldest years show a lower total of photosynthesis than the warmest years. It seems that in this ecosystem a higher sum of temperatures leads to more photosynthesis but that a longer growing season does not necessarily lead to more uptake of carbon.
Contrary to this complicated relation between growing season length and GPP, Figure 6.5c shows a clear relationship between growing season length and R_{eco}. This seems logical: a longer growing season leads to a longer period where respiration can take place and the total amount of respiration will increase. Respiration also increases with higher temperatures and therefore it is not surprising that R_{eco} would increase with the growing season temperature sum, as shown in Figure 6.5d.
Since both GPP and R_{eco} increase with higher summer temperatures, NEE depends on which of the two fluxes increases stronger. From Figure 6.5 it is clear that NEE showed no relationship with either growing season length or the sum of temperatures. If anything, the figure shows that it is unlikely that the uptake of carbon in this ecosystem is increased by a longer and warmer growing season. Years where the growing season was short or the total amount of summer temperatures were low, showed the highest uptake of carbon. Furthermore, the years where the growing season was long or warm, showed the least amount of uptake of carbon, with the exception of 2004. Also, the highest total of GPP occurred in 2007 but this estimate is possibly on the higher end. Figure 6.5 suggests that this year is an outlier and it is possible that the actual amount of carbon taken up in that growing season was much less, while it is unlikely it was even more.
These details from Figure 6.5 paint a pessimistic picture for the greenhouse gas exchange of this ecosystem for CO_2 alone. Arguably equally important is the observation that, even if

the net carbon uptake were to stay stable with higher summer temperatures, the longer growing season will definitely lead to more methane fluxes. And while methane fluxes from the studies site are very variable in between years because of different water availability and temperatures (*van der Molen et al.*, 2007), a longer snow free period leads to more time in which more methane fluxes can be emitted to the atmosphere. Importantly, a longer and warmer growing season does not necessarily lead to dryer conditions, since it was observed in the field that 2007 was very wet compared to other years and high methane fluxes were measured (not shown here). These emissions of methane cannot possibly be offset by an increase in carbon uptake and therefore the strength of the greenhouse gas sink of this ecosystem is likely to diminish in a warmer climate.

6.5 Conclusion

In this study, the net ecosystem exchange of a tundra site, measured over 8 consecutive years, has been split up in its components, gross primary production and ecosystem respiration. For 7 of the 8 years it was possible to ascertain the total fluxes of R_{eco} and GPP during the growing season, while for the remaining year a reasonable estimate could be made. The various carbon fluxes were subsequently compared to the climatic differences between years, with an emphasis on growing season length and the growing season temperature sum. While the length of the growing season showed an unclear relationship with GPP, it was shown that a higher growing season temperature sum led to a higher uptake of carbon. However, at the same time, a warmer growing season also led to more respiration.
The net carbon exchange that resulted from these two opposing fluxes showed no strong variation along the studied variables. However, it was found that the years that showed the highest net uptake of carbon, had the shortest growing season or the lowest temperatures. On the other hand, the years that showed the least amount of net carbon uptake mostly had long growing seasons or high summer temperatures.
This leads us to conclude that the amount of carbon which is taken up by this ecosystem is more likely to decrease rather than increase with longer growing seasons and higher summer temperatures. Additionally, it is expected that a longer growing season and higher temperatures also lead to more methane emissions. This study shows that this process cannot be compensated by an increase in carbon uptake and this makes it very likely that the greenhouse gas sink function of this ecosystem will significantly diminish in strength with longer and warmer growing seasons.

Acknowledgements
We like to acknowledge the people at the Institute for Biological Problems of the Cryolithozone SB RAS in Yakutsk for their assistance in and outside the field, without whom it would have been impossible to establish this long dataset. Also, we like to thank T.G. Strukova and the rangers of the Kytalyk Resource Reserve for their logistical support to and from the site and other assistance. Furthermore, we like to thank the engineering and electronics workshop at the VU University Amsterdam, without whom the successful installation, maintenance and operation of the equipment would not have been possible. Finally, we want to acknowledge the Darwin Center for Biogeosciences who supported this research with a grant to F.J.W. Parmentier (142.16.1041) and COordination action Carbon Observing Systems (COCOS) of the seventh framework programme (grant agreement no.: 212196) which provided additional funding to make this research possible.

References

Aubinet, M., et al., Estimates of the annual net carbon and water exchange of forests: The EUROFLUX methodology, *Advances In Ecological Research, Vol 30*, *30*, 113--175, 2000.

Aurela, M., T. Laurila, and J.-P. Tuovinen, The timing of snow melt controls the annual CO_2 balance in a subarctic fen, *Geophysical Research Letters*, *31*(16), L16,119, 2004.

Beringer, J., F. S. Chapin III, C. C. Thompson, and A. D. McGuire, Surface energy exchanges along a tundra-forest transition and feedbacks to climate, *Agricultural and Forest Meteorology*, *131*(3-4), 143--161, 2005.

Chapin III, F. S., et al., Role of land-surface changes in Arctic summer warming, *Science*, *310*(5748), 657--660, 2005.

Churkina, G., D. Schimel, B. H. Braswell, and X. M. Xiao, Spatial analysis of growing season length control over net ecosystem exchange, *Global Change Biology*, *11*(10), 1777--1787, 2005.

Corradi, C., O. Kolle, K. M. Walter, S. A. Zimov, and E.-D. Schulze, Carbon dioxide and methane exchange of a north-east Siberian tussock tundra, *Global Change Biology*, *11*(11), 1910--1925, 2005.

de Araújo, A. C., B. Kruijt, A. D. Nobre, A. J. Dolman, M. J. Waterloo, E. J. Moors, and J. S. de Souza, Nocturnal accumulation of CO_2 underneath a tropical forest canopy along a topographical gradient, *Ecological Applications*, *18*(6), 1406--1419, 2008.

Dorrepaal, E., S. Toet, R. S. P. van Logtestijn, E. Swart, M. J. van de Weg, T. V. Callaghan, and R. Aerts, Carbon respiration from subsurface peat accelerated by climate warming in the subarctic, *Nature*, *460*(7255), 616--U79, 2009.

Dye, D. G., Variability and trends in the annual snow-cover cycle in Northern Hemisphere land areas, 1972-2000, *Hydrological Processes*, *16* (15), 3065--3077, 2002.

Euskirchen, E. S., A. D. McGuire, F. S. Chapin III, S. Yi, and C. C. Thompson, Changes in vegetation in northern Alaska under scenarios of climate change, 2003-2100: implications for climate feedbacks, *Ecological Applications*, *19*(4), 1022--1043, 2009.

Falge, E., et al., Gap filling strategies for defensible annual sums of net ecosystem exchange, *Agricultural and Forest Meteorology*, *107* (1), 43--69, 2001.

Fan, S. M., S. C. Wofsy, P. S. Bakwin, D. J. Jacob, S. M. Anderson, P. L. Kebabian, J. B. McManus, C. E. Kolb, and D. R. Fitzjarrald, Micrometeorological measurements of CH_4 and CO_2 exchange between the atmosphere and sub-arctic tundra, *Journal Of Geophysical Research-Atmospheres*, *97* (D15), 16,627--16,643, 1992.

Groendahl, L., T. Friborg, and H. Soegaard, Temperature and snow-melt controls on interannual variability in carbon exchange in the high Arctic, *Theoretical And Applied Climatology*, *88*(1-2), 111--125, 2007.

Harazono, Y., M. Mano, A. Miyata, R. C. Zulueta, and W. C. Oechel, Inter-annual carbon dioxide uptake of a wet sedge tundra ecosystem in the Arctic, *Tellus Series B-Chemical And Physical Meteorology*, *55*(2), 215--231, 2003.

Hargreaves, K. J., D. Fowler, C. E. R. Pitcairn, and M. Aurela, Annual methane emission from Finnish mires estimated from eddy covariance campaign measurements, *Theoretical And Applied Climatology*, *70*(1-4), 203--213, 2001.

Høye, T. T., E. Post, H. Meltofte, N. M. Schmidt, and M. C. Forchhammer, Rapid advancement of spring in the High Arctic, *Current Biology*, *17*(12), R449--R451, 2007.

Kaufman, D. S., et al., Recent Warming Reverses Long-Term Arctic Cooling, *Science*, *325*(5945), 1236--1239, 2009.

Kutzbach, L., C. Wille, and E.-M. Pfeiffer, The exchange of carbon dioxide between wet arctic tundra and the atmosphere at the Lena River Delta, Northern Siberia, *Biogeosciences*, *4*(5), 869--890, 2007.

Kwon, H.-J., W. C. Oechel, R. C. Zulueta, and S. J. Hastings, Effects of climate variability on carbon sequestration among adjacent wet sedge tundra and moist tussock tundra ecosystems, *Journal of Geophysical Research-Biogeosciences*, *111*(G3), G03,014, 2006.

Lasslop, G., M. Reichstein, D. Papale, A. D. Richardson, A. Arneth, A. Barr, P. Stoy, and G. Wohlfahrt, Separation of net ecosystem exchange into assimilation and respiration using a light response curve approach: critical issues and global evaluation, *Global Change Biology*, *16*(1), 187--208, 2010.

Lloyd, J., and J. A. Taylor, On the temperature-dependence of soil respiration, *Functional Ecology*, *8*(3), 315--323, 1994.

Lund, M., et al., Variability in exchange of CO_2 across 12 northern peatland and tundra sites, *Global Change Biology*, *16*(9), 2436--2448, 2010.

McGuire, A. D., et al., Sensitivity of the carbon cycle in the Arctic to climate change, *Ecological Monographs*, *79*(4), 523--555, 2009.

Moffat, A. M., et al., Comprehensive comparison of gap-filling techniques for eddy covariance net carbon fluxes, *Agricultural and Forest Meteorology*, *147*(3-4), 209--232, 2007.

Myneni, R. B., C. D. Keeling, C. J. Tucker, G. Asrar, and R. R. Nemani, Increased plant growth in the northern high latitudes from 1981 to 1991, *Nature*, *386*(6626), 698--702, 1997.

Nakai, T., M. K. van der Molen, J. H. C. Gash, and Y. Kodama, Correction of sonic anemometer angle of attack errors, *Agricultural and Forest Meteorology*, *136*(1-2), 19--30, 2006.

Oechel, W. C., et al., A scaling approach for quantifying the net CO_2 flux of the Kuparuk River Basin, Alaska, *Global Change Biology*, *6*, 160--173, 2000.

Piao, S., P. Friedlingstein, P. Ciais, N. Viovy, and J. Demarty, Growing season extension and its impact on terrestrial carbon cycle in the Northern Hemisphere over the past 2 decades, *Global Biogeochemical Cycles*, *21*(3), GB3018, 2007.

Pop, E. W., S. F. Oberbauer, and G. Starr, Predicting vegetative bud break in two arctic deciduous shrub species, Salix pulchra and Betula nana, *Oecologia*, *124*(2), 176--184, 2000.

Post, E., et al., Ecological Dynamics Across the Arctic Associated with Recent Climate Change, *Science*, *325*(5946), 1355--1358, 2009.

Reichstein, M., et al., On the separation of net ecosystem exchange into assimilation and ecosystem respiration: review and improved algorithm, *Global Change Biology*, *11*(9), 1424--1439, 2005.

Schuur, E. A. G., et al., Vulnerability of permafrost carbon to climate change: Implications for the global carbon cycle, *Bioscience*, *58*(8), 701--714, 2008.

Serreze, M. C., et al., Observational evidence of recent change in the northern high-latitude environment, *Climatic Change*, *46*(1-2), 159--207, 2000.

Sitch, S., et al., Assessing the carbon balance of circumpolar Arctic tundra using remote sensing and process modeling, *Ecological Applications*, *17*(1), 213--234, 2007.

Smith, N. V., S. S. Saatchi, and J. T. Randerson, Trends in high northern latitude soil freeze and thaw cycles from 1988 to 2002, *Journal Of Geophysical Research-Atmospheres*, *109*(D12), D12,101, 2004.

Tarnocai, C., J. G. Canadell, E. A. G. Schuur, P. Kuhry, G. Mazhitova, and S. A. Zimov, Soil organic carbon pools in the northern circumpolar permafrost region, *Global Biogeochemical Cycles*, *23*, GB2023, 2009.

van der Molen, M. K., J. H. C. Gash, and J. A. Elbers, Sonic anemometer (co)sine response and flux measurement - II. The effect of introducing an angle of attack dependent calibration, *Agricultural and Forest Meteorology*, *122*(1-2), 95--109, 2004.

van der Molen, M. K., M. J. Zeeman, J. Lebis, and A. J. Dolman, EClog: A handheld eddy covariance logging system, *Computers and Electronics in Agriculture*, *51*(1-2), 110--114, 2006.

van der Molen, M. K., J. van Huissteden, F. J. W. Parmentier, A. M. R. Petrescu, A. J. Dolman, T. C. Maximov, A. V. Kononov, S. V. Karsanaev, and D. A. Suzdalov, The growing season greenhouse gas balance of a continental tundra site in the Indigirka lowlands, NE Siberia, *Biogeosciences*, *4*(6), 985--1003, 2007.

Welker, J., J. T. Fahnestock, G. H. R. Henry, K. W. O'Dea, and R. A. Chimner, CO_2 exchange in three Canadian High Arctic ecosystems: response to long-term experimental warming, *Global Change Biology*, *10*(12), 1981--1995, 2004.

Williams, M., W. Eugster, E. B. Rastetter, J. P. McFadden, and F. S. Chapin III, The controls on net ecosystem productivity along an Arctic transect: a model comparison with flux measurements, *Global Change Biology*, *6*, 116--126, 2000.

Zhou, L. M., C. J. Tucker, R. K. Kaufmann, D. Slayback, N. V. Shabanov, and R. B. Myneni, Variations in northern vegetation activity inferred from satellite data of vegetation index during 1981 to 1999, *Journal Of Geophysical Research-Atmospheres*, *106*(D17), 20,069--20,083, 2001.

Chapter 7

Synthesis, Conclusions and Recommendations

7.1 Introduction

This thesis discusses the dynamics of the exchange of CO_2 and methane to the atmosphere with a special emphasis on Northeastern Siberian tundra. A combination of different methods to measure trace gases has been used, together with modeling and lab analysis. First, the influence of water level on CO_2 fluxes and evaporation of a peatland in the Netherlands was studied. Hereafter, the focus switches to Siberia in a study on the spatial dynamics of methane emissions and the role that methanotrophic bacteria, that live within Sphagnum, play therein. The following chapter discusses the dynamics of methane emissions in tundra on a larger scale and the final chapter discusses the stability of net carbon uptake, and its components photosynthesis and respiration, to increasing summer temperatures and longer growing seasons.

7.2 Research Synthesis

7.2.1 Sensitivity of CO_2 fluxes and evaporation to water table

In a peatland in the Netherlands, the effect of shallow water table fluctuations on evaporation and CO_2-fluxes is investigated. These fluxes were measured from mid spring to the end of summer in 2005 and 2006 and simulated independently with process models. The observed and modeled data were then compared along a gradient of water levels. Any variation along the gradient would imply an influence of the water table on the flux. It became evident that changes in the water table had no effect on evaporation and CO_2-fluxes of the peatland. A probable cause could be the high water content of the soil, even for the low water tables, and the stable thermal conductivity of the soil. This study has implications for current land use management, which is aimed at reducing CO_2 emissions. Currently, regulations focus mostly on water levels while this study shows that soil water content should be focused on as well.
Furthermore, this study has implications for the research of carbon fluxes on tundra. The main study site of this thesis was situated in a very wet tundra type. Although significant changes in water table do occur, soil moisture content remains high. It is therefore likely that

respiration at the studied tundra site is more susceptible to changes in temperature than water level.

7.2.2 The role of endophytic methane oxidizing bacteria in submerged *Sphagnum* in determining tundra methane emissions

The role of microbial processes governing methane emissions in tundra ecosystem is receiving increasing attention. Recently, cooperation between methanotrophic bacteria and submerged *Sphagnum* was shown to reduce methane emissions but also to supply CO_2 for photosynthesis for the plant. Although this process was shown to be important in the laboratory, the differences that exist in methane emissions from inundated vegetation types with or without *Sphagnum* in the field have not been linked to these bacteria before.
In this study, chamber flux measurements, an incubation study and flux modeling were used to investigate the drivers and controls on the relative difference in methane emissions between a submerged *Sphagnum*/sedge vegetation and an inundated sedge vegetation without *Sphagnum*. It was found that methane emissions in the *Sphagnum* dominated vegetation type were 50% lower than in the vegetation type without *Sphagnum*. A model sensitivity analysis showed that these differences could not sufficiently be explained by differences in methane production and plant transport.
The model, combined with an incubation study, indicated that methane oxidation by endophytic bacteria, living in cooperation with submerged *Sphagnum*, plays a significant role in methane cycling at this site. This result is important for spatial upscaling spatially as oxidation by these bacteria plays a large role in 15% of the net methane emissions at this tundra site. Our findings support the notion that methane oxidizing bacteria are an important factor in understanding the processes behind methane emissions in tundra.

7.2.3 Spatial and temporal dynamics in eddy covariance observations of methane fluxes

In the past two decades, the eddy covariance technique has been used for an increasing number of methane flux studies at an ecosystem scale. Previously, most of these studies used a closed path setup with a tunable diode-laser spectrometer (TDL). Although this method worked well, the TDL has to be calibrated regularly and cooled with liquid nitrogen or a cryogenic system, which limits its use in remote areas.
Recently, a new closed path technique has been introduced that uses off-axis integrated cavity output spectroscopy that does not require regular calibration or liquid nitrogen to operate and can thus be applied in remote areas.
In the summer of 2008 and 2009, this eddy covariance technique was used to study methane fluxes from a tundra site in Northeastern Siberia. The measured emissions showed to be very dependent on the fetch area, due to a large contrast in water table between wind directions. Furthermore, the observed short and longterm variation of methane fluxes could be readily explained with a non-linear model that used relationships with atmospheric stability, soil temperature and water level. This model was subsequently extended to fieldwork periods preceding the eddy covariance setup and applied to evaluate a spatially integrated flux. The model result showed that average fluxes were 56.5, 48.7 and 30.4 nmol CH_4 m^{-2} s^{-1} for the summers of 2007 to 2009.
While previous models of the same type were only applicable to daily averages, the method

described can be used on a much higher temporal resolution, making it suitable for gap-filling. Furthermore, by partitioning the measured fluxes along wind direction, this model can also be used in areas with non-uniform terrain and still provide spatially integrated fluxes.

7.2.4 Longer growing seasons do not appear to increase net carbon uptake in Northeastern Siberian tundra

With global warming, snowmelt is occurring earlier and growing seasons are becoming longer around the Arctic. It has been suggested that this would lead to more uptake of carbon due to a lengthening of the period in which plants photosynthesize. To investigate this suggestion, 8 consecutive years of measurements at a Northeastern Siberian tundra site were investigated for patterns in net ecosystem exchange, photosynthesis and ecosystem respiration.
Net ecosystem exchange, measured with the eddy covariance, was split up with a partitioning method. By using day-time data to obtain model parameters, photosynthesis and ecosystem respiration could be well defined. For some years, springtime fluxes were missing and this data was gapfilled with the use of average parameters and average fluxes. The uncertainty that this method introduced could be well addressed.
While photosynthesis showed no clear increase with longer growing seasons, it was clearly increased by warmer summers. Due to these warmer temperatures however, the increase in uptake was mostly offset by an increase in respiration. Therefore, overall variability in net carbon uptake was low and no relationship with growing season length was found. Furthermore, the highest net uptake of carbon occurred with the shortest and the coldest growing season. Low uptake of carbon mostly occurred with longer or warmer growing seasons. We thus conclude that the net carbon uptake of this ecosystem is more likely to decrease rather than to increase under a warmer climate. Furthermore, a longer growing season also leads to more methane emissions. A lengthening of the growing season is therefore very likely to reduce the greenhouse gas sink of this ecosystem.

7.2.5 The growing season greenhouse gas balance of Northeastern Siberian tundra

The last two objectives of this thesis investigated the methane and CO_2 flux of tundra separately. By combining the measurements of greenhouse gas exchange in the growing seasons of 2007, 2008 and 2009, we can establish a greenhouse gas balance for those periods. In chapter 6, the net CO_2 exchange was shown to be -82.0$\pm$27.5 g C m^{-2}, -88.6 g C m^{-2} and -94. 9 g C m^{-2} for the growing seasons of 2007, 2008 and 2009. In chapter 5, it was established that the methane emissions in those same years was 56.5, 48.7 and 30.4 nmol CH4 m^{-2} s^{-1}, which equals 78.3 mg CH_4 m^{-2} day^{-1}, 67.5 mg CH_4 m^{-2} day^{-1} and 42.1 mg CH_4 m^{-2} day^{-1}. Assuming that these methane emission rates are valid for the entire growing season, we can multiply these amounts with the length of the growing seasons of 2007, 2008 and 2009. For the entire growing season, fluxes are then estimated to be 6.3 g CH_4 m^{-2}, 4.0 g CH_4 m^{-2} and 2.9 g CH_4 m^{-2}.
The global warming potential of 1 g of methane is equal to 25 g of CO_2 over a period of 100 years. However, carbon uptake is often expressed as grams of C, not CO_2. In this case, the relative global warming potential of 1 g of methane is equal to the global warming potential of 25x(12/44)=6.8 g C m^{-2} day^{-1}. By applying this conversion factor, the greenhouse gas sink of this site is estimated at -39$\pm$27.5 g CO_2-eq m^{-2}, -61.3 g CO_2-eq m^{-2} and -74.7 g

CO_2-eq m^{-2} for the growing seasons of 2007, 2008 and 2009. This shows that this site is a sink for both carbon and greenhouse gases, even during the very warm and long growing season of 2007. That year was very exceptional, with a growing season that was about 50% longer than normal. The growing seasons of 2008 and 2009 were much more typical and in those years we see that the site was a much stronger sink. However, outside of the growing season, this site is a net source of greenhouse gases. The full annual greenhouse gas balance of this site, which still remains to be determined, is expected to be smaller than the numbers represented here.

7.3 Conclusions

7.3.1 Sensitivity of CO_2 fluxes and evaporation to water table

- Studies on the relationship between respiration and water level show conflicting results.
- Fluxes of respiration, photosynthesis and evaporation were successfully modeled with varying techniques.
- While water table dropped significantly, soil moisture content remained high due to the high retention capacity of the soil.
- Fluxes of respiration, photosynthesis and evaporation showed no significant variation along a large range of water levels because soil moisture levels remained the same.
- When relationships between water table and respiration are studied, soil moisture should be measured as well.

7.3.2 The role of endophytic methane oxidizing bacteria in submerged *Sphagnum* in determining tundra methane emissions

- Methane fluxes in a *Sphagnum* dominated vegetation type were found to be 50% lower than in the vegetation type without *Sphagnum*.
- Although differences existed in vascular plant cover, this could not explain the observed differences.
- Incubation of *Sphagnum* samples found oxidation rates that were twice as high as the observed difference in the field, verifying the high oxidation potential in submerged. *Sphagnum*. These oxidation rates were due to methanotrophs living in a cooperation in or on the *Sphagnum* plants.
- A well established process model indicated that the observed differences were mostly due to differences in oxidation rates and in a much lesser sense due to methane production or plant transport rates.
- The above conclusions combined make it very likely that oxidation in submerged *Sphagnum* plays an important role in the spatial differences of tundra methane emissions.

7.3.3 Spatial and temporal dynamics in eddy covariance observations of methane fluxes

- During the summer of 2008 and 2009, methane fluxes were successfully measured with the use of a closed path eddy covariance setup that used a Los Gatos Fast Methane analyzer.
- Methane fluxes were found to be highly variable with wind direction and this was due to a difference in the amount of wet vegetation and ponds throughout the area.
- The difference in fluxes between years were related mostly to a difference in water level.
- Soil temperature explained some of the inter-annual variation but also variations within a season.
- Atmospheric stability could explain most of the within-day variation of fluxes.
- Fluxes could be modeled well by incorporating water level, soil temperature and atmospheric stability while partitioning the model along wind direction into three sectors with varying amounts of wet and dry vegetation.
- The model performed well when compared to chamber flux measurements, even when it was extended to other years.
- The model was successfully applied to estimate fluxes for each of the three sectors separately.
- Despite the highly heterogeneous terrain, a regional representative estimate of methane flux could be established by averaging the modeled flux of the three sectors.

7.3.4 Longer growing seasons do not appear to increase net carbon uptake in Northeastern Siberian tundra

- Carbon fluxes of 8 consecutive growing seasons (2003-2010) were successfully measured in a Northeastern Siberian tundra site.
- The measured fluxes could be separated well into ecosystem respiration and photosynthesis with the use of a day-based model.
- The start of the growing season proved to be highly predictable with cumulative air temperature.
- Early growing season gaps were gapfilled and uncertainties could be well addressed.
- GPP and R_{eco} varied more with summer temperatures than with growing season length.
- NEE showed no clear variation with growing season length. However, the highest net uptakes were observed for the coldest and the shortest growing seasons.
- The NEE at this site is more likely to decrease rather than to increase with warmer summer temperatures.
- Longer growing seasons will surely lead to more methane emissions and the greenhouse gas sink of this site is likely to decrease in a warmer climate.

7.3.5 The growing season greenhouse gas balance of Northeastern Siberian tundra

- The studies site is a sink for CO_2 but a source of methane
- The greenhouse gas balanse of the growing seasons of 2007, 2008 and 2009 are estimated to be -39±27.5 g CO_2-eq m^{-2}, -61.3 g CO_2-eq m^{-2} and -74.7 g CO_2-eq m^{-2}.

7.4 Research perspectives and recommendations

7.4.1 Sensitivity of CO_2 fluxes and evaporation to water table

The first objective has shown that when the sensitivity of evaporation and CO_2 fluxes to water level is studied, it is important to incorporate measurements of soil moisture content as well. Soil moisture remained high, while water level dropped significantly. This meant that, even during a very dry period, evaporation and photosynthesis were not limited. The small change in soil moisture also meant that respiration did not significantly change either.
If the studied fluxes were only compared to water table, it could be concluded that these are not sensitive to this parameter. However, this was mostly because soil moisture content remained high. In areas where soil moisture lowers much more rapidly with a low water table, a relationship between water table and respiration is probably more apparent.
This means that future research in this field should not only focus on water level. Soil moisture should be studied as well, since this might better explain physical changes in the unsaturated zone. Also, this finding suggests that fluxes in areas where soils remain wet, such as tundra, show little variation with a lower water table. However, soil moisture and water level studies in tundra are uncommon and this should be studied in more detail in the future.

7.4.2 Endophytic methane oxidizing bacteria in submerged *Sphagnum* and tundra methane emissions

The second objective showed that methanotrophic bacteria that live within *Sphagnum* have a large impact on methane emissions from these vegetation types. A microbiological analysis of submerged *Sphagnum* found very high oxidation rates, which was confirmed by the model. Future modeling work of methane fluxes should therefore include these high oxidation effects when considering submerged *Sphagnum* vegetation
Although this research has shown that the observed differences are most likely due to these methanotrophs, a more detailed analysis into these vegetation types might give more insight in the way that these bacteria interact within the ecosystem. While this study showed clearly that these bacteria reduce methane emissions, they also provide carbon to *Sphagnum*. Currently, no *in situ* studies have been done on the increase of carbon storage by these bacteria. A detailed study on soil type, vegetation composition, nutrient distribution in relation to methane production, methane oxidation and photosynthesis and respiration, perhaps combined with stable isotopes or labeling, might provide better insight in the carbon cycling within this vegetation type. Hopefully, this would lead to an understanding of how the cooperation between these bacteria and *Sphagnum* contributes to the high carbon storage found in *Sphagnum* dominated vegetation.

7.4.3 Spatial and temporal dynamics in eddy covariance observations of methane fluxes

The third objective showed that methane emissions can be measured accurately in highly heterogeneous terrain. A closed path eddy covariance setup was successfully applied and methane fluxes could be modeled accordingly. Furthermore, it was shown that diurnal methane fluxes were highly variable with atmospheric stability. By incorporating this parameter, a high resolution model was developed that can be used for gapfilling as well.
Future development in this field should extend measurements throughout the entire snow free season. The current power demands of the closed-path setup requires the use of a generator. This limits the use of the method to periods where people are present at the site. This problem could be aleviated by either a more reliable and stand alone power supply or the use of low power open-path setup, such as the recently released Licor-7700. By extending the measurements from (just before) snowmelt to soil re-freeze, the full dynamics of the methane emission of tundra can be assessed. Since large bursts of methane at the onset of re-freeze have been observed with chamber measurements, these end of season fluxes might prove to be critical in determining the full greenhouse gas balance of Siberian tundra. Also, the influence of other parameters, such as active layer depth, might be quantified better.

7.4.4 The influence of growing season length on net carbon uptake

The last objective showed that the uptake of carbon in tundra is highest with cold or short growing seasons. This is contrary to what was expected; longer growing seasons were thought to lead to more photosynthesis and thus more uptake of carbon. However, this research clearly shows that this is not the case, since the higher temperatures also lead to more respiration.
This finding could not have been made without long-term measurements of carbon exchange in tundra as in the current study. Continuation of the CO_2 flux measurements is therefore very important to observe how the net carbon exchange of tundra is changing in a warmer climate. Although the highest net uptakes of carbon are clearly occurring with cold and short growing seasons, vegetation changes might lag the temperature change. These vegetation changes will also lead to a different response of the ecosystem and this might be critical in determining the long-term stability of tundra carbon stocks. Long-term measurements require a significant effort in terms of logistics, personnel and costs but these types of measurements can provide us with insights that models cannot.

7.4.5 General recommendations

This research has shown that while tundra is a sink for carbon, it is a source of methane and while many of the dynamics of both systems were studied in detail, there are also areas where knowledge is lacking. For example, the methane emissions of thermokarst lakes are still poorly defined and knowledge of their emission in the studied area is limited. Other areas, such as floodplains, also emit high amounts of methane and have a high primary productivity but are less well studied. Also, the transfer of carbon into lakes (i.e. through mass wasting) and carbon transport through runoff are largely unknown. Future research should therefore incorporate these research areas to obtain a truly regional estimate of greenhouse gas exchange. To attain these research goals, a set of complimentary approaches should be used, including eddy covariance measurements, flux chambers, floating bubble traps and perhaps newly de-

veloped devices. To facilitate this much needed equipment, it is essential that the technical knowledge for building instrumentation and electronics is available at the research institute. This research has benefited largely from the extensive support by the instrumental and electronics workshops at the VU. Without their support, a successful completion of this research would have been much more problematic if not impossible. It would be wise to keep these facilities, and the knowledge of the technicians, to continue excellent field research in the future.

Chapter 8

Nederlandse samenvatting

8.1 Introductie

Dit proefschrift behandelt de dynamiek van de uitwisseling van CO_2 en methaan met de atmosfeer, waarbij in het bijzonder onderzoek gedaan is naar de toendra in Noordoost-Siberië. Een combinatie van verschillende methodes werd gebruikt om broeikasgassen te meten, samen met modelstudies en labanalyses. Als eerste werd onderzocht hoe veranderingen in het grondwaterniveau van een veengebied in Nederland invloed had op CO_2 uitstoot en verdamping. Hierna verplaatst de focus van het proefschrift naar Siberië in een studie waarin werd onderzocht hoe symbiotische bacteriën die in *Sphagnum* leven de ruimtelijke dynamiek van methaan emissies beïnvloeden. Het hoofdstuk daarna bespreekt de dynamiek van methaan op een grotere schaal en in het laatste hoofdstuk wordt geanalyseerd hoe de stabiliteit van de netto opname van CO_2, en diens componenten fotosynthese en ecosysteem respiratie, reageert op hogere zomertemperaturen en langere groeiseizoenen.

8.2 Onderzoeksynthese

8.2.1 De stabiliteit van CO_2 fluxen en verdamping met een variërende grondwaterstand

In een Nederlands veenweidegebied werd onderzocht welk effect variaties in de ondiepe grondwaterstand hebben op CO_2 fluxen en verdamping. Deze fluxen werden in 2005 en 2006 gemeten vanaf het midden van de lente tot het einde van de zomer en onafhankelijk van de grondwaterstand gesimuleerd met procesmodellen. De geobserveerde en gemodelleerde data werden vervolgens vergeleken langs een gradiënt aan waterstanden. Als daarin een afwijking te zien zou zijn, zou dat een indicatie zijn dat grondwaterstand een invloed heeft op de onderzochte fluxen.
Hieruit bleek dat een verandering in de grondwaterstand van het veenweidegebied geen effect had op verdamping en CO_2 fluxen. Een mogelijke oorzaak hiervoor zou kunnen zijn dat de bodem een erg hoge hoeveelheid bodemvocht bevatte, zelfs bij lage grondwaterstanden, en stabiele thermische eigenschappen vertoonde. Deze studie heeft gevolgen voor huidig landgebruik, wat gericht is op het reduceren van CO_2 emissies. Regelgeving legt op dit moment voornamelijk de nadruk op grondwaterstanden, terwijl deze studie laat zien dat ook

bodemvocht in acht moet worden genomen.
Verder heeft deze studie ook gevolgen voor onderzoek naar koolfstoffluxen op toendra. Het hoofdonderzoeksgebied van dit proefschrift is gelegen in een erg nat toendratype. Hoewel er zich significante veranderingen voordoen in de waterstand aldaar blijft de hoeveelheid bodemvocht hoog. Het is daarom aannemelijk dat respiratie in het onderzochte toendragebied ook meer vatbaar is voor veranderingen in temperatuur dan in grondwaterstand.

8.2.2 De rol van endofytische methaanoxiderende bacteriën in geïnundeerde *Sphagnum* bij het determineren van methaanemissies uit toendra

Recentelijk gaat er steeds meer aandacht uit naar de dynamische rol van microbiologische processen in de methaanemissies van toendra-ecosystemen. Onlangs werd er een samenwerking gevonden tussen methanotrofe bacteriën en geïnundeerde *Sphagnum* die leidt tot een vermindering van methaanemissies maar die ook CO_2 aan de plant levert voor fotosynthese. Alhoewel in het lab bleek dat dit proces belangrijk is, zijn in het veld de verschillen in methaanemissies tussen gebieden met of zonder *Sphagnum* nog niet eerder in verband gebracht met deze bacteriën.
In deze studie werden kamerfluxmetingen, een incubatiestudie en een methaanfluxmodel gecombineerd om te onderzoeken wat de oorzaken achter en de limitaties aan de relatieve verschillen in methaanemissie tussen vegetatietypes met of zonder *Sphagnum* zijn. Hieruit bleek dat methaanemissies in een vegetatietype gedomineerd door *Sphagnum* 50% lager waren dan in een vegetatietype zonder *Sphagnum*. Een modelgevoeligheidsanalyse liet zien dat deze verschillen niet voldoende uitgelegd konden worden door verschillen in methaanproductie en plantentransport.
Het model en de incubatiestudie gaven aan dat methaanoxidatie door endofytische bacteriën, die in een samenwerking leven met *Sphagnum*, een significante rol spelen in de methaancyclus van het onderzochte gebied. Dit resultaat is op grotere ruimtelijke schaal van belang omdat deze bacteriën een grote rol spelen in 15% van de netto methaanemissies van het onderzochte toendragebied. Onze bevindingen ondersteunen de notie dat deze methaanoxiderende bacteriën belangrijk zijn om de processen die methaanemissies in toendra bepalen beter te begrijpen.

8.2.3 Ruimtelijke en temporele dynamiek in eddy-covariantieobservaties van methaanfluxen

In de afgelopen twee decennia is de eddy-covariantietechniek meer en meer gebruikt in studies die methaanemissies trachten te bepalen op een ecosysteemschaal. Voorheen werden de meeste van deze studies uitgevoerd met een tunable diode-laser spectrometer (TDL). Alhoewel deze methode goed werkte, moet een TDL regelmatig gekalibreerd worden en daarnaast gekoeld worden met vloeibare stikstof of een koelsysteem, wat de toepassing in afgelegen gebieden aanzienlijk beperkt.
In de zomer van 2008 en 2009 werd de eddy-covariantietechniek gebruikt om methaanfluxen te meten van een toendragebied in Noordoost-Siberië. De gemeten emissies bleken erg afhankelijk te zijn van de windrichting, door het grote contrast in droge en natte gebieden in het gebied. Verder kon de korte- en langetermijnvariatie in de methaanflux verklaard worden aan de hand van een nonlineair model dat relaties gebruikte met de stabiliteit van de atmosfeer, bodem temperatuur en grondwaterniveau. Het modelresultaat liet zien dat de

gemiddelde fluxen 56.5, 48.7 en 30.4 nmol CH_4 m^{-2} s^{-1} waren voor de zomers van 2007 t/m 2009.
Alhoewel voorgaande modellen van hetzelfde type alleen toepasbaar waren op dagelijkse gemiddeldes, kan het hier beschreven model op een veel hogere tijdresolutie gebruikt worden, wat het bruikbaar maakt voor het opvullen van gaten in de data. Bovendien kan het model ook gebruikt worden in gebieden met een ongelijke vegetatie en toch ruimtelijke geïntegreerde fluxen opleveren, door het partitioneren van de gemeten flux langs de windrichting.

8.2.4 Langere groeiseizoenen leiden kennelijk niet tot een hogere netto opname van koolstof in Noordoost-Siberië

Door het versterkte broeikaseffect smelt sneeuw in arctische gebieden eerder in het jaar en worden de groeiseizoenen langer. Het is gesuggereerd dat dit zou leiden tot een hogere opname van koolstof doordat de periode waarin planten aan fotosynthese kunnen doen verlengt wordt. Om deze suggestie te onderzoeken, zijn acht opeenvolgende meetjaren van een site in Noordoost-Siberië onderzocht voor patronen in netto koolstofopname, fotosynthese en ecosysteemrespiratie.
De netto koolstofopname, zoals deze gemeten wordt met eddy-covariantie, was opgesplitst met een partitiemethode. Door dagwaardes te gebruiken om model parameters te optimaliseren, konden fotosynthese en ecosysteemrespiratie goed bepaald worden. Voor sommige jaren misten de metingen uit het voorjaar en deze data was opgevuld met behulp van gemiddelde parameters en gemiddelde fluxen. De onzekerheid die door deze methode werd geïntroduceerd kon goed bepaald worden.
Terwijl fotosynthese geen duidelijke toename liet zien met langere groeiseizoenen, was het duidelijk dat fotosynthese wel toenam met warmere zomers. De hogere opname van koolstof werd echter door deze warmere temperaturen grotendeels teniet gedaan door een toename in de respiratie. Daarom was de variabiliteit in netto koolstof opname laag en werd er geen duidelijke relatie gevonden met de lengte van het groeiseizoen. Sterker nog, de hoogste opname van koolstof werd geobserveerd voor het kortste en het koudste groeiseizoen uit de meetserie. Een lage opname van koolstof kwam voornamelijk voor bij langere of warmere groeiseizoenen. Wij concluderen daarom dat het eerder waarschijnlijker is dat de netto opname van koolstof van dit ecosysteem afneemt dan dat deze toeneemt in een warmer klimaat. Bovendien leidt een langer groeiseizoen tot een hogere uitstoot van methaan. Het is daarom waarschijnlijk dat een langer groeiseizoen de broeikasgasopname van dit ecosysteem vermindert.

8.2.5 De broeikasgasbalans van het groeiseizoen in Noordoost Siberische toendra

In de laatste twee doelstellingen van dit proefschrift werden de fluxen van CO_2 en methaan apart van elkaar onderzocht. Door de metingen van de groeiseizoenen van 2007, 2008 en 2009 te combineren kunnen we een broeikasgasbalans opstellen voor deze periodes. Uit hoofdstuk 6 kwam naar voren dat de netto koolstofopname in het groeiseizoen -82.0$\pm$27.5 g C m^{-2}, -88.6 g C m^{-2} and -94. 9 g C m^{-2} was, wanneer alleen naar CO_2 gekeken wordt. Uit hoofdstuk 5 kwam naar voren dat de methaanemissies in diezelfde jaren 56.5, 48.7 and 30.4 nmol CH4 m^{-2} s^{-1} was, wat gelijk is aan 78.3 mg CH_4 m^{-2} dag^{-1}, 67.5 mg CH_4 m^{-2} dag^{-1} and 42.1 mg CH_4 m^{-2} dag^{-1}. Als aangenomen wordt dat deze methaanemissies voor

het hele groeiseizoen gelden, kunnen we deze getallen vermenigvuldigen met de lengte van de groeiseizoenen uit 2007, 2008 en 2009. Voor het volledige groeiseizoen, zijn de methaanemissies dan 6.3 g CH_4 m^{-2}, 4.0 g CH_4 m^{-2} and 2.9 g CH_4 m^{-2}.
Het aardopwarmingsvermogen van 1 g methaan is gelijk aan dat van 25 g CO_2 over een periode van 100 jaar. De koolstofopname wordt echter meestal uitgedrukt in g C, niet in g CO_2. In dat geval is het relatieve aardopwarmingsvermogen van 1 g methaan gelijk aan het aardopwarmingsvermogen van 25x(12/44)=6.8 g C m^{-2} dag^{-1}. Na het toepassen van deze conversiefactor komt het aardopwarmingsvermogen van de groeiseizoenen van 2007, 2008 en 2009 uit op -39$\pm$27.5 g CO_2-eq m^{-2}, -61.3 g CO_2-eq m^{-2} and -74.7 g CO_2-eq m^{-2}. Dit resultaat laat zien dat het onderzochtte gebied een netto opname laat zien voor zowel koolstof als broeikasgassen, zelfs gedurende het warme en lange groeiseizoen van 2007. Dat jaar was zeer uitzonderlijk omdat het groeiseizoen 50% langer was dan gebruikelijk. De groeiseizoenen van 2008 en 2009 hadden een meer normale lengte en dan zien we dat de opname van broeikasgassen veel sterker is. Buiten het groeiseizoen is het gebied echter een bron van broeikasgassen en de volledige jaarlijkse broeikasgasbalans van dit gebied moet nog onderzocht worden. Het is te verwachten dat die getallen een lagere opname van broeikasgassen zal laten zien dan wat hier gepresenteerd is.

8.3 Conclusies

8.3.1 De stabiliteit van CO_2 fluxen en verdamping met een variërende grondwaterstand

- Studies die de relatie tussen respiratie en grondwaterstand onderzochten vertonen tegenstrijdige resultaten.
- Fluxen van respiratie, fotosynthese en verdamping konden succesvol gemodelleerd worden met verschillende methodes.
- Terwijl de grondwaterstand significant lager werd, bleef de hoeveelheid bodemvocht hoog door de hoge retentiecapaciteit van de bodem.
- Fluxen van respiratie, fotosynthese en verdamping vertoonden geen significante variatie langs een groot gradiënt van verschillende waterniveaus omdat de hoeveelheid bodemvocht grotendeels hetzelfde bleef
- Bij het onderzoeken van de relaties tussen grondwaterstand en respiratie, moet bodemvocht ook onderzocht worden.

8.3.2 De rol van endofytische methaanoxiderende bacteriën in geïnundeerde *Sphagnum* bij het determineren van methaanemissies uit toendra

- Methaanfluxen in een *Sphagnum* gedomineerd vegetatietype waren 50% lager dan in een vegetatietype zonder *Sphagnum*.
- Hoewel er verschillen waren in de bedekking van vaatplanten, kon dit niet de waargenomen verschillen verklaren

- Bij de incubatie van *Sphagnum* samples werden oxidatie niveaus gemeten die twee keer zo hoog waren als de verschillen die in het veld werden geobserveerd, wat de hoge oxidatiepotentie in *Sphagnum* bevestigt. Deze oxidatieniveaus werden veroorzaakt door bacteriën die in of op de *Sphagnum* leefden.
- Een procesmodel gaf aan dat de geobserveerde verschillen voornamelijk door oxidatie kwam en in veel mindere mate door planttransport of verschillen in methaan productie.
- De combinatie van de eerdergenoemde conclusies maakt het zeer waarschijnlijk dat oxidatie in geïnundeerde *Sphagnum* een belangrijke rol speelt in de ruimtelijke verschillen van methaanemissies uit toendra.

8.3.3 Ruimtelijke en temporele dynamiek in eddy-covariantieobservaties van methaanfluxen

- Gedurende de zomer van 2008 en 2009, werden methaanemissies succesvol gemeten met het gebruik van een *closed path* eddy-covariantiesysteem dat een Los Gatos fast methane analyser gebruikte.
- Methaanfluxen bleken erg variabel te zijn met de windrichting en dit kwam door een verschil in de hoeveelheid natte vegetatie en meertjes in het gebied.
- De verschillen tussen de jaren werden het best verklaard door de verschillen in waterniveau.
- Bodemtemperatuur verklaarde een deel van het verschil tussen de jaren maar ook de variatie binnen een seizoen.
- De stabiliteit van de atmosfeer verklaarde de meeste variatie binnen een dag.
- De fluxen konden goed gemodelleerd worden door relaties met de grondwaterstand, bodemtemperatuur en de stabiliteit van de atmosfeer in een nonlineair model dat verdeeld werd langs drie windrichtingen met verschillende vegetatie.
- Het model werkte goed in vergelijking met kamerfluxmetingen en het was mogelijk om het naar andere jaren door te trekken.
- Het model kon succesvol gebruikt worden om de emissies van de drie verschillende sectoren apart te berekenen.
- Ondanks het erg heterogene terrein kon een regionaal representatieve schatting van de methaanflux gemaakt worden door de gemodelleerde flux te middelen over de drie sectoren.

8.3.4 Langere groeiseizoenen leiden kennelijk niet tot een hogere netto opname van koolstof in Noordoost-Siberië

- De koolstoffluxen van 8 opeenvolgende groeiseizoenen (2003-2010) van een toendra gebied in Noordoost-Siberië zijn succesvol gemeten.
- De gemeten fluxen konden goed opgesplitst worden in ecosysteemrespiratie en fotosynthesie met behulp van een model dat gekalibreerd werd op dagwaardes.

- De start van het groeiseizoen bleek erg voorspelbaar te zijn aan de hand van de cumulatieve luchttemperatuur.
- Gaten in de data van het vroege groeiseizoen werden opgevuld en onzekerheden konden goed benoemd worden
- GPP en R_{eco} varieerden meer met zomertemperatuur dan met de lengte van het groeiseizoen.
- NEE liet geen duidelijke variatie met de lengte van het groeiseizoen zien. Echter, de grootste netto opname werd gemeten in het kortste en het koudste groeiseizoen.
- Het is waarschijnlijk dat de NEE van dit gebied afneemt in plaats van toeneemt met hogere zomertemperaturen.
- Een langer groeiseizoen leidt zeker tot meer methaanemissies en de opname van broeikasgassen in dit gebied neemt daardoor waarschijnlijk af in een warmer klimaat.

8.3.5 De broeikasgasbalans van het groeiseizoen in Noordoost Siberische toendra

- Het onderzochtte gebied laat een netto opname van CO_2 zien maar is een bron voor methaan.
- De broeikasgasbalans van de groeiseizoenen in 2007, 2008 en 2009 wordt geschat op -39$\pm$27.5 g CO_2-eq m^{-2}, -61.3 g CO_2-eq m^{-2} and -74.7 g CO_2-eq m^{-2}.

8.4 Onderzoeksperspectief en aanbevelingen

8.4.1 De stabiliteit van CO_2 fluxen en verdamping met een variërende grondwaterstand

De eerste doelstelling laat zien dat het belangrijk is om metingen van bodemvocht erbij te betrekken als de gevoeligheid van verdamping en CO_2 fluxen voor veranderingen in de grondwaterstand wordt onderzocht. Bodemvocht bleef hoog, terwijl de grondwaterstand significant verlaagde. Dit betekent dat, zelfs tijdens een erg droge periode, verdamping en fotosynthese niet gelimiteerd waren. De kleine verandering die plaatsvond in bodemvocht betekende ook dat respiratie niet significant veranderde.
Als de onderzochte fluxen alleen vergeleken waren met grondwaterstand, had geconcludeerd kunnen worden dat deze fluxen niet gevoelig zijn voor deze parameter. Dit kwam echter vooral omdat de hoeveelheid bodemvocht hoog bleef. In gebieden waar bodemvocht veel sneller vermindert samen met een lagere grondwaterstand zal een relatie tussen respiratie en grondwaterstand duidelijker zijn.
Dit betekent dat toekomstig onderzoek in dit vakgebied zich niet alleen moet richten op grondwaterstand. Bodemvocht moet ook onderzocht worden, aangezien dit wellicht beter kan verklaren wat de fysische veranderingen zijn in de onverzadigde zone. Ook suggereert dit resultaat dat er in gebieden waar de bodem nat blijft, zoals in toendra, weinig variatie te zien zal zijn met een veranderende grondwaterstand. Bodemvocht- en grondwaterstandonderzoek in toendra is echter zeldzaam en moet daarom meer onderzocht worden in de toekomst.

8.4.2 De rol van endofytische methaanoxiderende bacteriën in geïnundeerde *Sphagnum* bij het determineren van methaanemissies uit toendra

De tweede doelstelling liet zien dat methanotrofe bacteriën die in *Sphagnum* leven, een grote invloed kunnen hebben op de methaanemissie van deze vegetatietypes. Een microbiologische analyse van geïnundeerde *Sphagnum* liet erg hoge oxidatieniveaus zien, wat bevestigd werd door de modelstudie. Toekomstig modelleerwerk van methaanemissies zou deze hoge oxidatieniveaus moeten meenemen wanneer deze vegetatie onderzocht wordt.
Alhoewel dit onderzoek laat zien dat de waargenomen verschillen waarschijnlijk door deze methanotrofen veroorzaakt worden, zou een meer gedetailleerde analyse van deze vegetatietypes meer inzicht geven in de interactie tussen deze bacteriën en het ecosysteem. Deze studie liet duidelijk zien dat deze bacteriën emissies kunnen verlagen maar ze stimuleren ook het vastleggen van koolstof door *Sphagnum*. Op dit moment zijn er geen *in situ* experimenten gedaan naar de toename van koolstofopname die aan activiteit van deze bacteriën toegeschreven zou kunnen worden. Een gedetailleerde studie naar het bodem type, de vegetatiecompositie, nutriëntendistributie in relatie tot methaanproductie, methaanoxidatie, fotosynthese en respiratie, wellicht gecombineerd met stabiele isotopen of labelen, zou meer inzicht kunnen verschaffen in de koolstofcyclus in dit vegetatietype. Hopelijk leidt dit tot een beter inzicht van hoe de samenwerking tussen deze bacteriën en *Sphagnum* bijdragen aan de hoge koolstofopslag die in *Sphagnum* gedomineerde vegetatie gevonden wordt.

8.4.3 Ruimtelijke en temporele dynamiek in eddy-covariantieobservaties van methaanfluxen

De derde doelstelling liet zien dat methaan emissies nauwkeurig gemeten kunnen worden in een zeer heterogeen gebied. Een *closed path* eddy-covariantiesysteem werd succesvol toegepast en methaanfluxen konden vervolgens gemodelleerd worden. Het bleek bovendien dat de dagelijkse gang van methaan fluxen varieerde met de stabiliteit van de atmosfeer. Door deze parameter erbij te betrekken kon een model met een hoge tijdsresolutie ontwikkeld worden, dat gebruikt kan worden voor het opvullen van gaten in de gemeten data.
Toekomstig onderzoek in dit gebied zou de metingen moeten doortrekken naar het hele sneeuwvrije seizoen. Het huidige stroomverbruik van het *closed path* systeem vereist het gebruik van een generator. Dit limiteert het gebruik tot de periodes dat mensen in het gebied aanwezig zijn. Dit probleem kan opgelost worden door een meer betrouwbare en meer zelfstandige stroomvoorziening of door het gebruik van een *open path* systeem, zoals de recent uitgebrachte Licor-7700. Door metingen te verlengen van net voordat de sneeuw smelt totdat de bodem weer opvriest, kan de volle dynamiek van de methaanemissie van toendra bepaald worden. Aangezien er bij een andere studie op Groenland in kamerfluxmetingen aan het einde van het seizoen, bij de start van het opvriezen van de bodem, een hoge uitstoot waargenomen is, zouden de emissies aan het einde van het seizoen ook wel eens kritiek kunnen zijn om de volle broeikasgasbalans van Siberische toendra te bepalen. Ook kan bij een langere meetperiode de invloed van andere parameters, zoals de diepte van de ontdooide laag, beter bepaald worden.

8.4.4 De invloed van groeiseizoenlengte op de netto opname van koolstof

Uit de laatste doelstelling bleek dat de opname van koolstof in toendra het hoogst was met koude of korte groeiseizoenen. Dit was tegenstrijdig met wat verwacht werd; een langer groeiseizoen leidt immers tot meer fotosynthese en dus meer opname van koolstof. Dit onderzoek laat echter duidelijk zien dat dit niet het geval is omdat de hogere temperatuur ook tot meer respiratie leidt.
Deze conclusie had niet getrokken kunnen worden zonder langetermijnmetingen van de koolstofuitwisseling in toendra als in deze studie. Voortzetting van de CO_2 flux metingen is daarom erg belangrijk om te blijven waarnemen hoe de netto uitwisseling van koolstof op de toendra verandert met een warmer klimaat. Alhoewel de hoogste netto opnames van koolstof duidelijk met de korte en koude groeiseizoenen plaats vonden, kunnen vegetatieveranderingen wellicht een langere respons vertonen. Deze eventuele vegetatieveranderingen zullen ook tot een andere respons van het ecosysteem leiden en dit kan kritiek zijn in het bepalen van de langetermijnstabiliteit van de opgeslagen koolstof in toendra. Lange termijn metingen vereisen een aanzienlijke opdracht in logistiek, personeel en kosten maar dit soort metingen kan ons inzichten verschaffen die een model ons niet kan leveren.

8.4.5 Algemene aanbevelingen

Dit onderzoek heeft laten zien dat toendra koolstof opneemt, een bron is voor methaan en alhoewel veel van de dynamiek van beide systemen tot in detail onderzocht is, zijn er ook onderdelen waar kennis ontbreekt. De methaan emissies van thermokarstmeren zijn bijvoorbeeld slecht gedefinieerd en de kennis van hun emissie in het onderzochte gebied is beperkt. Andere gebieden, zoals het riviergebied, stoten ook hoge hoeveelheden methaan uit en hebben een hoge primaire productie maar dit is minder goed onderzocht. Verder is het onbekend hoeveel koolstof in meren eindigt of via de rivieren getransporteerd wordt. Toekomstig onderzoek zou deze onderwerpen moeten meenemen om een echte regionale schatting van de broeikasgasbalans te kunnen maken.
Om deze doelen te behalen, zal een reeks aan toepassingen gebruikt moeten worden, waaronder eddy-covariantiemetingen, fluxkamers, drijvende fluxkamers en wellicht nieuw te ontwikkelen systemen. Om in dit zeer nodige materieel te voorzien, is het essentieel dat de technische kennis voor het bouwen van dit soort instrumentatie en elektronica beschikbaar is op het onderzoeksinstituut. Dit onderzoek heeft zeer veel baat gehad bij de uitgebreide ondersteuning van zowel de fijnmechanische werkplaats als de afdeling elektronica van de VU. Zonder hun ondersteuning zou een succesvolle afronding van dit onderzoek problematischer, zo niet onmogelijk, zijn geweest en het zou zeer verstandig zijn om deze faciliteiten en de kennis van de technici te behouden, om zo uitstekend veldonderzoek te kunnen blijven waarborgen.

List of Figures

List of Tables

List of symbols and abbreviations

The following list gives a short description of the symbols used throughout this thesis.

Symbol	Description and unit
α	Priestley-Taylor parameter or canopy light utilization efficiency [µmol C J^{-1}]
β	Maximum CO_2 uptake rate of the canopy at light saturation [µmol C m^{-2} s^{-1}]
γ	The psychometric constant
λ	Thermal conductivity of the soil [W m^{-1} K^{-1}]
Φ	Result of the atmospheric stability function [> 0]
E_0	Temperature sensitivity [°K]
f_{ox}	Within plant oxidation factor (0-1), reducing the amount of emitted CH_4 from plants.
f_{shoots}	Fraction (0-1) of net primary production (NPP) allocated to aboveground shoots.
F_s	Flux of gas 's' [µmol m^{-2} s^{-1}] or [nmol m^{-2} s^{-1}]
FU	Cumulative forcing units [°C]
G	Flux density of heat into the soil [W m^{-2}]
GPP	Gross Primary Production [µmol m^{-2} s^{-1}]
L	Monin-Obukhov length [m]
NEE	Net Ecosystem Exchange [µmol m^{-2} s^{-1}]
NPP	Net Primary Production [µmol m^{-2} s^{-1}]
NRMSD	Normalized root mean square deviation
P_{max}	Maximum daily NPP [0.001-0.005 kgC m^{-2} day^{-1}].
R_{eco}	Ecosystem CO_2 respiration rate [µmol m^{-2} s^{-1}]
r^2	Coefficient of determination
R_{ref}	Reference respiration at T=10°C [µmol m^{-2} s^{-1}]
R_n	Net radiation [W m^{-2}]
R_g	Incoming short-wave radiation [W m^{-2}]
s	Slope of the saturation water vapor-temperature curve at air temperature
s'	Deviation of the concentration of gas 's' from the mean [µmolm^{-3}]
T_{air}	Air temperature [°C]
T_{soil}	Soil temperature [°C]
$u*$	Friction velocity [m s^{-1}]
VPD	Vapour pressure deficit [hPa]
V_{transp}	Plant transport factor (0-15), increasing the amount of emitted CH_4 from plants.
w'	Deviation from mean vertical wind speed [m s^{-1}]
w_l	Water level [m]
z	Measurement height [m]
Z_{roots}	Maximum root depth [0.1-0.6 m].